



AN ABSTRACT OF THE THESIS OF

Kyle Richard Hogrefe for the degree of Master of Science in Geography presented on June 5, 2008.

Title: Derivation of Near-shore Bathymetry from Multispectral Satellite Imagery used in a Coastal Terrain Model for the Topographic Analysis of Human Influence on Coral Reefs

Abstract approved:

---

Dawn J. Wright

The analysis of material and energy exchange between the marine and terrestrial components of island ecosystems enables research into the impact of human population and land use on the health of coral reef habitat. Satellite and acoustic remote sensing technologies enable the collection of data to produce high resolution bathymetry for integration with terrestrial digital elevation models (DEMs) into coastal terrain models. An integrated terrain surface that incorporates the land-sea interface, grounded by a geographic information system, is a powerful analytical tool for geomorphic studies of watersheds and coastal processes. The island of Tutuila, American Samoa is an ideal case study due to its high relief terrain, data availability and local interest in impacts to coral reef resources. The Tutuila model integrates a USGS DEM, multibeam bathymetry from 15 to 500 m and near shore bathymetric data from 0 to 15 m derived from IKONOS satellite imagery. The high spatial resolution of IKONOS imagery is suitable for

detection of features with subtle relief and intricate structure. Shallow water bathymetry is derived by quantifying the relative attenuation of blue and green spectral band radiance as a function of depth. The procedure used to derive bathymetry, Lyzenga (1985), is identified as the most effective of several proposed in the recent literature. The product is error-checked using control points extracted from multibeam sonar data and collected during recent field surveys, as well as terrain profiles. The coastal terrain model provides morphological detail of fine resolution and high accuracy for terrain and land use analysis to enhance the study of ecosystem interconnectivity and the effects of anthropogenic inputs to coral reef habitats. Subsequent topographic analyses of the Tutuila model use drainage patterns to identify contiguous marine/terrestrial basins within which the marine environment is most directly impacted by land use through freshwater inputs from affiliated catchments. Human population density serves as an indicator of intensified land use and urbanization, which has been shown to increase pathogen and sediment loads in runoff, while percent coral cover, coral colony density and coral genera diversity are used as indicators of reef health. Spatiotemporal correlation analyses of population density against the three reef health indices within each of the marine/terrestrial basins reveal a decline in reef health associated with increased population density. This paper integrates and builds upon established methods of satellite imagery analysis and terrain modeling to create the Tutuila coastal terrain model and uses it to refine the scale of other studies linking human terrestrial activities to the physical condition of coral reefs.

©Copyright by Kyle Richard Hogrefe  
June 5, 2008  
All Rights Reserved

Derivation of Near-shore Bathymetry from Multispectral Satellite Imagery used in a  
Coastal Terrain Model for the Topographic Analysis of Human Influence on Coral Reefs

by  
Kyle Richard Hogrefe

A THESIS

submitted to

Oregon State University

in partial fulfillment of  
the requirements for the  
degree of

Masters of Science

Presented June 5, 2008  
Commencement June 2009

Master of Science thesis of Kyle Richard Hogrefe  
presented on June 5, 2008.

APPROVED:

---

Major Professor, representing Geography

---

Chair of the Department of Geosciences

---

Dean of the Graduate School

I understand that my thesis will become part of the permanent collection of Oregon State University libraries. My signature below authorized release of my thesis to any reader upon request.

---

Kyle Richard Hogrefe, Author

## ACKNOWLEDGMENTS

I would like to express deep appreciation for the contributions of Dawn Wright (Oregon State University) and Eric Hochberg (University of Hawaii) whose contributions and advice greatly enhanced the depth and breadth of this research and writing. I also offer a special thanks to my graduate committee members Anne Nolin, Hannah Gosnell and Joe Beatty, as well as the rest of my colleagues and mentors within the Department of Geosciences, for their support and insight during my graduate program.

I also want to acknowledge the data contributions that made these investigations possible. Thanks to NOAA's Pacific Islands Benthic Habitat Mapping Center for providing the multi-beam sonar bathymetry and contacts to acquire IKONOS satellite imagery; to NOAA's Pacific Island Fisheries Science Center, Coral Reef Ecosystem Division for providing coral species distribution data and for collecting field control points during a busy deployment schedule on the 2008 American Samoa Research and Management Program research cruise aboard the NOAA Vessel *Hi'ialakai*; and to NOAA's Center for Coastal Monitoring and Assessment, Biogeography Team and NOAA's Coastal Services Center for providing the at-sensor IKONOS imagery needed for deriving bathymetry.

Finally, I want to convey deep gratitude to my fiancé and soon to be wife, Jeanette Hawkins, for her patience and unwavering support and to my family for providing the foundation of who I am and for their part in my growth over the last 39 years.

## CONTRIBUTION OF AUTHORS

Dr. Wright, as my major advisor, provided technical advice regarding GIS techniques, data sources and scientific method in the completion of both chapters 2 and 3, as well as editorial advice in the design and writing of this entire thesis.

Dr. Hochberg provided essential technical advice in identifying and then pursuing the most accurate procedure for deriving depth from multispectral satellite imagery as detailed in chapter 2. He also provided editorial comment concerning the design and focus of chapter 2.

## TABLE OF CONTENTS

	<u>Page</u>
Chapter 1 Introduction .....	1
Chapter 2 Derivation and Integration of Shallow-water Bathymetry: Implications for Coastal Terrain Modeling and Subsequent Analyses .....	4
Abstract.....	5
2.1 Introduction .....	6
2.2 Methods .....	8
2.2.1 Study Area .....	8
2.2.2 Data.....	9
2.2.2.1 IKONOS Imagery.....	9
2.2.2.2 Multibeam Sonar Data.....	10
2.2.2.3 Digital Elevation Model .....	10
2.2.2.4 Ground-Truth Data .....	11
2.2.3 Bathymetric Derivations from IKONOS Satellite Imagery .....	12
2.2.4 Dataset Integration.....	16
2.3 Results .....	17
2.3.1 Derived Bathymetry Error Analysis.....	17
2.3.2 CTM Error Analysis .....	22
2.3.3 Dataset Seams and Morphological Detail .....	25
2.4 Discussion.....	30
2.4.1 Improvement and Repeatability of Derivation Method.....	30
2.4.2 Issues with Merging Datasets.....	31
2.4.2.1 Data Gaps .....	31
2.4.2.2 Vertical Datum Issue .....	32

2.4.3	Continuing Research .....	34
2.5	Conclusion .....	35
	Acknowledgments .....	36
	References .....	37
Chapter 3 Human Population Density and Coral Reef Diversity: A Topographic Analysis .....		39
	Abstract.....	40
3.1	Introduction .....	41
3.2	Methods .....	42
3.2.1	Study Area .....	42
3.2.2	Data.....	44
3.2.2.1	Tutuila Coastal Terrain Model .....	44
3.2.2.2	Population Density Data.....	45
3.2.2.3	Coral Reef Health Criteria.....	46
3.2.3	Identification of Marine Terrestrial Units .....	52
3.3	Results .....	53
3.3.1	MTU Analysis .....	53
3.3.2	Comparison of Population Density and Reef Criteria by MTU .....	56
3.4	Discussion.....	59
3.5	Conclusion .....	62
	Acknowledgments .....	63
	References .....	64
Chapter 4. Conclusion .....		66
	References .....	71

## LIST OF FIGURES

<u>Figure</u>	<u>Page</u>
2.1: The island of Tutuila, American Samoa.....	7
2.2: Error analyses for four published methods to derive bathymetry. ....	14
2.3: Derived bathymetry error analysis by linear regression .....	18
2.4: Error analysis by linear regression performed on integrated derived bathymetry. .	21
2.5: Error analysis by linear regression performed on estimated bathymetry.....	23
2.6: Error analysis by linear regression performed on complete CTM mosaic.....	24
2.7: Tutuila CTM with terrain profile transects.....	26
2.8: Terrain profile of Transect 1.....	27
2.9: Terrain profile of Transect 2. ....	27
2.10: Terrain profile of Transect 3. ....	28
2.11: Terrain profile of Transect 4. ....	29
3.1: Location map of Tutuila, American Samoa. ....	43
3.2: 2004 and 2006 REA locations with coral cover and coral density. ....	48
3.3: 2004 and 2006 REA Locations with Generic Diversity and Coral Community Composition.. ....	49
3.4: Identification of Marine Terrestrial Units. ....	53
3.5: Marine Terrestrial Units and REA Site Locations. ....	55
3.6: 2004 Reef Assessment Criteria Correlation to Population Density. ....	58
3.7: 2006 Reef Assessment Criteria Correlation to Population Density. ....	58
3.8: 2004-2006 Percent Change in Reef Assessment Criteria Correlation to Population Density. ....	59

## LIST OF TABLES

<u>Table</u>	<u>Page</u>
2.1: IKONOS spatial and spectral resolutions.....	9
3.1: MTU Population Density. ....	45
3.2: 2004 and 2006 REA Data Summary by MTU .....	51
3.3: Percent Change in REA Data between 2004 and 2006 per MTU .....	51
3.4: 2000 MTU Population Densities with REA Data: sorted by density .....	57
3.5: Population Density / REA Data Correlation Co-efficients .....	57

## LIST OF APPENDICES

<u>Appendix</u>	<u>Page</u>
Appendix A: Tutuila, American Samoa Costal Terrain Model .....	73
Appendix B: Data processing “Cookbook” of instructions to derive bathymetry .....	74
Appendix C: U.S. Census Bureau Data .....	96
Appendix D: REA Coral Reef Assessment Data MTU Summary .....	99
Appendix E: Correlation Coefficient Calculations .....	101
Appendix F: Data processing “Cookbook” of processing steps taken in Arc Hydro..	105

## LIST OF APPENDIX TABLES

<u>Appendix Tables</u>	<u>Page</u>
C.1: Census Data MTU Assignments.....	96
C.2: Multiple MTU Census Tract Data Allocations.....	98
D.1: REA Coral Reef Assessment Data MTU Summary.....	99
E.1: Correlation Co-efficient Calculations.....	101
F.1: Tags defined in Arc Hydro “Terrain Preprocessing” used for MTU analysis.....	107

# **Chapter 1. Derivation of Near-shore Bathymetry from Multispectral Satellite Imagery used in a Coastal Terrain Model for the Topographic Analysis of Human Influence on Coral Reefs**

## **Introduction**

The research goal of this thesis is the derivation of shallow water bathymetry to enable the completion of a terrain model and its subsequent use in a topographic analysis to compare human land use with the health of nearby coral reefs. The research question is how does terrain influence the impact of human land use intensification to the physical condition of coral reefs? The logical sequence through two manuscripts establishes the validity of using multispectral satellite imagery to deduce bathymetry and describes the technical steps for deriving accurate depth data and integrating it into a seamless terrain surface. The resulting coastal terrain model (CTM) is then used to determine combined marine/terrestrial units (MTUs) in which human activity would be most likely to influence the near shore environment. Subsequent analyses indicate spatiotemporal correlations between human population density and three criteria commonly used to assess the condition of coral reefs.

In Chapter 2, the research goal is the identification of the most accurate method to derive bathymetry from multispectral satellite imagery and its use to provide near-shore data for the creation of a CTM. The research question is what errors are associated with derived bathymetry and its use in a CTM? Though several methods have been developed to calculate depth from multispectral data by gauging the relative attenuation rate of different wavelengths of light as they pass through water, research using this derived bathymetry in any capacity is scarce. This paper identifies Lyzenga (1985) as the most accurate of several published methods, relying on a multiple linear regression analysis to

establish the statistical relationship between the differential attenuation rate of the blue and green spectral bands as they pass through water. This multivariate linear relationship is then used to derive depths to fill a data gap between terrestrial and deeper seafloor data, in order to complete a CTM of Tutuila Island, American Samoa. The errors associated with interim products and the final model are assessed through regression analyses and terrain profiles.

In Chapter 3, the research goal is to conduct a terrain analysis using the Tutuila CTM to answer the question how does island terrain influences the impact of increased human land use intensity on the physical condition of coral reefs? The Tutuila CTM is analyzed to determine MTUs, defined as areas of contiguous terrestrial and marine terrain as identified by drainage patterns that would occur if the whole area were dry land. This classification distinguished terrain units in which nutrients, sediment and pathogens contained in freshwater inputs are most likely to impact the physical condition of coral reefs. The comparison of population density to percent coral cover, coral colony density and coral generic diversity within each MTU reveals correlations between increased human population density and the health of coral reefs. Strong negative correlations between population density and the percent change of both colony density and generic diversity between 2004 and 2006 indicate that increased population density leads to an increased rate of decline of these two indices. A positive correlation between population density and percent change in coral cover poses a less definitive relationship, but the island wide decrease of this criterion still implies an impact as population has increased.

The synthesis of these two manuscripts (one submitted for publication to the journal *Marine Geodesy*, and the other in submission to a journal to be determined) contributes to the advancement of scientific knowledge by integrating two established analytical approaches to create an original product and using this product to refine the scale of previous research. The identification of the most accurate of multiple published methods of bathymetric derivation, the integration of bathymetry derived by this method, and the error analyses conducted on the product establish an accurate and cost effective data source for coastal terrain modeling in remote areas. The division of Tutuila's terrain into MTU allows for the refinement of previous island scale analyses of correlations between population density and coral community diversity to a smaller, drainage basin scale. In doing so, the MTU approach demonstrates the influence of terrain on land use and how this ultimately impacts coral reefs.

### **Reference**

Lyzenga, D. R. 1985. Shallow-water bathymetry using combined LIDAR and passive multispectral scanner data. *International Journal of Remote Sensing* 6 (1):115-125.

**Chapter 2. Derivation and Integration of Shallow-water Bathymetry: Implications for Coastal Terrain Modeling and Subsequent Analyses**

Kyle R. Hogrefe, Dawn J. Wright and Eric J. Hochberg

Submitted to *Marine Geodesy*

Publication office:

Taylor and Francis, Inc

325 Chestnut St. Suite 800

Philadelphia, PA 19106

6<sup>th</sup> Special Issue on Marine and Coastal Geographical Information Systems

**Abstract**

Satellite and acoustic remote sensing enable the collection of high-resolution seafloor bathymetry data for integration with terrestrial elevations into coastal terrain models. A model of Tutuila Island, American Samoa is created using depths derived from IKONOS satellite imagery to provide data in the near-shore gap between sea level and the beginning of sonar data at 10-15 m depth. A derivation method gauging the relative attenuation of blue and green spectral radiation is proven the most effective of several proposed in recent literature. The resulting coastal terrain model is shown to be accurate through statistical analyses and topographic profiles.

## 2.1 Introduction

Coastal terrain models (CTM) incorporating both topography and bathymetry, grounded by a geographic information system (GIS), have proven to be powerful analytical tools for the modeling of watershed and coastal morphology. The integration of environmental and societal datasets into a CTM enable investigations into the relationships and interactions of island ecosystems and provide information about terrestrial influences to coral reefs from human activities (Mumby et al. 2004). The marine and terrestrial components of island ecosystems are linked by fresh water inputs that reach miles out to sea and provide for nutrient exchange and larval transport, but they also carry sediment and pollutants that diminish the species diversity of coral reef community structure (Andrefouet et al. 2002, Shapiro and Rohmann 2005). Other research links diminished reef species diversity to human development density through the increased turbidity that it causes at the island scale (Sealey 2004). A finer scale investigation, at the watershed level, may reveal more direct relationships between land use practices, freshwater plumes and coral reef health.

Satellite and acoustic remote sensing technologies produce readily accessible data to create coastal terrain models detailed enough to run oceanographic, hydrographic and atmospheric simulations (Mumby et al. 2004, Shapiro and Rohmann 2005). However, a challenge in the creation of a CTM is the acquisition of data from 0 to 15 m where surf conditions and shallow terrain features make the operation of bathymetric survey vessels hazardous (Figure 2.1). In clear water conditions, both LIDAR (light detection and ranging) surveys and processed satellite imagery show promise for filling this data gap. Though LIDAR data are more accurate, survey costs may be prohibitive and satellite

imagery is more easily available and cost effective, particularly in remote locations or poor countries (Mumby et al. 1999). Recent work (Hochberg et al., unpublished) investigates the accuracy of several methods proposed to derive bathymetry and points to one process (Lyzenga 1985) as the most effective. Similar methods, coupled with processing steps to eliminate surface glint, are used to derive bathymetry from IKONOS satellite imagery. These data are used in creation of a CTM for the island of Tutuila and its surrounding bathymetry and are subjected to error analysis during CTM integration.

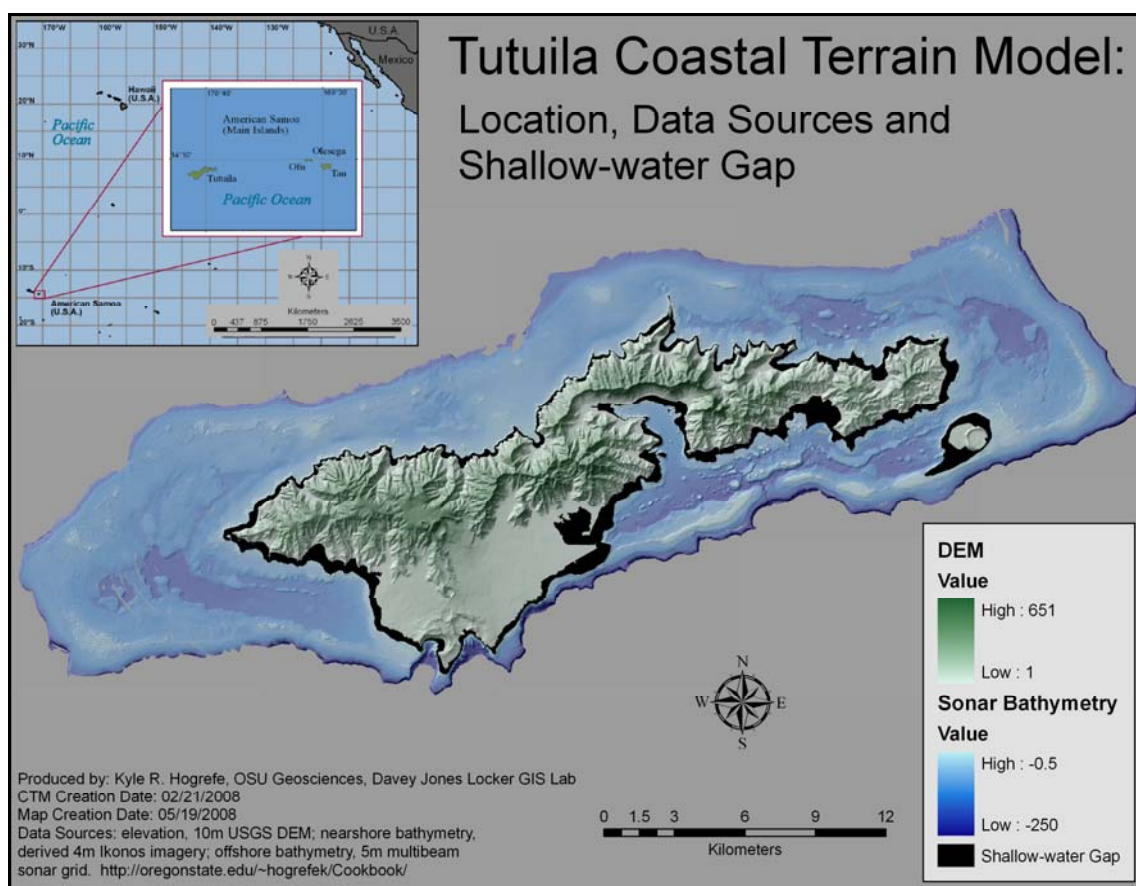


**Figure 2.1:** The island of Tutuila, American Samoa. Data sources include a 10-m USGS digital elevation model (DEM), near shore bathymetry derived from 4-m IKONOS imagery, and offshore bathymetry at 5-m resolution, (more information online at [oregonstate.edu/~hogrefek/Cookbook](http://oregonstate.edu/~hogrefek/Cookbook/)). Projection and datum are Universal Transverse Mercator (UTM) Zone 2 South, World Geodetic System (WGS) 1984. Notice the gap in data between the island and the deepwater bathymetry.

## **2.2 Methods**

### **2.2.1 Study Area**

This research focuses on deriving bathymetry to complement pre-existing datasets for the creation of a CTM for the island of Tutuila, American Samoa (Appendix A) and testing its accuracy for the assessment of human population and land use practices on coral reefs. Tutuila is ideal for a case study of human driven terrestrial impacts. Its volcanic origin and the tropical climate of the South Seas have resulted in topography of well-defined ridgelines and valleys that extend beyond the shoreline to significant depth. These distinct marine/terrestrial units provide naturally defined topographic basins for comparing land use impacts to adjacent reefs. The population pattern of the island consists of valleys that contain human settlements ranging from cities such as Pago Pago (population ~ 4000) to small villages of populations less than 100, with some small valleys remaining uninhabited. Though most of the settlement is concentrated on relatively flat coastal terrain, population pressure pushes development up steeper valley slopes and traditional land use, such as small plot agriculture and the harvest of fruit and wood, occurs farther up in the valleys. Pago Pago Harbor supports industrial activities such as a fish cannery and port services to support an extensive fishing fleet and international commerce. Densely-populated areas spreading to the southwest of Pago Pago Harbor along the coast cross through several watersheds, support a large percentage of the island's population and have many impervious surfaces that probably enhance runoff and contribute to pollutant loads.

Personal experience with community leaders, resource managers and the general population on Tutuila as well as recent research (Wright 2002) indicate a strong desire to

take action to protect marine resources. However, the mitigation of pollutants in terrestrial runoff is problematic because it requires changing social practices, which further requires either extensive outreach and education or passage of regulations to modify people's actions. These solutions demand scientific information to convince individuals of the necessity of change or to justify the implementation of new policies (Hoffman 2002b, Mumby et al. 1999).

## 2.2.2 Data

### 2.2.2.1 IKONOS Imagery

The IKONOS satellite is a high spatial resolution “push broom” sensor with a sun synchronous polar orbit operated by GeoEye, Inc. The instrument obtains multi-spectral data in four bands at 4 m nominal resolution and panchromatic data at 1 m nominal resolution (Table 2.1). IKONOS images were originally obtained by NOAA Coastal Services center in 2001 and used to create a mosaic covering the islands of Tutuila and Aunu'u for the Pacific Islands GIS project. NOAA's National Centers for Coastal Ocean Science, Center for Coastal Monitoring and Assessment (CCMA) provide original imagery for this research. The images were acquired on 11/07/2001, 12/02/2001 (two images) and 02/03/02 at approximately 21:44 hours and delivered as NTF files.

**Table 2.1:** IKONOS Spatial and Spectral Resolutions.

<b>Band</b>	<b>Spectral Range (µm)</b>	<b>Color Range</b>	<b>Resolution (m at nadir)</b>
1	0.45 – 0.52	Blue	4 x 4
2	0.52 – 0.60	Green	4 x 4
3	0.63 – 0.69	Red	4 x 4
4	0.76 – 0.90	Near-infrared	4 x 4
Pan	0.45 – 0.90	Panchromatic	1 x 1

#### **2.2.2.2 Multibeam Sonar Data**

The Coral Reef Ecosystem Division (CRED) of NOAA's Pacific Islands Fisheries Science Center (PIFSC) in conjunction with the University of Hawaii's Pacific Islands Benthic Habitat Mapping Center provides bathymetry at a depth range of 15 – 250 m. The data were collected from January to March, 2004 and February to March, 2006 using the 30 kHz Simrad EM300 and 300 kHz Simrad EM3002D sonar systems aboard the NOAA *R/V Hi'ialakai*, a 218' research ship, and the 240 kHz RESON 8101-ER sonar system aboard the *R/V AHI* (Acoustic Habitat Investigator), a 25' survey launch operated by the PIFSC. The effort supports the Coral Reef Conservation Program goal of mapping all coral reefs in less than 30 m depth, and select reefs in deeper water, by 2009. Sonar soundings were processed into a 5 m resolution raster grid and the data were provided as an ASCII file.

The projection and resolution of the deepwater bathymetry were chosen as project defaults so that, once the file was converted to an ESRI raster and defined in its projection, no further processing was required prior to CTM mosaicing. However, data gaps are apparent in the bathymetry in areas where sonar swaths did not overlap (Figure 1). An expression is employed using the ArcGrid command line window to close these data gaps using a moving average algorithm that assigns a mean value to "NoData" cell values without changing the original data.

#### **2.2.2.3 Digital Elevation Model**

The source of terrestrial data is a 10 m resolution mosaic of 1:24,000 scale USGS digital elevation models (DEMs) produced in April, 2001 for the American Samoa Land

Grant Extension program and provided to the American Samoa GIS User Group. Raster data grids derived from the original DEMs were mosaicked using ArcGIS to create the compilation. This product is the baseline dataset for terrain analysis on Tutuila and has previously been merged with bathymetric data around the island, but the shallow-water data gap prevents a seamless surface (Figure 2.1). To prepare the DEM for integration into the CTM, it is reprojected from the North American Datum of 1983, Geodetic Reference System (GRS) 1980 ellipsoid to World Geodetic System (WGS) 1984, Universal Transverse Mercator (UTM) 2S and resampled from a 10 m to a 5 m resolution.

#### **2.2.2.4 Ground-Truth Data**

Data points used to conduct error analysis on the derived bathymetry and the CTM are from two sources: recently collected control points and points created in ArcGIS with depth extracted from the PIBHMC multibeam sonar bathymetry. NOAA CRED's Oceanography Team collected most of the field survey control points during the 2008 American Samoa Research and Management Program research cruise. At each control point, position and depth data are collected either haphazardly or at specific waypoints; a small number of additional points are gleaned from oceanographic sampling records (CTD casts) from previous cruises. Each data point was collected using a Garmin76 GPS unit and an echosounder. The resulting 140 control points fall within all categories of bathymetric data used in the CTM. To more fully explore the range of error associated with the data, two additional sets of point features are used to extract sonar and derived depth values for comparison. The first set entails the same point features

used to extract the linearized spectral values used in determining the depth/spectral decay relationship (next section). Using these same points to evaluate derived depths may be considered biased; however, given that they were chosen in areas where image conditions looked most favorable for a clean spectral signal, they are useful for an analysis focused on areas likely to have a reasonable result. For an error analysis with greater geographic coverage and less bias, features of over 800 points with haphazard distribution were created for each IKONOS image to extract derived values from depths shallower than 20 m as defined by the sonar bathymetry.

### **2.2.3 Bathymetric Derivations from IKONOS Satellite Imagery**

Digital image processing techniques allow for the derivation of shallow water bathymetry by assessing the relative radiance of blue and green bands (Table 1) of the electromagnetic spectrum as they are attenuated as a function of depth. Bathymetric derivation procedures require starting with “at sensor” data, as provided by the CCMA, to assure accurate tracking of processing lineage and the validity of derived depth. The high spatial resolution of the IKONOS imagery makes the data suitable for detection of features with subtle relief and intricate structure (Stumpf et al. 2003, Mumby et al. 2004, Shapiro and Rohmann 2005). Depth derivation from spectral data is a multi-phase procedure using ArcGIS 9.2 (Environmental Systems Research Institute, Inc., Redlands, CA) ENVI 4.3 (ITT Industries, Inc., Boulder, CO) Microsoft Excel (Microsoft Corporation, Redmond, WA), and S-Plus (Insightful Corporation, Seattle, WA).

The four images required to provide spatial coverage of Tutuila and Aunu'u were georectified and then radiometrically calibrated (converted from digital number to

radiance values), using standard processing techniques (Appendix B). Sea surface glint effects were corrected using methods first described in (Hochberg et al. 2003) and refined by (Hedley et al. 2005) using the equation  $R'_i = R_i - b_i(R_{NIR} - Min_{NIR})$ ; where  $R_i$  = radiance of band  $i$ ,  $b_i$  = regression line slope of band  $i$  (y axis) against the NIR band (x axis),  $R_{NIR}$  = NIR radiance, and  $Min_{NIR}$  = minimum NIR value. The variable  $b_i$  is determined using a spatial subset of image pixels over optically deep water (> 15 m) to obtain radiance values for the linear regression;  $Min_{NIR}$  may also be determined from this subset. The values  $R_i$  and  $R_{NIR}$  are drawn from the input image as it is processed. However, Tutuila CTM bathymetric derivations employ a modified version of this formula by not subtracting the  $Min_{NIR}$  value to correct for atmosphere in the same manner as a “dark pixel subtraction” (Chavez 1988). Therefore, corrections for both sea surface glint and atmospheric effects are conducted using the formula  $R'_i = R_i - b_i(R_{NIR})$ . The linear regression between band  $i$  radiance and NIR radiance is calculated using MS Excel, while ENVI 4.3 enables other processing steps.

In recent work, bathymetric derivation procedures proposed since 1978 are tested using imagery from various sites across the Pacific (Hochberg et al., unpublished). Figure 2.2 shows the results of an error analysis of the four most effective methods compared with SHOALS (Scanning Hydrographic Operational Airborne LIDAR Survey) data in Kaneohe Bay, Oahu, Hawaii. One method (Lyzenga 1985) far outperforms the others achieving an error range of  $\pm 5$  m, half the magnitude of other methods. Note the 5 m overestimate that occurs at a depth of 5 m and the 5 m underestimate that occurs at a depth of 20 m. Similar results are obtained when methods based on Lyzenga (1985) are used to derive shallow water bathymetry for inclusion in the Tutuila CTM.

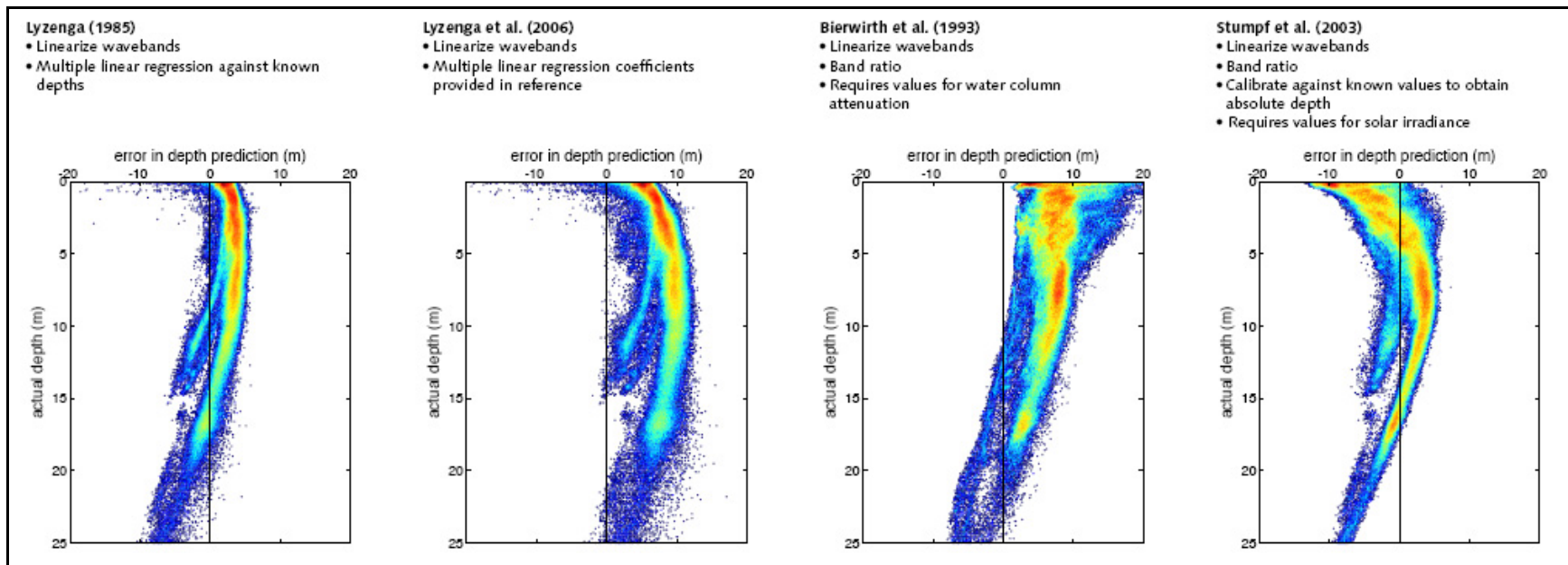


**Figure 2.2:** Error analyses for four published methods to derive bathymetry. Derived depths from an image of Kaneohe Bay, Hawaii are compared to SHOALS (Scanning Hydrographic Operational Airborne LIDAR Survey) data. The y-axis represents increasing depth while the x-axis shows the negative and positive error of the derived depth. Source: Hochberg (unpublished data, 2007).

Bathymetric data are derived by gauging the relative attenuation rates of blue (450-520 nm) and green (520-600 nm) spectral radiation as it passes through the water column. Spectral radiance values are first linearized using the formula  $R_{Linear} = \ln(R_i - R_{imin})$ ; where  $R_i$  = radiance of band  $i$ , and  $R_{imin}$  = minimum radiance of band  $i$ . The variable  $R_i$  is drawn from the input image as it is processed while  $R_{imin}$  is determined using a spatial subset over optically deep water from the glint/atmosphere corrected image. With this step completed in ENVI 4.3, the linearized spectral data for the blue and green bands are exported to ArcGIS 9.2 for data extraction, a process greatly facilitated by the ENVI Reader for ArcGIS plug-in (<http://www.itvis.com/>), to establish correlation with depth in a multiple linear regression using S-PLUS.

In ArcMap, features containing between 150 – 200 points are created for each IKONOS image extent in depths of less than 20 m and then used to extract sonar depth and linearized blue and green spectral values at each location. Multiple linear regression analysis is conducted with depth as the dependant variable and the linearized spectral radiance values as the independent variables. The outputs of interest are y-intercept, and the slope for each spectral band. Depth is then derived in ENVI 4.3 using the equation  $D = a + (b_i)(x_i) + (b_j)(x_j)$ ; where  $a$  = y-intercept,  $b$  = slope,  $x$  = linearized spectral radiance and  $i$  and  $j$  indicate spectral band. The variables  $x_i$  and  $x_j$  are drawn from the input image as it is processed. The four ENVI raster files containing derived bathymetry are then opened in ArcGIS, converted to ESRI Grid files and mosaicked into a single raster grid. The derived bathymetry mosaic is then resampled to a resolution of 5 m and erroneous values from cells over optically deep water are trimmed in preparation for final integration into the CTM.

#### **2.2.4 Dataset Integration**

The CTM mosaic provides terrain data from the 650 m peak of the island to 250 m depth using the IKONOS derived bathymetry to fill the critical shallow water gap between 0-15 m (Appendix A). The integration of the CTM is accomplished using ArcGIS 9.2. Original datasets for the CTM are standardized to the geographic reference of the WGS94, UTM Zone 2 South.

The integration sequence entails merging the derived data from each image into a mosaic, combining the multibeam and derived bathymetry grids, and adding the DEM data. To assure that the most accurate data are retained during the mosaicking process, priority is first given to derived values from images that perform best in the error analysis described below, then to the sonar values so that they replace derived values in areas of overlap and finally to the DEM. After the derived / sonar data integration, a gap fill expression is then applied through a sequence of 46 iterations to completely fill all “NoData” values. Most of the smaller gaps, between swath widths, from terrain shadows and in surf zones, are filled after four iterations of the expression, but large voids remain from extensive areas of cloud cover. The last 42 iterations are required to provide information in these areas and result in far more dubious values; this issue is explored further below. The expression also adds values around the perimeter and into the center of the combined bathymetry grids, which are resolved by trimming the perimeter and by the DEM prioritization, described above.

## **2.3 Results**

The accuracy of both the derived bathymetry and integrated CTM data are assessed at multiple stages of data processing and integration using depth control points collected during field surveys and points features created to extract sonar depth data as controls. The ability of the derived data to detect terrain features, as well as the utility of the integrated CTM for providing seamless terrain across datasets, are evaluated using linear transects that cross both natural features and transition zones between the data sources.

### **2.3.1 Derived Bathymetry Error Analysis**

Control points from both field surveys and sonar data extraction are used for linear regression analyses plotting the control depth (x) against the derived depth (y) to compare the accuracy of derivations from each image (Figure 2.3). The image specific datasets are then combined to extract values from the derived imagery mosaic after resampling (Figure 2.4). The four images needed to cover the extent of Tutuila are referred to as West Tutuila, West-central Tutuila, East-central Tutuila, and East Tutuila and they are presented in this geographic order across the columns of Figure 2.3. The indicators of quality and error in these graphs are the slope of the linear fit to the data and the  $r^2$  value. The plotted control depths represent a “correct” linear relationship with a slope of 1. The further the value of the regression line’s slope is from 0 toward 1, the greater the sensitivity to spectral signal attenuation with depth in the derived bathymetry values. The closer the  $r^2$  value it to 1, the more effective the derived values are at predicting the control values.

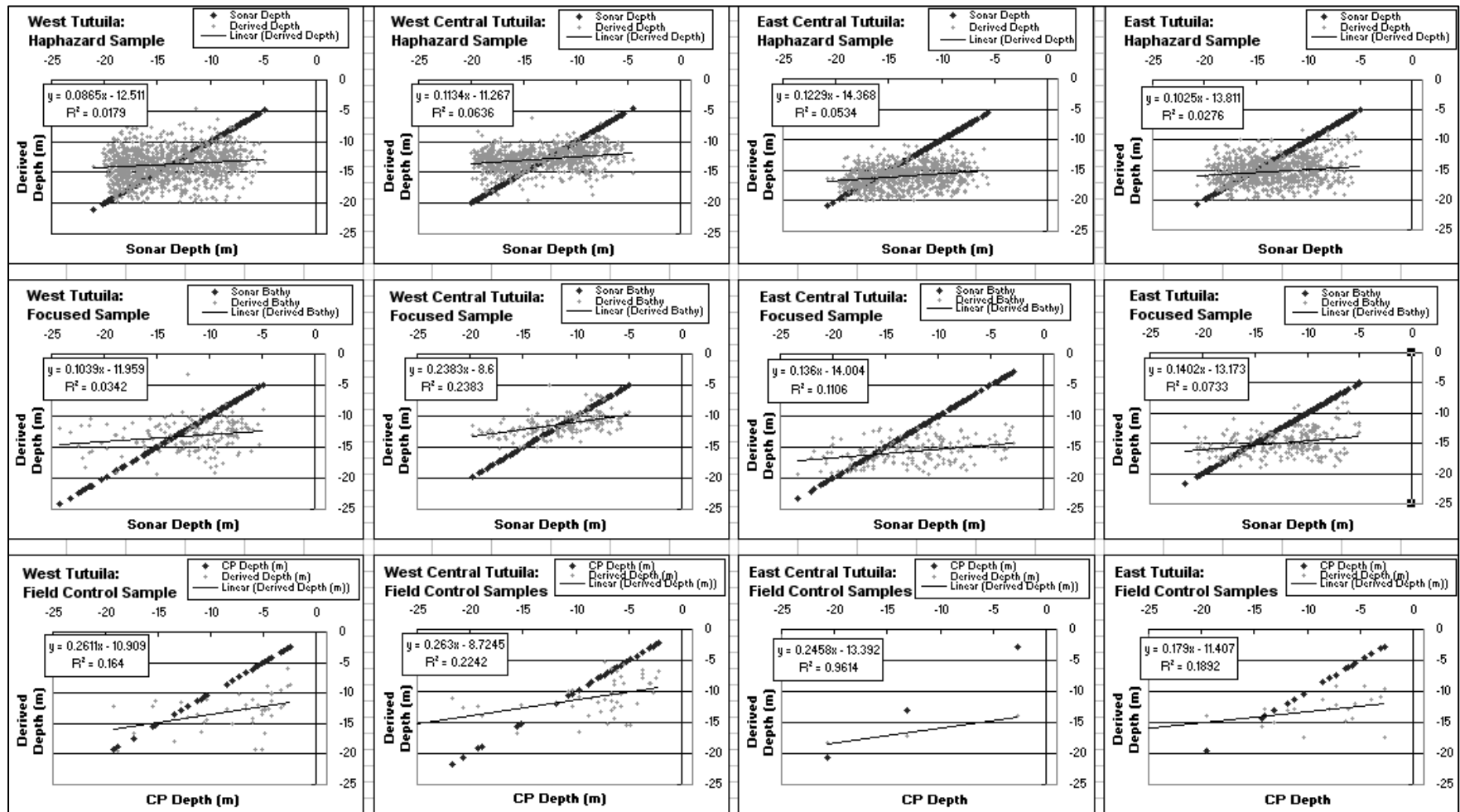


**Figure 2.3:** Derived bathymetry error analysis by linear regression. Notice that each column represents a satellite image and each row represents a point sample type.

Looking to the focused sample data for example, it is clear that the derived bathymetry from West-central image is the best product with a slope of 0.238 and an  $r^2$  value of 0.238, followed by the East-central with a slope of 0.136 and an  $r^2$  value of 0.110, East with a slope of 0.140 and an  $r^2$  value of 0.073, and West Tutuila with a slope of 0.103 and an  $r^2$  value of 0.034. Though the magnitude of these measures varies between the focused, haphazard and control point error analyses, this pattern of data quality is consistent between images. The fact that the most favorable results are exhibited by the control point data set, the most direct measurement of depth at location, has positive implications for the use of these data for terrain modeling. In a more immediate sense this information guided the prioritizing of image values during the mosaic process so that the best results were retained. However, the second best image, East-central, had such extensive data loss due to cloud cover that it made sense to prioritize the data from the third best image, East, in the derived bathymetry data mosaic. The only data available for western portion of the island was that with the most tenuous result.

The progression of derived depth quality across the images is explained by variable atmospheric and sea-state conditions at the time of data acquisition of each of the four images. The images were acquired on three dates over the course of three months and exhibit a range of ocean swell, wind wave (chop), sea spray conditions. More wave action causes a greater range of sea-glint values and frothy waves within a pixel's ground coverage area create erroneous spectral signals that result in less accurate sea glint corrections. Wind-blown sea spray, a particular problem in near shore areas close to breaking waves, increases the non-selective scattering of spectral energy and therefore

increases the error in atmospheric correction for the effected pixels. These errors compound through processing and result in less accurate depth derivations as exemplified by the results in Figure 2.3, where the best results correlate with the best environmental conditions in the original imagery.

The prioritization of datasets during mosaic integration and interpolations during the resampling of the mosaic grid from a 4 m to a 5 m resolution result in new values at many locations in the derived bathymetry mosaic. Therefore, the point features are aggregated and used to extract values from the mosaic for a final quality assessment previous to integration into the greater CTM (Figure 2.4). The same pattern of increasing slope and  $r^2$  values through the haphazard, focused and control point datasets apparent in the image specific analysis is also obvious in the mosaic data error analysis. Though this trend may be attributable to decreasing sample size, it has positive implications for the inclusion of the derived bathymetry in the CTM. The haphazard sample clearly shows the potential error in the derived bathymetry in the depth of the data cloud, but even this “broadest net” sample of derived values shows a weak correlation. The statistical results improved markedly using the data points from the focused sample, but these data are suspect for error analysis since the same points were used to extract the linearized spectral radiance values used in the depth derivation process. Herein lays the particular value of the CRED control point data, which were collected in a haphazard manner as the Oceanography Team completed other deployment duties around Tutuila. Where positions were provided to guide their efforts, they were chosen only on the presumption of shallow depths in the area and the only guiding criteria was that control point depths be less than 15 m. The control point slope value of 0.264 and  $r^2$  value of 0.182 demonstrate a

high degree of correlation between on site depth measurements and derived depth values using unbiased sample locations.

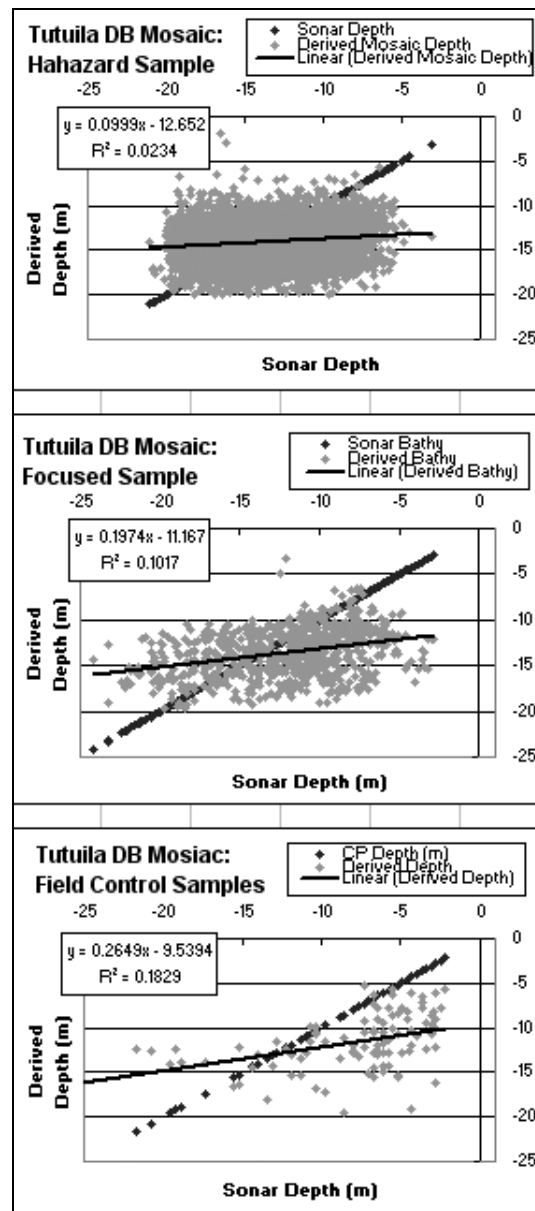


**Figure 2.4:** Error analysis by linear regression performed on integrated derived bathymetry.

### 2.3.2 CTM Error Analysis

With the derived bathymetry integrated into the full CTM mosaic, the CRED control points serve for two final error analyses. Of the original 140 control points, 103 fell within areas of derived bathymetry and have been used in the previous analysis (41 in West, 47 in West-central, 3 in East-central and 21 in East Tutuila – with overlap), 32 fell within areas of estimate depth and 5 fell in areas covered by multibeam sonar. The points within areas of estimated depth are used to assess the values calculated by the ArcGrid moving mean expression in areas void of data, while the full set of 140 points is used to extract values from the CTM for a final analysis of the fully integrated mosaic. Because of this control point spread, the final CTM error analysis can be considered inclusive of all data types with a focus on the derived bathymetry.

Cloud cover in the original IKONOS imagery necessitates that a significant area of the near shore bathymetry is estimated using the mean value of surrounding cells. Multiple iterations of the algorithm are needed to fill the larger gaps with the estimated surface error increasing with distance from the edge of valid data values. Figure 2.5 demonstrates the utility and relative accuracy of the estimated depths with a slope of 1.115 that is actually steeper than that of the control data and a high  $r^2$  of 0.343, however, the large potential error in the data is illustrated by the outliers in the range of 30-35 m of estimated depth and 5-12 m control depth.

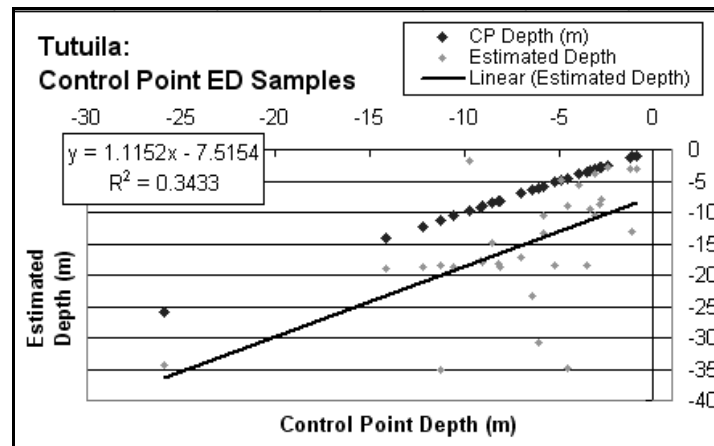


**Figure 2.5:** Error analysis by linear regression performed on estimated bathymetry.

With the derived and estimated bathymetry thus validated, and the DEM and multibeam sonar datasets presumed to be accurate on their own merits, a final error assessment of the integrated CTM is conducted using the 140 CRED control points to extract depth data from the CTM. Regression analyses of these data results in an initial slope of 0.585 and  $r^2$  value of 0.285 which improve to a slope of 0.601 and  $r^2$  value of 0.414 with the removal of 3 outliers (Figure 2.6) signifying a statistically valid representation.

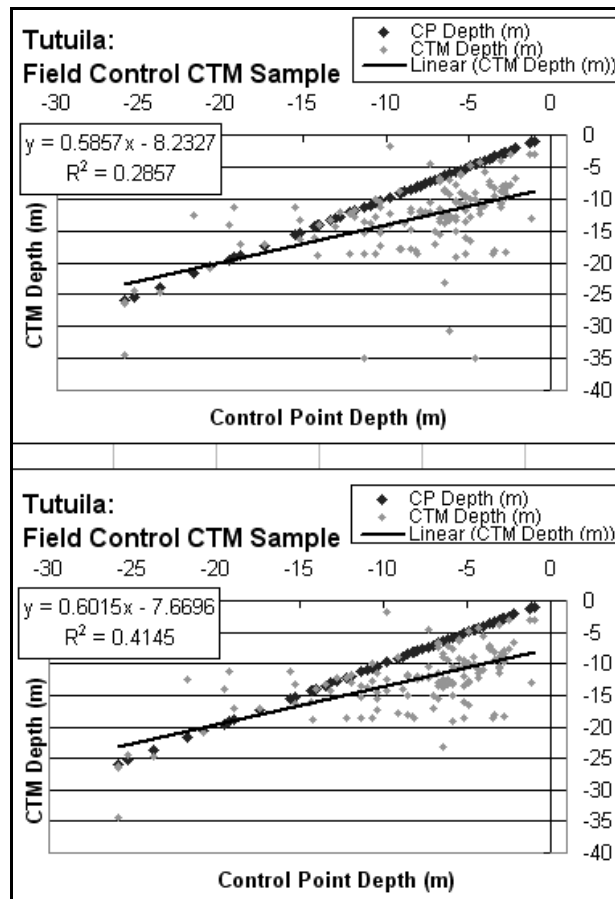


**Figure 2.6:** Error analysis by linear regression performed on complete CTM mosaic.

These final figures conclude the extended error analysis of multiple stages in the process of bathymetric derivation and CTM integration and provide support for the use of bathymetry derived from IKONOS imagery to provide shallow water depth data for coastal terrain modeling. Though the model is not perfect, analyses show that the derived depths represent a realistic measure of depth and that overall error decreased as the datasets are mosaicked into the CTM. Further analyses provide evidence that the derived data's range of error is small enough to provide realistic terrain through the sea-land transition and justifies additional steps to smooth seams between the datasets.

### 2.3.3 Dataset Seams and Morphological Detail

Having assessed the error associated with derivation of depth from spectral data and integration of the derived surface into the CTM, linear transects are used to extract elevation and depth data across the land-sea interface to visualize and quantify the vertical offset at the seams between the DEM, derived bathymetry, and multibeam sonar datasets. The transect profiles are also used to explore the CTM's representation of subtle topographic transitions and detection of specific terrain features. Four transects are created as point features in ArcGIS with a value extracted from each contiguous raster cell over distances of 800 m or 1200 m (Figure 2.7). The extracted data result in terrain profiles with a 5 m horizontal spacing and vertical reliefs of 50 m, 80 m, or 200 m over transitions between the DEM, derived bathymetry (DB), ArcGrid expression estimated bathymetry (EB) and sonar bathymetry (SB) data (Figures 2.8-2.11).

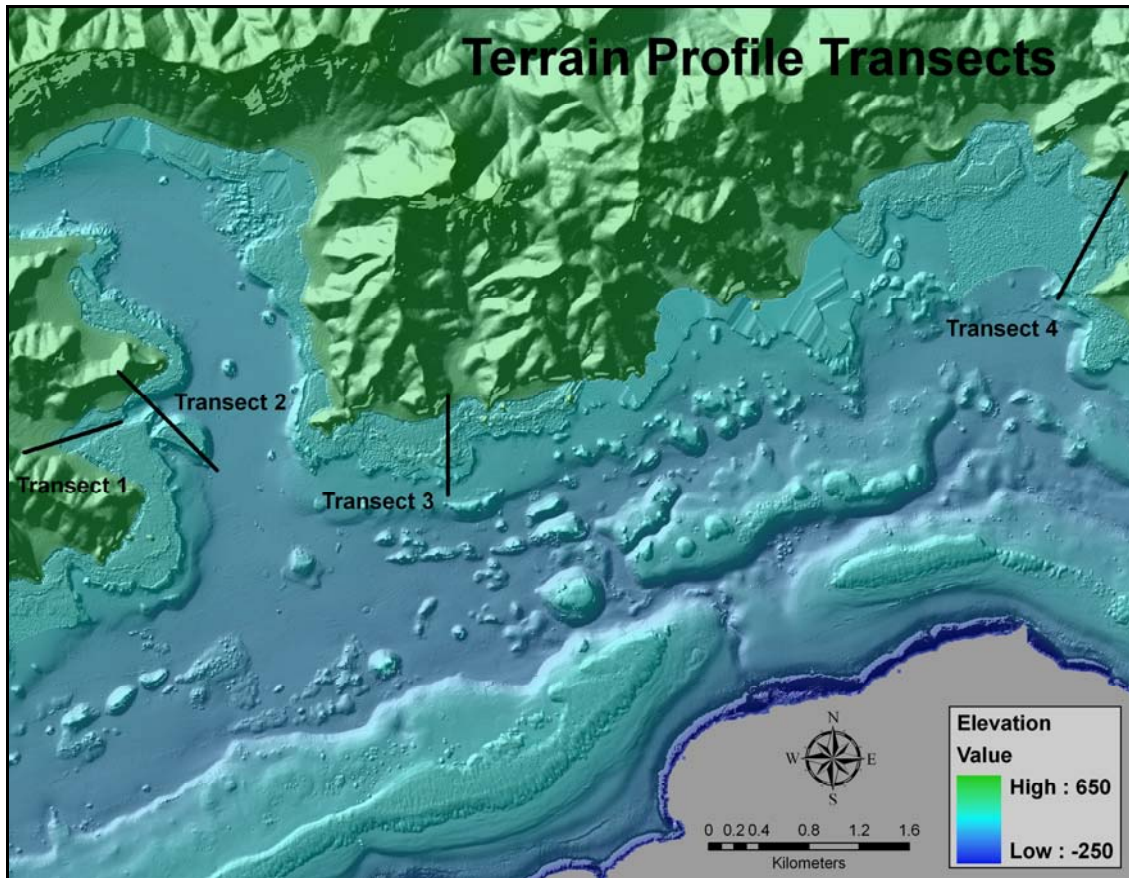


**Figure 2.7:** Tutuila CTM with terrain profile transects.

Transect 1 (Figure 2.8) begins on the floodplain of a small watershed and follows the hollow of the basin into an offshore submarine channel. The “stepping” on the left side of the profile is an artifact inherent on low slopes in data originating as an integer DEM. A vertical offset of 6.7 m is readily apparent at the transition between the DEM and EB. However, no offset exists at the transitions from EB to DB (at a distance of 510 m), which is as should be expected since the ArcGrid expression derived the EB values as the mean of nearby DB values, or from DB to SB (at a distance of 720 m), which simply shows excellent corroboration between the two sources of depth data.

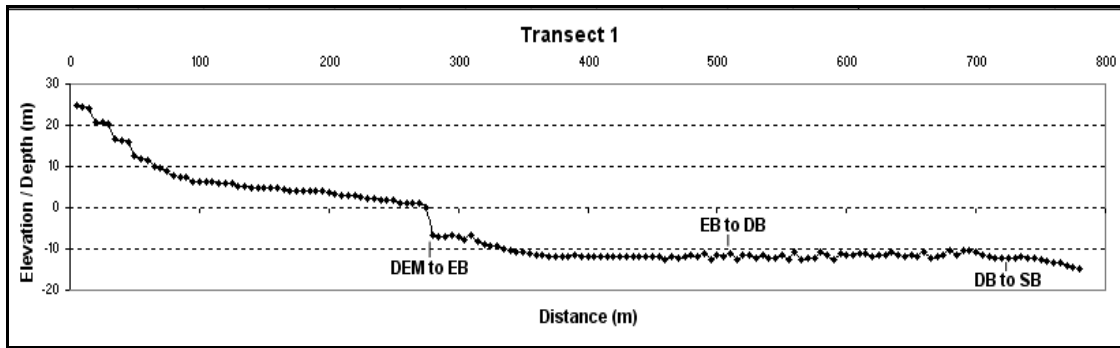


**Figure 2.8:** Terrain profile of Transect 1.

Transect 2 (Figure 2.9) starts at the top of a ridge, descends quickly before crossing a narrow reef flat, proceeds across a channel with two small ridges and then crosses a large coral plateau. At the land-sea transition, the first DB value has a large vertical offset of 19.2 m, but subsequent DB values are much more realistic and provide for good terrain representation across the reef flat to a seam without vertical offset between DB and SB at a distance of 215 m. From this point to a distance of 435 m ridges in the bottom of the channel are clearly indicated by SB data, then there are two transitions from SB to DB and back at 440 m and 665 m with vertical offsets of only 2.5 m and 2.3 m as the transect crosses the coral plateau.

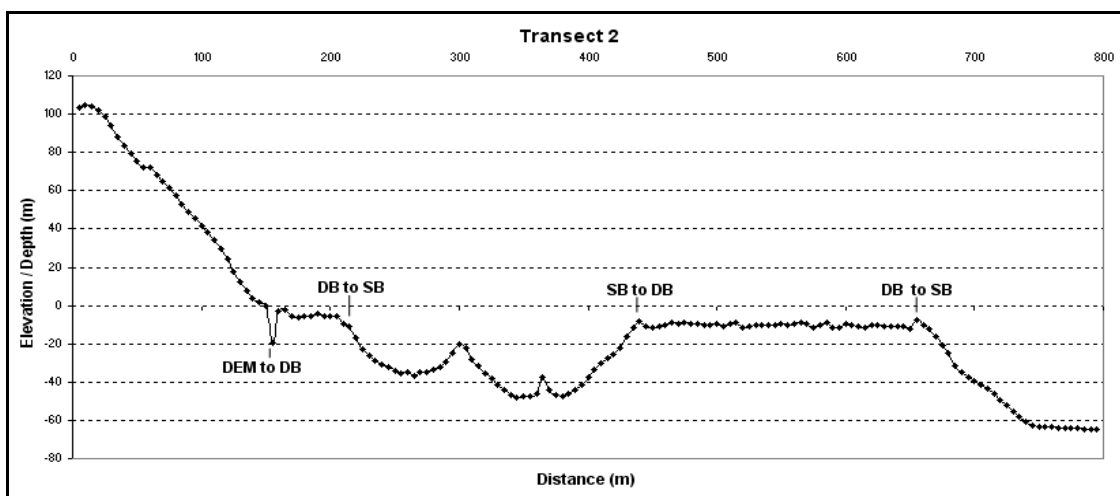


**Figure 2.9:** Terrain profile of Transect 2.

Transect 3 (Figure 2.10) initiates at the base of a ridge crossing a steep grade to the shoreline, proceeds across a broad back reef and reef crest before ending on the fore reef slope. There is a vertical offset of 5.67 m between the DEM and the DB at the land-sea interface. From this transition to a distance of 400 m, the profile exhibits typical back reef terrain with moderate rugosity and variable depth that increases until a sudden decrease at the reef flat, which causes a notable data issue. At a distance of 330 m the DB values began to thin out (in the derived bathymetry mosaic) due to surf conditions and breaking waves on the reef flat, and the depth values become “more estimated” to the right. The other side of this surf zone data gap is at a distance of 675 m in the SB data where the depth values become “more estimated” to the left on the profile. The drastic vertical offset of 19.5 m between distances of 575 m and 590 m is the transition between EB calculated from original DB and SB data during several iterations of the ArcGrid expression run to fill the data gap. The large error at this seam is a result of the EB data failing to capture the real change in depth from the shallows at the edge of the DB values to the deeper reef slope SB values.

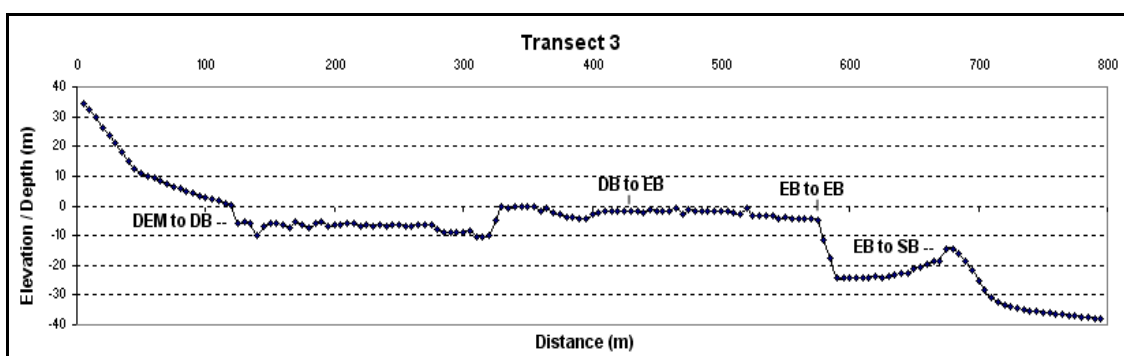


**Figure 2.10:** Terrain profile of Transect 3.

Transect 4 (Figure 2.11) runs from the base of a ridge across a moderately sloped coastal plain to the shoreline, proceeds across a narrow back reef and then continues

along the fore reef while crossing a channel and then finally descends the reef slope. There is a vertical offset of 6.74 m between the DEM and the DB at the land-sea interface. From this point to a distance of 640 m the DB profile again indicates typical back reef / fore reef morphology and closer inspection of the terrain that transect 4 crosses reveals that the DB data provide a high degree of detail allowing for the detection of potholes in the variable terrain of the shallows and the channel in the fore-reef at a distance of about 400 m. One of the limitations of the bathymetric derivation method is evident between the distances of 665 m and 1000 m. The derived depth data bottoms out at the lower range of the derivation procedure's effective limit of around 15 m (in this case) until the transect crosses the tip of a fore reef outcrop that is in range from of 835 m to 875 m distance. The vertical offset of 9.1 m at distance of 1005 m is the transition between this “false floor” artifact and the SB data. This data artifact is also apparent in Figure 7, in the middle of the bay to the west of transect 4, where most of the data in the central bay is false floor with a vertical offset of up to 35 m at the seam. Fortunately for the model, this is the only area around the island with such a large gap between the effective range of the derived bathymetry and the extent of the sonar bathymetry dataset.

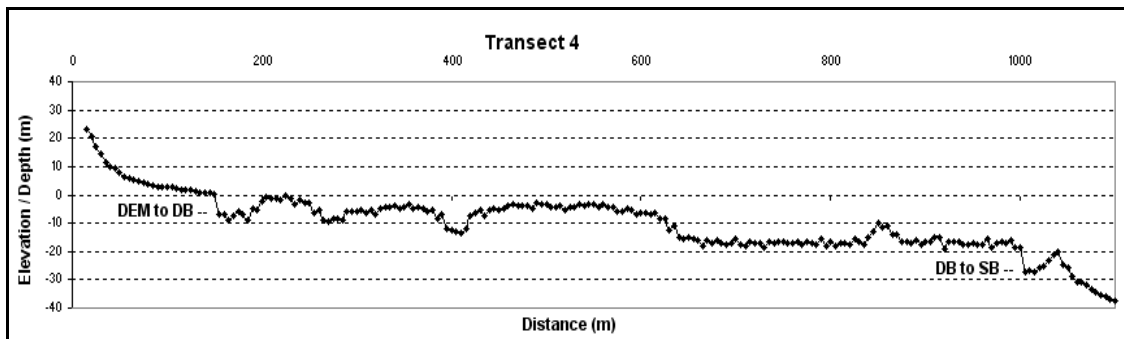


**Figure 2.11:** Terrain profile of Transect 4.

This generation of the Tutuila CTM was integrated with the intent of leaving the artifacts and errors that are inherent in the original data or that result from derived bathymetry processing and CTM integration so they might be scrutinized. The error analyses presented in this section demonstrate that, though the data are not perfect, the derived bathymetry is reasonably correlated to control data and effective at detecting subtle terrain features, thus supporting its integration into the final CTM mosaic. It is further demonstrated by the terrain transect profiles that the combined topo/bathymetric product, though the transition between data sets are not always seamless, is an accurate enough representation of reality to justify its continued refinement and further use in terrain analysis research.

## **2.4 Discussion**

### **2.4.1 Improvement and Repeatability of Derivation Method**

The current iteration of Tutuila CTM provides a foundation for efforts to smooth extreme values at the seams of datasets and explore options to provide better data in areas where clouds, surf or depths beyond the detection floor create a data gap should also be explored. Metadata for the sonar bathymetry indicate that the raw sonar data were cleaned of erroneous “noise” values and then smoothed with a high pass filter previous to conversion to a raster grid. These pre-processing steps remove extreme values and improve the modeled terrain surface and, therefore, should be conducted with the derived bathymetry mosaic, particularly the high pass filter. Further, when the derived depth grid is mosaicked with the sonar bathymetry, the edges of the datasets should be “feathered”, a commonly available processing option, to create a transition zone of averaged values from both datasets to reduce the vertical offset at the seams.

Step by step documentation of processing methods and suggestions concerning the nuances of using ENVI, ArcGIS, Excel and S-Plus to derive bathymetry and create the CTM are provided in a processing “cookbook” should enable similar products at other locations (Appendix B). However, the cookbook does not represent a formal set of instructions as several of the steps require familiarity with GIScience concepts and technology along with the judgment of experience when the “recipe” needs to be adjusted. Creation of a model using the guidance of the cookbook would support the validity of this research and meet a goal of this study in creating repeatable method for creation coastal zone models.

## **2.4.2 Issues with Merging Datasets**

### **2.4.2.1 Data Gaps**

The issues of whether and how to fill areas of “NoData” values in the derived and sonar bathymetry grids remain to be considered. As the IKONOS data are processed, areas of cloud cover and breaking surf are masked out of the imagery as unsuitable spectral data for depth estimation. As the multibeam sonar data are collected, data gaps result in strips where sonar swaths do not overlap and behind sharp terrain features that cause “signal shadow”. Regardless of the cause, these data gaps raise the question of whether they should be left in the data or filled using data interpolation methods. It may be argued that filling these areas with estimated values results in a product of dubious validity because the data is not from the direct sensing of depth in that area. However, a continuous surface should prove superior for terrain and current modeling, so the goal for this research is the creation and testing of such a surface.

To this end, an ArcGrid command line expression is used to apply a moving average algorithm that assigns the mean value from a 6x6 window to “NoData” cells without changing original data values. The estimated surface could be further improved by using control points and other data to “seed” the large data gaps with depth measurements to provide accurate input for the ArcGrid algorithm as it calculates depth. This measure will not only create more site-specific precision, but will also result in less extreme vertical offsets for the feathering function to address at dataset seams. Of course, new satellite imagery without clouds in the same locations would be the best solution for filling the cloud gaps, but this analysis seeks solutions with the given materials.

#### **2.4.2.2 Vertical Datum Issue**

A matter concerning the accurate integration of bathymetric and topographic datasets remains in the form of the vertical datum issue. Having assured two of three primary components of a common geospatial framework with the same coordinate system and horizontal datum, the more intractable problem of converting to a common vertical datum is circumvented, but not actually resolved. Vertical data may be tidal, based on regional tidal measurement, orthographic, derived from gravity potential, or geodetic, created using space based systems. Bathymetric data are usually referenced to a tidal datum such as mean lower low water (MLLW) while topographic data are usually based off an orthographic datum such as the National Geodetic Vertical Datum of 1929 (NGVD29), which is the specific case with the Tutuila DEM and multibeam sonar bathymetry. The Tampa Bay (Florida) Topobathy Project has developed tools that provide for conversions between 28 commonly used vertical data using a numerical hydrodynamic circulation models and spatial interpolations of tide level between gauge

stations. The conversion to a common vertical datum avoids data conflicts at the sea/land interface, however, to date this tool is only available for limited regions of the continental US and not available for American Samoa (Gesch and Wilson 2001, <http://chartmaker.ncd.noaa.gov/bathytopo/>).

While seeking a permanent solution for the conversion of the Tutuila data to a common vertical datum, the CTM integration is allowed to progress due to the nature of the datasets. The DEM and the deepwater bathymetric data do not overlap so that there is no specific data conflict at the sea-land interface, a common problem associated with the vertical datum issue. The error introduced by the vertical datum issue is also manageable. Though not applicable to Tutuila, the datum conversion tool indicates a vertical offset between NGVD29 and MLLW at Tampa Bay (28° N latitude) of only 0.326 m. Given that Tutuila (14° S latitude) is about half as far from the equator, with less tidal flux, it may be presumed that the vertical offset at this position would be even less, further, the island's steep topography allows for little horizontal displacement of shoreline position even at a real tidal flux in the 1 m range. It is also relevant to note that the derived bathymetry is not vertically referenced at all, though a tide correction for the specific time the image was recorded might be considered. However, the error at the shallow and deep end of derivation method's range is greater than either this potential tidal correction of 0-.5 m or that of the vertical datum offset.

To solve the problem of establishing sea-level, which would still need to be addressed with the grids converted to the same vertical datum since neither dataset actually crosses the sea-land interface, a ring of raster cells is added to the DEM with a value of 0.000001. This is accomplished by adding a ring of new raster values one to

three cells thick around the DEM perimeter, reclassifying the entire new raster to the value 0.000001 (chosen since the value zero is involved several processing steps and can be problematic), and mosaicking it back to the original DEM. The result is a ring of sea level values that separate land and sea once the adjusted DEM is mosaicked to the previously integrated derived and sonar bathymetry grid.

### **2.4.3 Continuing Research**

When a freshwater plume enters the ocean from its watershed, dispersal is affected by seafloor bathymetric interactions with shallow and deep currents determining the distribution of the plume's payload across the reef. Pathogens, nutrient loading and high turbidity in the plumes are presumed to have a detrimental effect on reef health. The negative effects of these factors can be measured as a function of the diversity and distribution of coral, algae, invertebrate and reef fish species (Salas et al. 2006, Mumby 2001). Differences in human settlement, population density and land use patterns may lead to variable stream sediment load, nitrification or pathogen levels in Tutuila's watersheds and have a corresponding effect on the species composition and diversity of coral and fish populations of adjacent reefs.

Topographically-defined units over the sea-land interface should enable analyses of material and energy exchange that will help to identify the impact of terrestrial inputs to near shore marine environments. In terrestrial studies, hydrologic units are defined through the assessment of slope, aspect and ridgeline location and enable the analysis of groundwater and surface runoff as a function of variable rainfall levels (Clarke and Burnett 2003, Miller et al. 2007). The expansion of this concept using the CTM to define island terrain in terms of marine-terrestrial units (MTU) that span the land-sea interface

should enable quantitative scientific information correlating land use and development practices to the vitality of reef communities as measured by coral and fish species composition and diversity. This effort will contribute to island scale comparison conducted in the Caribbean by (Sealy 2004), which found a correlation between population density and decreased reef species diversity, by refining its geographic focus. Such scientifically valid information may enable managers and community leaders to make informed decisions regarding the stewardship of the island's terrestrial and marine resources (White et al. 2006, Hoffmann 2002b). This level of analysis will be undertaken as the next phase of the primary author's research.

Further applications enabled by the classification of Tutuila's terrain into MTU's might include advanced investigations into the dispersal of inputs from specific watersheds into their affiliated marine catchments and allow for comparisons between MTU's. The greater CTM could then enable the analysis of topographic effects on terrestrial freshwater flows as well as surface and deep-sea currents to model the systemic dispersal of terrestrial plume loads.

## **2.5 Conclusion**

Coral reefs are in decline across the globe and scientific literature increasingly points to anthropogenic factors, many of them with terrestrial origins, as primary drivers behind the degradation. Coastal terrain models that enable the modeling of material and energy exchange across the land-sea interface are effective analytical tools to study the interconnectivity of terrestrial and marine systems. Multiple publications since 1978 establish the efficacy of deriving bathymetry from spectral data, recent research indicates the most accurate of several proposed methods and analyses of the Tutuila CTM product

prove that it is a truthful representation of reality. Though steps to improve the CTM during mosaic compilation are proposed, the current CTM is deemed of sufficient quality to be used in terrain studies employing the concept of marine/terrestrial units.

Marine/terrestrial units will be used to compare human development and the vitality of coral reefs within the same topographical regions. Correlations would indicate that terrain restrains material flows between the land and sea while defining the impact of terrestrial inputs to the system. Specific results may be used to determine the impact of differing land use practices and population levels on adjacent coral reefs. This scientifically defensible information could then enable informed decision making by local community leaders and resource managers.

### **Acknowledgments**

Sincere thanks to NOAA's Pacific Islands Benthic Habitat Mapping Center for providing the multibeam sonar bathymetry. Thanks also to NOAA's Pacific Island Fisheries Science Center, Coral Reef Ecosystem Division, whose oceanography team collected field control points during a busy deployment schedule on the 2008 American Samoa Research and Management Program research cruise aboard the NOAA R/V *Hi'ialakai*. These data proved essential to product analysis. Finally, thanks to the Biogeography Group of NOAA's Center for Coastal Monitoring and Assessment, and NOAA's Coastal Services Center for providing the at-sensor IKONOS imagery needed for deriving bathymetry.

## References

- Andrefouet, S., P. J. Mumby, M. McField, C. Hu, and F. E. Muller-Karger. 2002. Revisiting coral reef connectivity. *Coral Reefs* 21 (1):43-48.
- Chavez, P. S. (1988) An improved dark-object subtraction technique for atmospheric scattering correction of multispectral data. *Remote Sensing of Environment*, 24, 459-479.
- Clarke, S. and K. Burnett. 2003. Comparison of digital elevation models for aquatic data development. *Photogrammetric Engineering and Remote Sensing* 69: 1367-1375.
- Gesch, D. and R. Wilson. 2001. Development of a Seamless Multisource Topographic / Bathymetric Elevation Model for Tampa Bay. *Marine Technology Society Journal* 35: 58-64.
- Hedley, J. D., A. R. Harborne, and P. J. Mumby. 2005. Simple and robust removal of sun glint for mapping shallow-water benthos. *International Journal of Remote Sensing* 26 (10):2107-2112.
- Hochberg, E. J., S. Andrefouet, and M. R. Tyler. 2003. Sea surface correction of high spatial resolution IKONOS images to improve bottom mapping in near-shore environments. *IEEE Transactions on Geoscience and Remote Sensing* 41 (7):1724-1729.
- Hochberg, E.J., S. Vogt, J.E. Miller and K.R. Hogrefe. 2007. Remote sensing of shallow water bathymetry for integration with multibeam SONAR data. *Pacific Region Integrated Data Enterprise principle investigators conference*, Honolulu, HI, Poster. Available from: [http://apdrc.soest.hawaii.edu/PRIDE/pride\\_meetings.html](http://apdrc.soest.hawaii.edu/PRIDE/pride_meetings.html). (Accessed 7 March 2008)
- Hoffmann, T. C. 2002. The reimplementation of the Ra'ui: Coral reef management in Rarotonga, Cook Islands. *Coastal Management* 30 (4):401-418.
- Hogrefe, K.H. 2008. Digital image processing “cookbook”: a method to derive bathymetric data from high spatial resolution multispectral imagery. Corvallis, Oregon State University. Available from: <http://oregonstate.edu/~hogrefek/Cookbook/>. (Accessed 10 March 2008)
- Jiang, Y. W., O. W. H. Wai, H. S. Hong and Y. S. Li. 2004. A geographical information system for marine management and its application to Xiamen Bay, China. *Journal of Coastal Research*. 254-264.
- Li R., J. Liu and Y. Felus. 2001. Spatial modeling and analysis for shoreline change detection and coastal erosion monitoring. *Marine Geodesy*. 24:1-12.
- Lyzenga, D. R. 1985. Shallow-water bathymetry using combined LIDAR and passive multispectral scanner data. *International Journal of Remote Sensing* 6 (1):115-125.
- Miller S.N., D.J. Semmens, D.C. Goodrich, M. Hernandez, R.C. Miller, W.G. Kepner and D.P. Guertin. 2007. The automated geospatial watershed assessment tool. *Environmental Modeling and Software*. 22:365-377.
- Mumby, P. J. 2001. Beta and habitat diversity in marine systems: a new approach to measurement, scaling and interpretation. *Oecologia* 128 (2):274-280.

- Mumby, P. J., E. P. Green, A. J. Edwards, and C. D. Clark. 1999. The cost-effectiveness of remote sensing for tropical coastal resources assessment and management. *Journal of Environmental Management* 55 (3):157-166.
- Mumby, P. J., W. Skirving, A. E. Strong, J. T. Hardy, E. F. LeDrew, E. J. Hochberg, R. P. Stumpf, and L. T. David. 2004. Remote sensing of coral reefs and their physical environment. *Marine Pollution Bulletin* 48 (3-4):219-228.
- Salas F., C. Marcos, J.M. Neto, J. Patricio, A. Perez-Ruzafa and J.C. Marques. 2006. User-friendly guide for using benthic ecological indicators in coastal and marine quality assessment. *Ocean and Coastal Management*. 49:308-331.
- Sealey, K. S. 2004. Large-scale ecological impacts of development on tropical islands systems: comparison of developed and undeveloped islands in the central Bahamas. *Bulletin of Marine Science* 75 (2):295-320.
- Shapiro, A. C., and S. O. Rohmann. 2005. Summit-to-sea mapping and change detection using satellite imagery: tools for conservation and management of coral reefs. *Revista De Biologia Tropical* 53:185-193.
- Stumpf, R. P., K. Holderied, and M. Sinclair. 2003. Determination of water depth with high-resolution satellite imagery over variable bottom types. *Limnology and Oceanography* 48 (1):547-556.
- White, A., E. Deguit, W. Jatulan, and L. Eisma-Osorio. 2006. Integrated coastal management in Philippine local governance: Evolution and benefits. *Coastal Management* 34 (3):287-302.
- Wright, D. 2002. Mapping and GIS capacity building in American Samoa. *Proceedings of the 22nd Annual ESRI User Conference*. San Diego, CA, Paper 101.

**Chapter 3. Human Population Density and Coral Reef Diversity: A Topographic Analysis**

Kyle R. Hogrefe and Dawn J. Wright

Not yet submitted for publication.

**Abstract**

Coral reefs are under stress across the globe and research indicates that increased loads of sediment, nutrients and pollutants in freshwater inputs are a major contributing factor. One investigation establishes a correlation between increased human population density and a reduction in percent coral cover along with changes to coral species diversity at the island scale. In this study, a recently completed coastal terrain model (CTM) is used to conduct a finer scale investigation into this phenomenon with a focus on the island of Tutuila, American Samoa. Terrain analyses using the CTM identify topographic units using drainage patterns that span the transition from land to sea. These marine/terrestrial units (MTUs) associate the marine environment around the island with terrestrial drainages most likely to influence local reef ecology. Population density is compared with percent coral cover, coral colony density and coral genera diversity within each MTU. A significant drop in each criterion between survey years and strong correlations between population density and this decline indicate a general decline in reef conditions around the island with intensified land use as a potential driver.

### 3.1 Introduction

Coral reefs are under pressure from human activities across the globe with one of the major factors being sediment, nutrient and pathogen loaded terrestrial inputs (Mumby et al. 2004, Abelson et al. 2005, Duke et al. 2005). Island ecosystems are comprised of both marine and terrestrial components that are linked by fresh water inputs originating miles inland and reaching over 100 miles out to sea. These plumes provide the benefits of nutrient exchange and larval transport but also increasingly carry nutrient loaded sediment and pollutants that diminish the species diversity of coral reef community structure (Andrefouet et al. 2002, Shapiro and Rohmann 2005). Island-scale analyses of human population and the health of adjacent coral reefs reveals that increased turbidity levels associated with greater development density change the species composition and reduce the species diversity of coral reefs (Sealey 2004).

Coastal terrain models (defined as terrain models incorporating both topography and bathymetry) have proven to be powerful analytical tools for the geomorphic modeling of watersheds and coastal morphology (Li et al. 2001). The data for their creation are easily accessible (Shapiro and Rohmann 2005, Clarke and Burnett 2003, Li et al. 2001), and proper documentation of methodology allows for the tracking of uncertainty so that model data output is quantitatively defensible (Gahegan and Ehlers 2000). Satellite and acoustic remote sensing technologies have enabled the collection of data to produce detailed coastal terrain models that include benthic habitat classification, ground cover characteristics and terrain detailed enough to run oceanographic, hydrographic and atmospheric simulations (Mumby et al. 2004, Shapiro and Rohmann 2005). Such models must be geographically grounded by a geographic information

system (GIS) for the integration and analysis of topographic, environmental and societal datasets to enable investigations into the relationship and interactions of island ecosystems (Miller et al. 2007, Jiang et al. 2004).

This study uses a recently created CTM of the island of Tutuila, American Samoa to compare human population density with coral species diversity and percent coral cover (Hogrefe et al., submitted). Previous research conducted on 12 islands in the central Bahamas has established the validity of such a comparison for assessing the impact of variable population levels to coral reefs (Sealey 2004). Terrain analyses of the Tutuila CTM allow for a refined assessment by analyzing drainage patterns to divide the island into marine/terrestrial units (MTU) that span the land-sea interface. Such an approach allows for the focused comparison of the health of reefs in a particular area with the terrestrial activities that are most likely to affect them.

## **3.2 Methods**

### **3.2.1 Study Area**

Tutuila (Figure 3.1) is ideal for a case study of human driven terrestrial impacts. Its volcanic origin and the tropical climate of the South Seas have resulted in topography of well-defined ridgelines and valleys that extend beyond the shoreline to significant depth. These distinct marine/terrestrial units provide naturally defined topographic basins for comparing land use impacts to adjacent reefs. The population pattern of the island consists of valleys that contain human settlements ranging from cities such as Pago Pago (population ~ 4000) to small villages of populations less than 100, with some small valleys remaining uninhabited (Craig et al. 2000). Though most of the settlement is concentrated on relatively flat coastal terrain, population pressure pushes development up

steeper valley slopes and traditional land use, such as small plot agriculture and the harvest of fruit and wood, occurs farther up in the valleys. Pago Pago Harbor supports industrial activities such as a fish cannery and port services to support an extensive fishing fleet and international commerce. Densely-populated areas spreading to the southwest of Pago Pago Harbor along the coast cross through several watersheds, support a large percentage of the island's population and have many impervious surfaces that probably enhance runoff and contribute to pollutant loads (Craig et al. 2000).

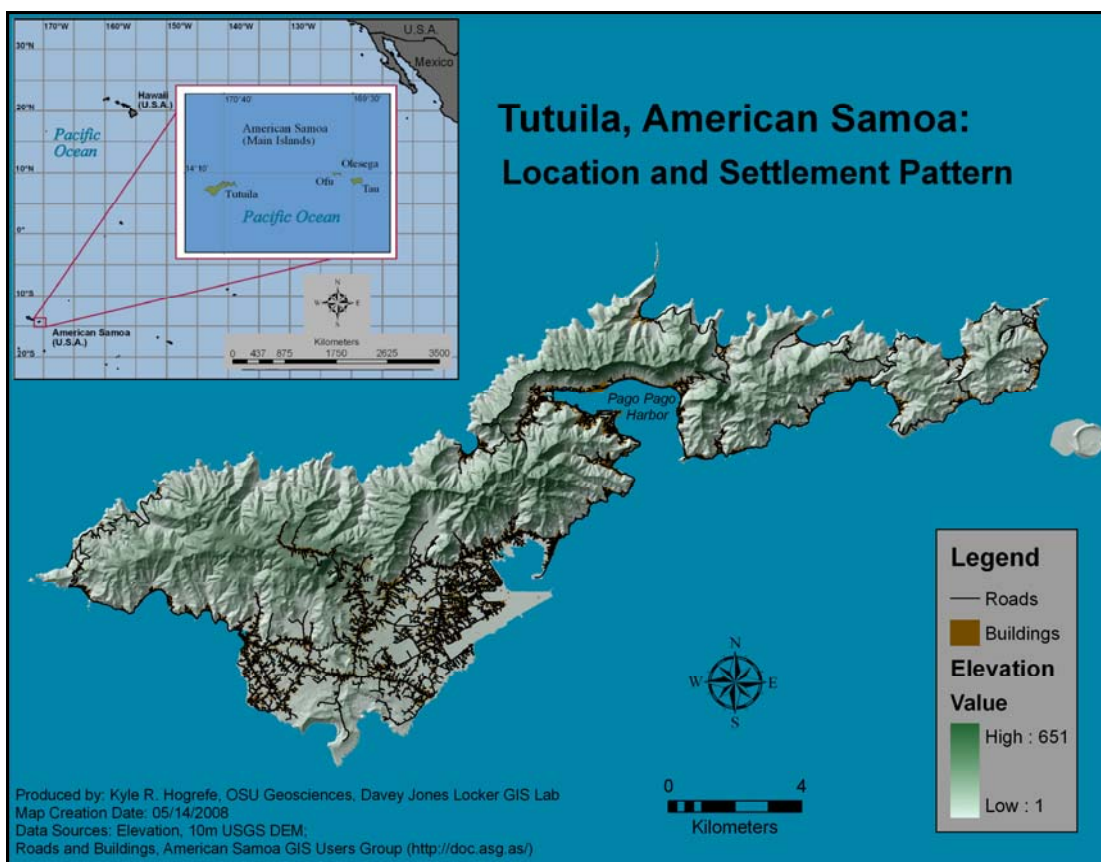


**Figure 3.1:** Location map of Tutuila, American Samoa. American Samoa is a United States Territory that includes 5 volcanic islands and 2 coral atolls, Tutuila is the main Island. Geographically, it is part of the Samoan archipelago. Note how the island's terrain determines settlement pattern as expressed by the distribution of roads and buildings.

Personal experience with community leaders, resource managers and the general population on Tutuila, as well as recent research (e.g., Wright 2002), indicate a strong desire to take action to protect marine resources. However, the mitigation of pollutants in terrestrial runoff is problematic because it requires changing social practices, which further requires either extensive outreach and education or passage of regulations to modify people's actions. These solutions demand scientific information to justify the necessity of change and the implementation of new policies that should accommodate local concerns and traditional knowledge (Mumby et al. 1999, Hoffmann 2002a, Hoffmann 2002b).

### **3.2.2 Data**

#### **3.2.2.1 Tutuila Coastal Terrain Model**

The Tutuila CTM integrates data from three different sources to provide a seamless topographic surface from 651 m elevation to 250 m depth (Hogrefe et al. submitted). Terrestrial data originated as a 10 m resolution DEM, seafloor bathymetry for depths ranging from 15 m to 250 m were processed from multibeam sonar data, while near-shore bathymetry from 0 m to 15 m were derived from high spatial resolution satellite imagery. The three datasets were converted to a common geographic reference and spatial resolution and combined to create the CTM. Regression analyses were performed at multiple points during depth derivation and dataset integration to assess the error associated with interim results as well as the final product. Terrain profiles were used to assess the model's representation of terrain and offsets that may exist at the seams between the datasets. The model proved statistically accurate and was determined to be a

realistic representation of Tutuila's topography through all datasets (Hogrefe et al. submitted).

### 3.2.2.2 Population Density Data

Population density for each MTU was derived from year 2000 United States Census Bureau data downloaded from the American Samoa GIS Users Group website (<http://doc.asg.as/>) (Table 3.1). After MTU definition (below), data from all census tracts within a unit were combined to calculate its total population and land area. Total population was divided by total land area to determine population density within each MTU (Appendix C, Table 1). In most cases of a census tract falling within multiple MTU the percentage of the tract that fell within each unit determined the population and area that is was assigned. In other cases the population distribution indicated in Figure 3.1 and backed by field experience was used to apportion the data. (Appendix C, Table 2).

**Table 3.1:** MTU Population Density.

<b>MTU</b>	<b>AREA (km<sup>2</sup>)</b>	<b>2000 Population</b>	<b>2000 Population Density (People/km<sup>2</sup>)</b>
<b>1</b>	28.1991	8042	285
<b>2</b>	15.1551	1162	77
<b>3</b>	7.7480	1178	152
<b>4</b>	21.5051	3730	173
<b>5</b>	48.4437	29275	604
<b>6</b>	10.6253	10395	978
<b>7</b>	2.4469	693	283
<b>8</b>	0.6941	0	0

### 3.2.2.3 Coral Reef Health Criteria

The data used as criteria to gauge the vitality of reefs around Tutuila were collected by NOAA Fisheries' Pacific Island Fisheries Science Center, Coral Reef Ecosystem Division (CRED) as part of the Pacific Reef Assessment and Management Program. One of the many methods used by CRED to collect data for monitoring the status of coral reefs and associated organisms is their rapid ecological assessment (REA) surveys. These surveys are conducted by teams of 1-3 scientists using SCUBA gear with each team focusing on a different component of the reef biota and provide for data with a high degree of taxonomic resolution of coral, algae, macroinvertebrate, and reef fish communities (Brainard et al. in review). REA sites are evenly distributed around Tutuila.

This analysis will focus on three types of data collected by the coral team in their 2004 and 2006 surveys: percent live coral cover, coral colony density and generic diversity (Figures 3.2 and 3.3). Percent live coral cover was determined by visual estimate in 2004 and by line point surveys in 2006. Visual estimates were qualitative assessment of live cover made by the coral diver as data points associated with each belt line transect. They were a subjective estimate made through visual inspection of the transect area. To conduct the line point intercept surveys, a coral biologist swam along two 25 m transect lines (actual cords deployed across the reef) at each REA site. All benthic elements occurring directly beneath the line at a 50 cm interval were recorded to the lowest feasible taxonomic level. These raw data were later used to determine live coral cover. Coral colony density and generic diversity were ascertained using the belt line transect method in both survey years. Belt line transects were conducted by a second coral diver swimming along the 25 m line and recording the genus and maximum

diameter of each coral colony. Only colonies falling within 0.5 m to 1 m of the line, dependant on the density perceived by the diver at the start of the survey, were recorded resulting in 1 m or 2 m “belts” along the transect. From these data, coral colony density was computed as colonies per m<sup>2</sup> while generic diversity was determined by a total count of all coral genera at each REA site (Brainard et al. in review).

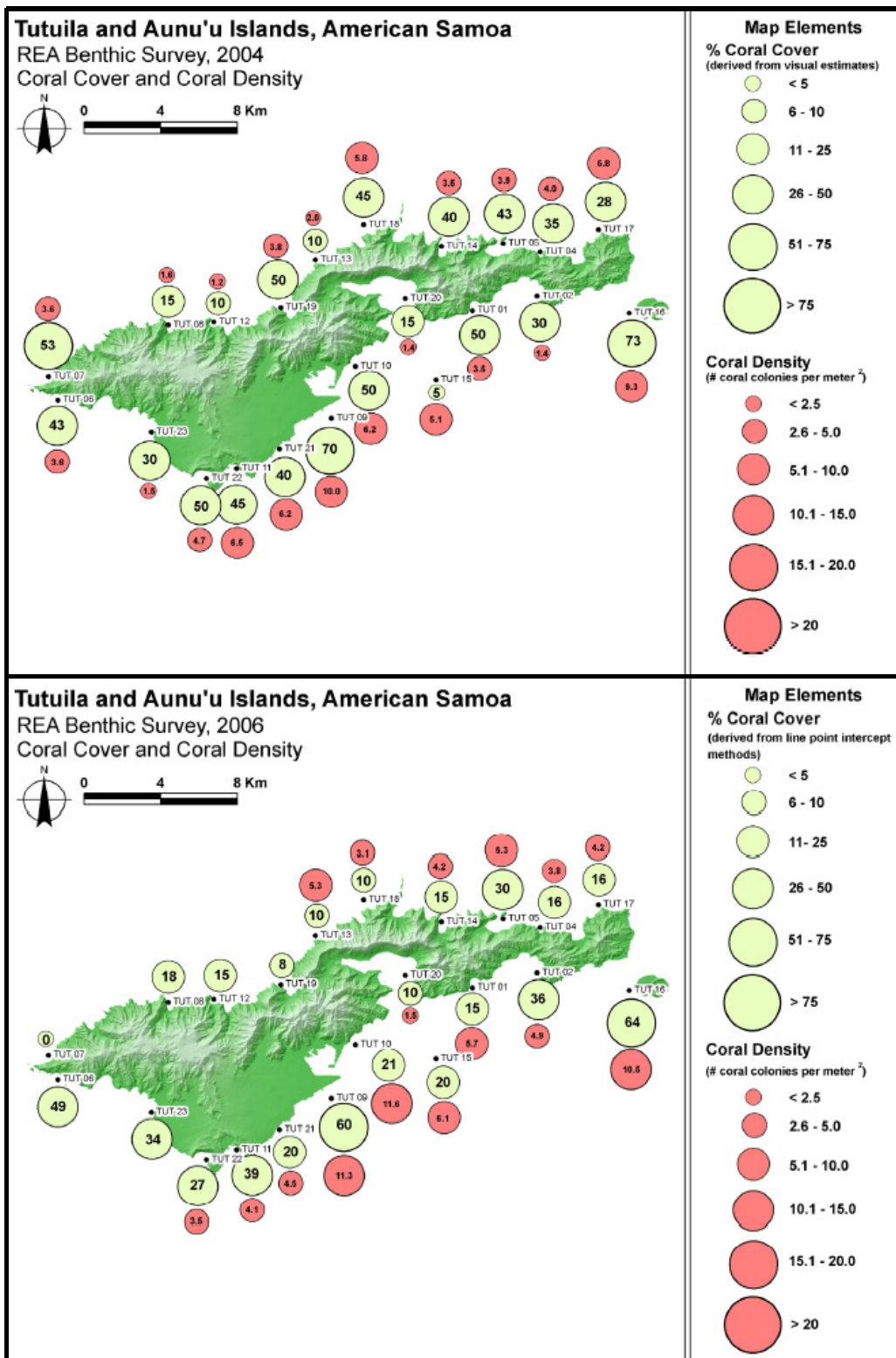


**Figure 3.2:** 2004 and 2006 REA locations with coral cover and coral density (Source: Brainard et al. in review).

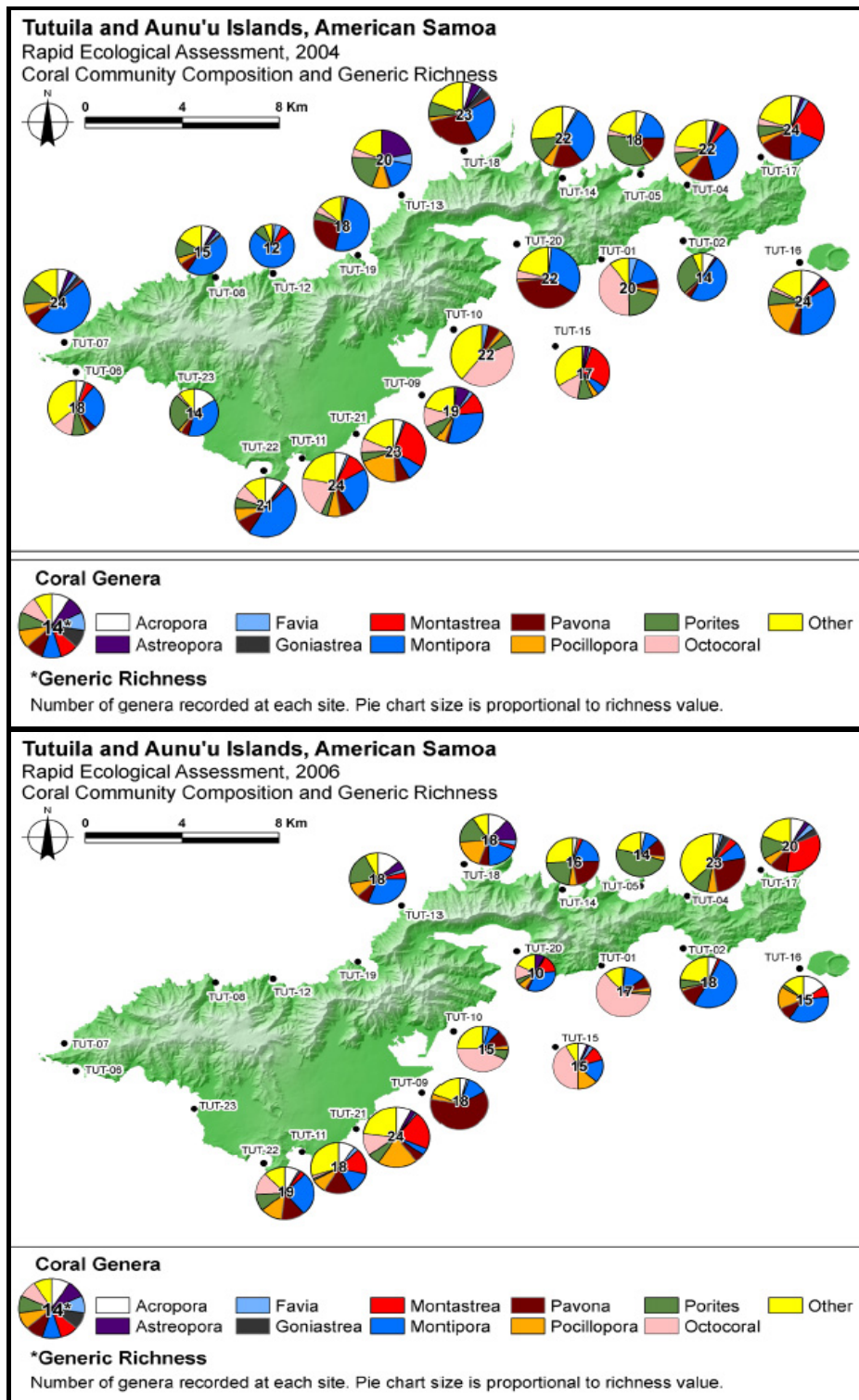


Figure 3.3: 2004 and 2006 REA locations with generic diversity and coral community composition (Source: Brainard et al. in review).

For this analysis, data from all REA sites that fell within an MTU were combined to create composite figures for all three indices by reworking the 2004/2006 REA spreadsheet provided by CRED (Appendix D). Live coral cover, colony density and generic diversity were all averaged to provide a mean value for each MTU. In an attempt to capture the full diversity of coral communities around the island, total generic diversity was also determined for each MTU (Table 3.2). Percent change was calculated for each criterion by subtracting 2006 values from 2004 values, dividing the difference by the original 2006 figure, multiplying by 100 and finally multiplying by -1 so that the output reflected the negative change between years (Table 3.3). As a final metric to quantify observed relationships in the data, correlation co-efficients were calculated for population density and each of these criteria using the formula:  $\text{Correlation}(r) = \frac{N\Sigma XY - (\Sigma X)(\Sigma Y)}{\text{Sqrt}([N\Sigma X^2 - (\Sigma X)^2][N\Sigma Y^2 - (\Sigma Y)^2])}$  (Appendix E).

**Table 3.2:** 2004 and 2006 REA Data Summary by MTU

<b>MTU</b>	<b>Average % Coral Cover</b>	<b>Average Coral Density (colonies/m<sup>2</sup>)</b>	<b>Average Generic Richness</b>	<b>Total Generic Richness</b>
<b>2004</b>				
<b>1</b>	42	5.9	19.3	29
<b>2</b>	13	2.7	13	17
<b>3</b>	35	7.7	20.7	30
<b>4</b>	37	8.7	21.5	28
<b>5</b>	37	14.2	23	37
<b>6</b>	55	30.8	24	28
<b>7</b>	45	21.1	26	26
<b>8</b>	50	16.5	24	24
<b>2006</b>				
<b>1</b>	28	N/A	N/A	N/A
<b>2</b>	16	N/A	N/A	N/A
<b>3</b>	9	4.2	15.5	17
<b>4</b>	19	4.7	16.8	24
<b>5</b>	28	6.6	14.3	27
<b>6</b>	40	10.1	19	25
<b>7</b>	39	8.2	19	19
<b>8</b>	27	7	19	19

**Table 3.3:** Percent Change in REA Data between 2004 and 2006 per MTU

<b>MTU</b>	<b>Average % Coral Cover</b>	<b>Average Coral Density (colonies/m<sup>2</sup>)</b>	<b>Average Generic Richness</b>	<b>Total Generic Richness</b>
<b>1</b>	-33	N/A	N/A	N/A
<b>2</b>	23	N/A	N/A	N/A
<b>3</b>	-74	-45	-25	-43
<b>4</b>	-49	-46	-22	-14
<b>5</b>	-24	-54	-38	-27
<b>6</b>	-27	-67	-21	-11
<b>7</b>	-13	-61	-27	-27
<b>8</b>	-46	-58	-21	-21

### 3.2.3 Identification of Marine Terrestrial Units

The concept of using MTU to affiliate near shore marine environments with the terrestrial areas most likely to affect them through freshwater sediment, nutrient and pathogen loads was untried prior to this research. Such an investigation was enabled by the seamless transition between terrestrial topography and seafloor bathymetry provided by the Tutuila CTM. The terrain analyses required to determine the MTU was facilitated by the Arc Hydro data model and associated data processing tools (Maidment 2002). Arc Hydro was developed by a consortium established by the Center for Research in Water Resources of the University of Texas at Austin and the Environmental Systems Research Institute. The use of the Arc Hydro data model and the user defined parameters set while employing specific processing functions during the MTU terrain analyses are detailed in Appendix F.

The Tutuila CTM was input as the original digital elevation model (DEM) required by the data model and taken through multiple processing steps for watershed delineation. The processing steps relied on the elevation data from the DEM to determine flow direction and then assigned each raster cell an accumulation value based on how many other cells contributed to it. Stream definition parameters were then set to identify cells with an accumulation value of 2500 as “streams” running through both the land and seafloor terrain. These stream locations were used to identify minor catchments that would contribute to their flow and then to determine drainage pattern for the entirety of the terrain in the CTM. Finally, the drainage lines were used to detect all minor catchments affiliated by the drainage pattern and combine them into adjoining catchments or watersheds. Because the terrain in this analysis included both land and sea

components, the pertinent adjoining catchments were termed “marine terrestrial units” (Figure 3.4).

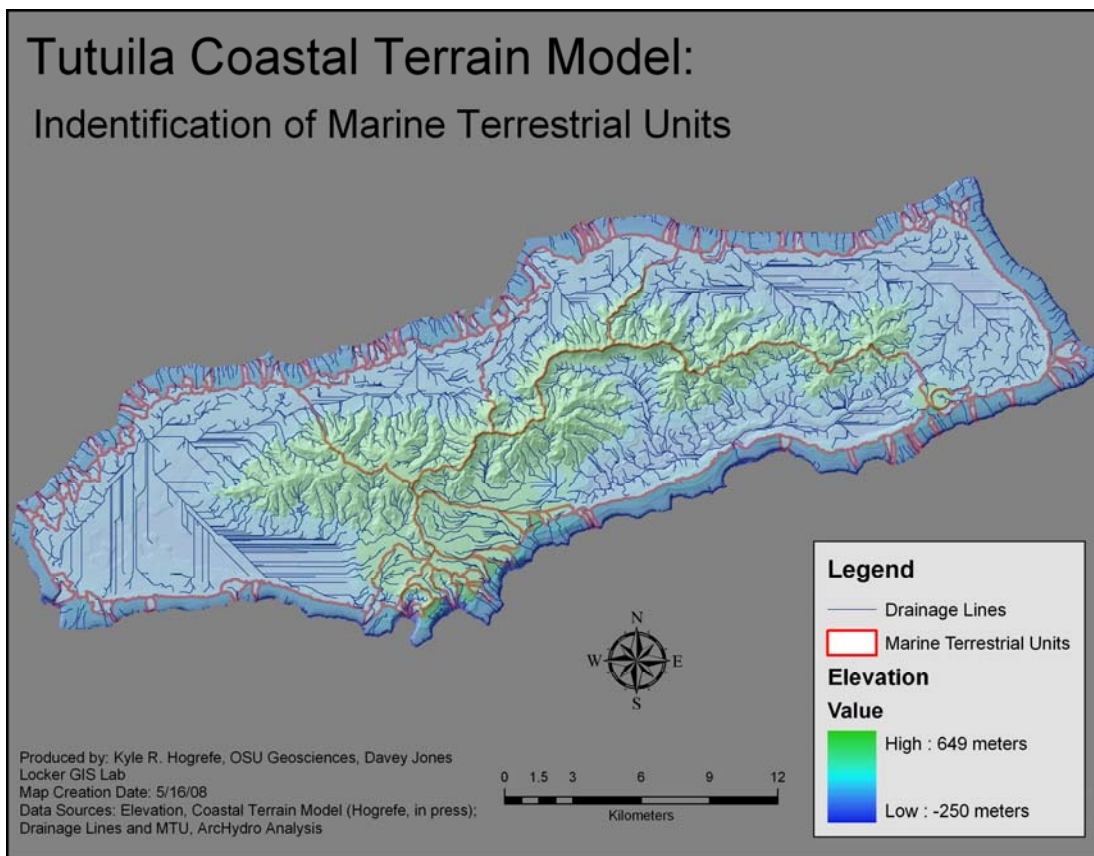


**Figure 3.4:** Identification of marine terrestrial units. MTU were defined using the Tutuila CTM and the terrain analysis capabilities of Arc Hydro. Note that the drainage pattern within each MTU has only one exit point. The straight drainage lines will be discussed in the next section.

### 3.3 Results

#### 3.3.1 MTU Analysis

The terrain analysis conducted with Arc Hydro was very effective in identifying topo-bathymetric catchments when applied to the Tutuila CTM. The comparison of the “stream” location and flow direction products defined 3585 minor catchments. Drainage

lines were used to amass these minor catchments into groups that contribute to the same drainage pattern resulting in 1520 intermediate basins which were further compiled “on the fly” by the data model into 94 adjoining catchments (Figure 3.5). Out of this total, 74 of the catchments contain no land area and flowed to the outside of the model due to the deep, fossil reef that fringes the basin around Tutuila. An additional six catchments do not contain REA sites. Of the 14 catchments that are germane to this study, five provide for excellent MTU (designated MTU 1 - MTU 5) with no further consideration. The complicated nature of the terrain in the south-central portion of the CTM required further visual analysis to group five catchments into MTU 6, two catchments into MTU 7, and two catchments into MTU8. MTU 6 and MTU8 also contain small areas not identified as part of a catchment.

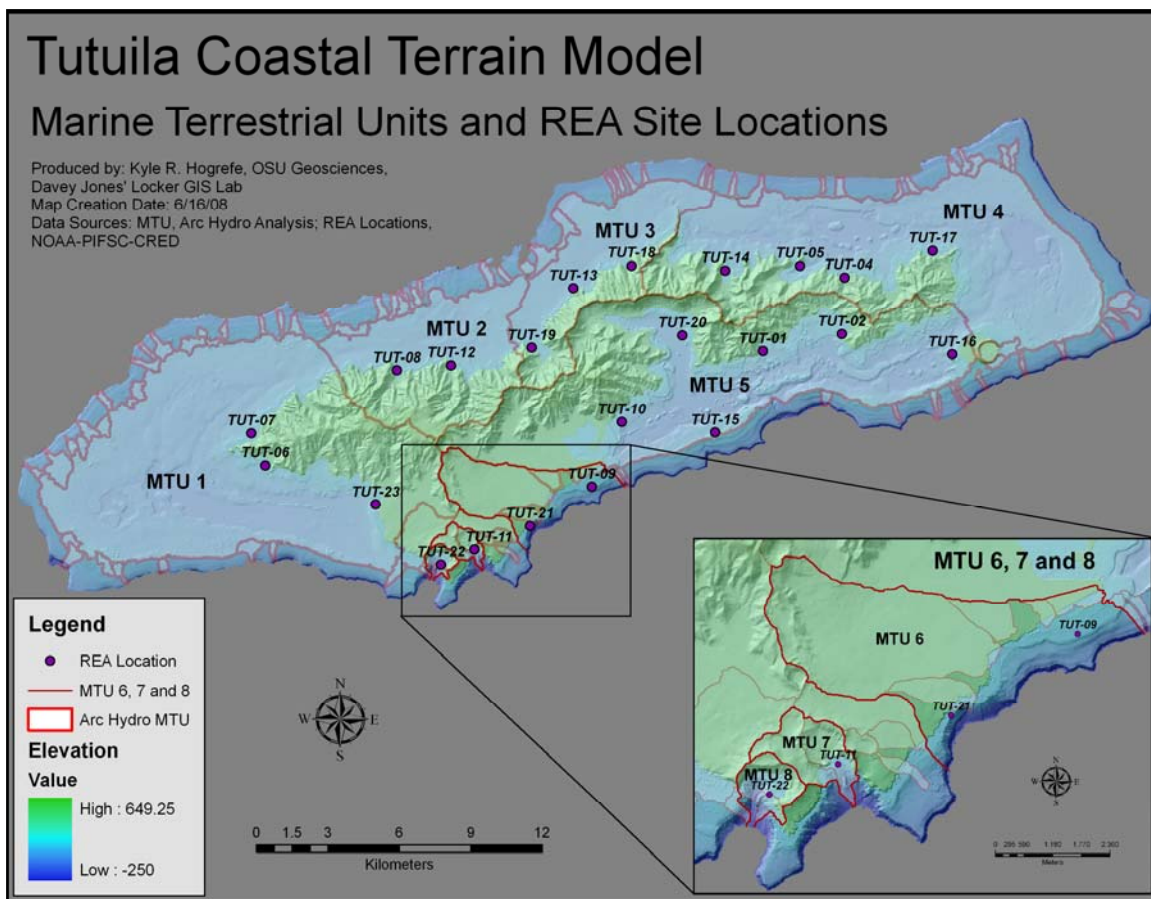


**Figure 3.5:** Marine terrestrial units and REA site locations.

A potential issue arose from the second step in the Arc Hydro processing series called “fill sinks” that resulted in straight drainage lines, primarily in the west and northeast portions of the CTM (Figure 3.4). During this step the data model assures that all catchments will flow to the edge of the DEM by locating low areas that would act as sinks and increasing the elevation values within them. Arc Hydro was originally designed for large scale terrestrial watershed applications where it can be expected that riverine systems flow to an outlet and that such sinks represent a data error (Maidment 2002). This is not the nature of the seafloor where basins with no outlet are common. Advanced processing techniques allowed for the possibility to fine tune the effects of “fill sink”.

However, this option was not pursued because the flattened seafloor terrain did not impact the determination of land area adjacency to coral reefs which primarily occur close to shore as indicated by REA positions (Figure 3.5).

### **3.3.2 Comparison of Population Density and Reef Criteria by MTU**

With MTU established to affiliate marine habitat with terrestrial catchments, land area population density was compared to average percent coral cover, average coral density and average generic richness within each MTU. Total generic diversity was not used in this continued analysis due to bias detected in the criteria. Larger MTU contained more REA sites which increased the chances for detection of rare genera, thus skewing the total generic diversity count in favor of the larger units. Using the average generic diversity minimized this bias and increased consistency of the data used in the comparison by using all mean values.

Once these datasets were combined into a common table and sorted by increasing population density (Table 3.4) and graphed as scatter-plots (Figures 3.6 and 3.7), patterns became immediately apparent between population density and the assessment criteria. Correlation co-efficients quantify these relationships (Table 3.5) with values from -1 to 1. Values closer to -1 indicate a stronger negative correlation and values closer to 1 indicate stronger positive correlations. For both 2004 and 2006 there was a positive correlation between population density and each of the criteria. Coral density had the most significant correlation with co-efficient values of 0.715 in 2004 and 0.691 in 2006. Percent coral cover had moderate correlations with values of 0.469 and 0.587 while generic diversity had the least significant correlation, particularly in 2006, with values of 0.374 and 0.012.

**Table 3.4:** 2000 MTU Population Densities with REA Data, Sorted by Density

MTU	2000 Population Density (People/km <sup>2</sup> )	Average % Coral Cover	Average Coral Density	Average Generic Richness
<b>2004 REA Data</b>				
8	0	50	16.5	24
2	77	13	2.7	13
3	152	35	7.7	20.7
4	173	37	8.7	21.5
7	283	45	21.1	26
1	285	42	5.9	19.3
5	604	37	14.2	23
6	978	55	30.8	24
<b>2006 REA Data</b>				
8	0	27	7	19
3	152	9	4.2	15.5
4	173	19	4.7	16.8
7	283	39	8.2	19
5	604	28	6.6	14.3
6	978	40	10.1	19
<b>2004 - 2006 % Change in REA Data</b>				
8	0	-46	-58	-21
3	152	-74	-45	-25
4	173	-49	-46	-22
7	283	-13	-61	-27
5	604	-24	-54	-38
6	978	-27	-67	-21

**Table 3.5:** Population Density / REA Data Correlation Co-efficients

Criterion	2004 CC	2006 CC	2004 - 2006 % Change CC
Average % Coral Cover	0.469	0.587	0.518
Average Coral Density	0.715	0.691	-0.609
Average Generic Richness	0.374	0.012	-0.209

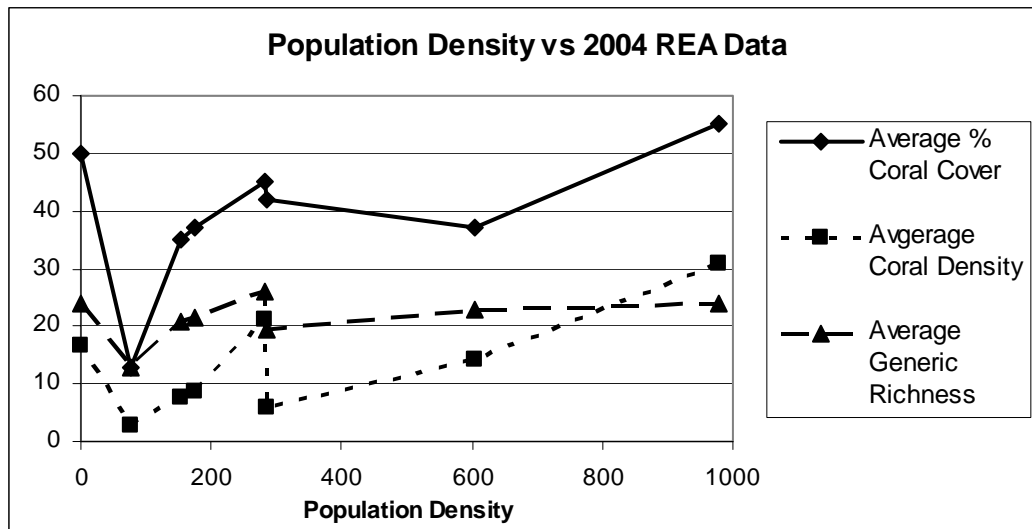


**Figure 3.6:** 2004 reef assessment criteria correlation to population density.

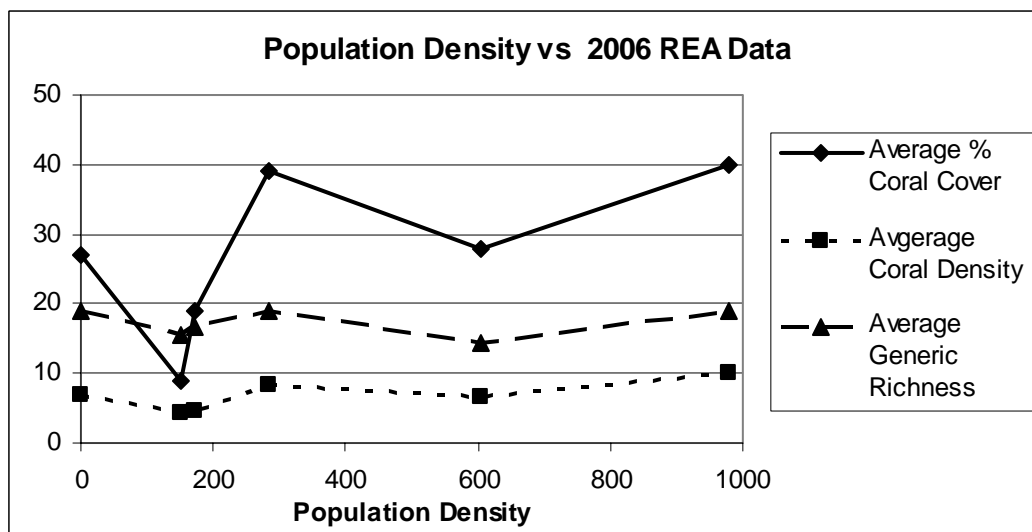


**Figure 3.7:** 2006 reef assessment criteria correlation to population density.

A drop in the values of each of the assessment criteria was readily apparent in both the tabular (Table 3.2) and graphic representations of the data, which inspired the calculation of percent change between the 2004 and 2006 (Table 3.3). When this metric was compared with population density (Figure 3.8), the percent change of percent coral

cover held a moderately positive correlation with a value of 0.518. However, there was a shift in the results with the other two criteria. The percent change of coral colony density and generic richness both exhibited negative correlations with coefficient values of -0.609 and -0.209 respectively (Table 3.5).

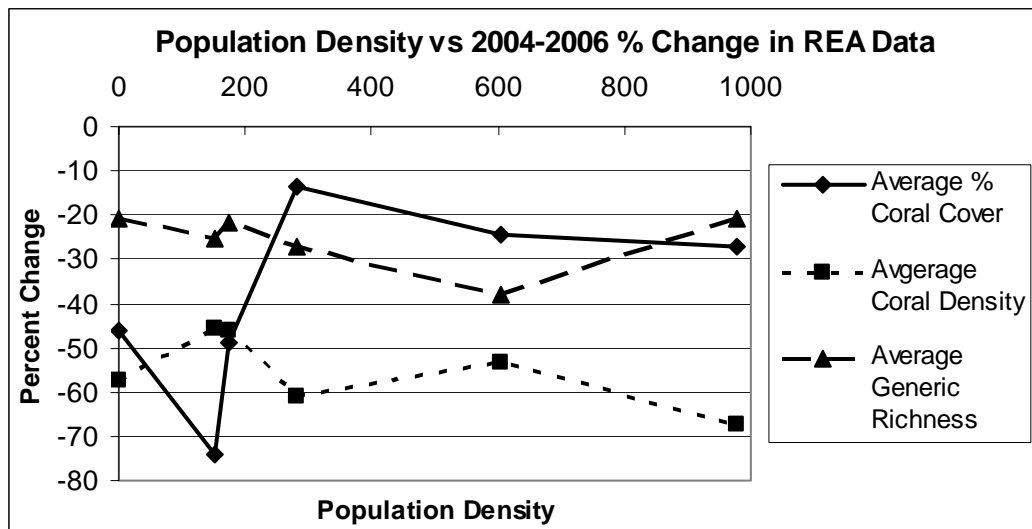


**Figure 3.8:** 2004-2006 percent change in reef assessment criteria correlation to population density.

### 3.4 Discussion

The MTU approach to studying the interconnectivity of marine and terrestrial systems provided some interesting insights into the relationship between intensified land use, using population density as a proxy, and the health of coral reef ecosystems. A potential shortcoming of the concept was rooted in the treatment of bathymetry as dry land terrain to determine drainage pattern. It did not account for the fact that as freshwater enters the marine environment it mixes with seawater through wave and current action. Even when calm environmental conditions minimize the mixing, the

higher density of the seawater causes freshwater to spread across its surface. This mixing and differential density makes it highly unlikely that freshwater inputs would follow the drainage patterns used to determine MTU. However, this was never the claim and the validity of the approach is supported by the nature of suspended sediment loads and the outcome of the correlation analysis.

Suspended loads that are introduced by freshwater plumes settle to the seafloor over time. The turbidity of the water while the load remains suspended prevents light penetration and interrupts photosynthesis by the symbiotic organism within the coral polyp. As the load settles out, it causes the siltation of the reef which smothers living corals and prevents the recruitment of coral larvae to the substrate. Both of these factors have been identified as major impacts to coral reef vitality and community diversity (Devlin and Brodie 2005, Richmond et al. 2007, Sealey 2004). Larger particulate matter would settle out close to input sources while the finer material moves farther out into the marine environment. During this progressive settlement the material would be most likely to remain in the marine catchment identified by the drainage lines even if it wouldn't precisely flow along them.

The hypothesis driving the creation of MTU was that watershed scale analyses using the Tutuila CTM would identify near shore areas most likely impacted by affiliated terrestrial drainages. Urbanization and intensive agriculture lead to higher suspended sediment loads in freshwater inputs to the marine environment (Devlin and Brodie 2005). Therefore, if the hypothesis it held true, one would expect to see an inverse relationship between increasing population density and criteria that indicate reef health. Initial comparisons did not support the premise due to the positive correlations between

population density and the criteria of percent coral cover, coral colony density and generic diversity (Table 3.5). However, the variable nature of Tutuila's terrain provides for differentiated substrates and uneven exposure to prevailing currents and weather patterns which results in diverse coral community composition around the island (Brainard et al., in review). This knowledge and the similarly shaped plot lines between 2004 and 2006 (Figures 3.6 and 3.7) lead to the suspicion that site specific environmental factors caused the correlation.

The consistent drop in the value of all reef health criteria between the 2004 and 2006 survey years spurred the examination of the percent change of each criterion. Adding this temporal aspect to the analysis reduced the spatial bias by assessing the change within an MTU for comparison to population density rather than simply looking at differences between sites. Percent coral cover was still correlated with population density to a similar degree, however, average coral density had a strong negative correlation with a coefficient of -0.609 and average generic richness had a negative correlation with a coefficient of -0.209 (Table 3.5 and Figure 3.8). As mentioned in the methods section, the 2004 REA percent cover data was collected by visual assessment, which is subjective between divers or even when collected by one diver as environmental conditions change or as fatigue increases. Thus the data and results from visual assessments may be considered suspect. It is conceivable that one or two particularly robust genera of coral could account for increased cover with fewer but larger colonies as generic diversity declines. However, a coral community in such a state would still represent a system thrown out of balance. Also note that the positive correlation does not indicate growth in coral cover between sites, just less loss between 2004 and 2006

surveys. Therefore, this correlation analysis indicates that increased human population density and the land use changes associated with it have a negative impact to the diversity and vitality of coral reef communities.

### **3.5 Conclusion**

Coral reefs are in decline around the world as indicated by diminishing geographic coverage and shifts in the biotic community diversity of those that remain. The ramifications of this decline are enormous. As reefs disappear, so does their capacity to fill their vital niche in the greater oceanic food web. Also lost are reefs ability to provide food for human consumption, protection in the face of severe weather events, cultural identity to traditional societies, and aesthetic value to society at large. Coastal terrain models enable the assessment of coastal change and the comparison of geomorphic, environmental and societal datasets to study the factors driving such change. The application of the MTU concept to the Tutuila CTM provided for an outcome similar to previous work in demonstrating a correlation between human population density and diminished coral reef diversity. Further, it refined other efforts that assessed the phenomenon at the island scale or larger to one focused on contiguous land/sea catchments. Approaching the problem at this scale should allow for discrete assessments of resource uses within a catchment and their impact to affiliated marine ecosystems.

Continued effort could be focused on enhancement of the terrain analysis, further investigation into the effects of terrain on suspended load dispersal or assessment of input levels from various sources. Though the Tutuila CTM provided a suitable topobathymetric surface for this analysis there is room for improvements in reducing the “noise” in the derived bathymetry and offsets at dataset transitions (Hogrefe et al.,

submitted). This would potentially eliminate the need for the “fill sinks” processing step and allow for improved terrain analyses by avoiding the filling of basins that represent real topography. With these improvements, the CTM could be used to model the effects of variable precipitation rates, winds and currents on the input and dispersal of suspended sediment loads. Such modeling efforts would be greatly enhanced by the collection of site specific stream flow, suspended sediment, and nutrient level data to both feed into the modeling analyses and proof results.

### **Acknowledgments**

Thanks to NOAA’s Pacific Island Fisheries Science Center, Coral Reef Ecosystem Division for their diligent work in collecting data to monitor reefs throughout the United States affiliated Pacific Islands and in particular their provision of the REA data that made this analysis possible.

## References

- Abelson, A., R. Olinky & S. Gaines (2005) Coral recruitment to the reefs of Eilat, Red Sea: temporal and spatial variation, and possible effects of anthropogenic disturbances. *Marine Pollution Bulletin*, 50, 576-582.
- Andrefouet, S., P. J. Mumby, M. McField, C. Hu & F. E. Muller-Karger (2002) Revisiting coral reef connectivity. *Coral Reefs*, 21, 43-48.
- Brainard R, Asher J, Gove J, Helyer J, Kenyon J, Mancini F, Miller J, Myhre S, Nadon M, Rooney J, Schroeder R, Smith E, Vargas-Angel B, Vroom P. (draft, in review) *Coral Reef Ecosystem Monitoring Report for American Samoa: 2002-2006*. NOAA Special Report National Marine Fisheries Service (NMFS) Pacific Islands Fisheries Science Center (PIFSC).  
<http://www.pifsc.noaa.gov/cred/hmapping/amsareport.php> (Last accessed 19 June 2008).
- Clarke, S. & K. Burnett (2003) Comparison of digital elevation models for aquatic data development. *Photogrammetric Engineering and Remote Sensing*, 69, 1367-1375.
- Craig, P., L. Peau, V. Filiga, M. Dworsky, M. McCuddin, S. Wiegman, G. Brighthouse, M. McPhee, J. Seamon, C. Seitz, N. Daschbach, M. Kirshman, J. Craig, F. Curren, & M. Turituri (2000) *Impacts of Rapid Population Growth in American Samoa: A Call to Action*, American Samoa Government and Coral Reef Advisory Group, 31 pp. <http://doc.asg.as/crag/population> (Last accessed 19 June 2008).
- Devlin, M. J. & J. Brodie (2005) Terrestrial discharge into the Great Barrier Reef Lagoon: nutrient behavior in coastal waters. *Marine Pollution Bulletin*, 51, 9-22.
- Duke, N. C., A. M. Bell, D. K. Pederson, C. M. Roelfsema & S. B. Nash (2005) Herbicides implicated as the cause of severe mangrove dieback in the Mackay region, NE Australia: consequences for marine plant habitats of the GBR World Heritage Area. *Marine Pollution Bulletin*, 51, 308-324.
- Gahegan, M. & M. Ehlers (2000) A framework for the modelling of uncertainty between remote sensing and geographic information systems. *Isprs Journal of Photogrammetry and Remote Sensing*, 55, 176-188.
- Hoffmann, T. C. (2002a) Coral reef health and effects of socio-economic factors in Fiji and Cook Islands. *Marine Pollution Bulletin*, 44, 1281-1293.
- Hoffman, T.C. (2002b) The reimplementation of the Ra'ui: Coral reef management in Rarotonga, Cook Islands. *Coastal Management*, 30, 401-418.
- Hogrefe, K.R., D.J. Wright & E.J. Hochberg (submitted) Derivation and Integration of Shallow-water Bathymetry: Implications for Coastal Terrain Modeling and Subsequent Analyses. *Marine Geodesy*.
- Jiang, Y. W., O. W. H. Wai, H. S. Hong & Y. S. Li (2004) A geographical information system for marine management and its application to Xiamen Bay, China. *Journal of Coastal Research*, 254-264.
- Li R., J. Liu and Y. Felus. 2001. Spatial modeling and analysis for shoreline change detection and coastal erosion monitoring. *Marine Geodesy*. 24:1-12.
- Maidment, D.R. editor (2002) *Arc Hydro: GIS for Water Resources*, ESRI Press
- Miller S.N., D.J. Semmens, D.C. Goodrich, M. Hernandez, R.C. Miller, W.G. Kepner and D.P. Guertin. 2007. The automated geospatial watershed assessment tool. *Environmental Modeling and Software*. 22:365-377.

- Mumby, P. J., E. P. Green, A. J. Edwards & C. D. Clark (1999) The cost-effectiveness of remote sensing for tropical coastal resources assessment and management. *Journal of Environmental Management*, 55, 157-166.
- Mumby, P. J., W. Skirving, A. E. Strong, J. T. Hardy, E. F. LeDrew, E. J. Hochberg, R. P. Stumpf & L. T. David (2004) Remote sensing of coral reefs and their physical environment. *Marine Pollution Bulletin*, 48, 219-228.
- Richmond, R. H., T. Rongo, Y. Golbuu, S. Victor, N. Idechong, G. Davis, W. Kostka, L. Neth, M. Hamnett & E. Wolanski (2007) Watersheds and coral reefs: Conservation science, policy, and implementation. *Bioscience*, 57, 598-607.
- Sealey, K. S. (2004) Large-scale ecological impacts of development on tropical islands systems: comparison of developed and undeveloped islands in the central Bahamas. *Bulletin of Marine Science*, 75, 295-320.
- Shapiro, A. C. & S. O. Rohmann (2005) Summit-to-sea mapping and change detection using satellite imagery: tools for conservation and management of coral reefs. *Revista De Biologia Tropical*, 53, 185-193.
- Wright, D. 2002. Mapping and GIS capacity building in American Samoa. *Proceedings of the 22nd Annual ESRI User Conference*. San Diego, CA, Paper 101.

## Chapter 4. Conclusion

In the completion of this thesis, its research goal was attained while the answers provided to the research questions of each manuscript provide direction for additional courses of inquiry. During the creation of the Tutuila CTM, bathymetry derived from multispectral data was shown to be statistically accurate and to provide for realistic terrain profiles through all data sets and therefore suitable for use in terrain modeling. The identification of the most accurate published method to derive bathymetry and the error assessment conducted throughout CTM creation established the efficacy of using these derived depths to model near shore terrain. The Tutuila CTM enabled the MTU approach to terrain analysis used to investigate the second manuscript's research question of whether terrain influences the impact of intensified land use to coral reefs. The MTU drainage pattern analysis allowed for a spatiotemporal comparison of population density and the change in three reef assessment criteria within marine/terrestrial catchments in which land use would have the most direct impact to coral reefs. Significant negative correlations were shown for two of the three criteria, with the significance of positive correlation deemed questionable, suggesting that terrain affects the impact of terrestrial inputs to the coral reef ecosystems. How can this knowledge be applied to the management of coral reef resources?

This research suggests potential courses of action by establishing both a method by which the impact of land use to coral reef health can be quantified and the baseline data that demonstrates this impact. Without a scientifically quantified cause and effect relationship between a human action and an environmental response, it is difficult to justify management actions. Scientific data are also essential in continued monitoring of

the environmental responses to management decisions to suggest future courses of action and demonstrate the efficacy of management measures to the public (Hoffmann 2002b, Mumby et al. 1999). Knowing that increased population density decreases the community diversity of coral reefs within a marine/terrestrial drainage leads to questions concerning which components of freshwater inputs have the greatest impact to reefs and how they move once they've entered the marine environment. The MTU identified for Tutuila could be used as geographical assessment areas to determine the distribution of freshwater runoff monitoring units to gauge precise levels of freshwater contaminants such as pathogens, increased nutrient loads and high suspended sediment loads. Once these precise inputs are better understood, oceanic current modeling could be conducted to better understand how the island terrain directs the flow of near shore currents. Knowing how the currents move would enable assessments of how contaminant loads are distributed once they enter the marine environment and the identification of areas where suspended loads might settle as opposed to being washed away to the deep ocean. This full range of information would enable resource managers to first establish that some changes to land use practices are necessary to mitigate their impact to coral reefs. Subsequent monitoring using the MTU approach could identify which inputs are most important to control and then the land uses identified as primary sources could be managed. The decline of coral reef resources has been identified as a concern around Tutuila and marine protected areas (MPAs) are increasingly used as a management tool for conservation. However, lack of adherence to MPA regulations is pointed out as a common problem that reduces their effectiveness as a management measure (Hoffmann

2002b, McClanahan et al. 2006). Does the “social capital” required for conservation measures to succeed exist on Tutuila?

Polynesian and Melanesian cultural traditions developed around island settlement patterns in coastal valleys separated by steep ridges, give the authority over land and sea resources within a catchment to the village and its chief. This direct link between the population and the resources that they depend on for sustenance, typically lead to sustainable harvest with a deep understanding of the balance between the terrestrial and marine components of the system and limits to population growth by resources availability (Hoffmann 2002a, Hoffmann 2002b, Cinner, Marnane and McClanahan 2005a, Cinner et al. 2005b). The shift from a traditional Polynesian/Melanesian values system to one focused on western ideas of development and resource management explain actions that cause declines in reef health. To a large degree the failings of the western approach of centralized authority are a matter of scale. National regulations often establish broad resource management policies that operate at a spatial scale larger than the precise local knowledge needed to understand and manage the highly heterogeneous ecology of coral reefs. Another issue is the shift in the perception of reef resources from having a value based in their provision of sustenance and cultural identity to having a purely economic value which encourages overharvest in pursuit of profit. The inclusion of cultural traditions and local concerns in the management of coral reef resources address these issues and are effective measure to reverse the decline of the worlds coral reef resources (Hoffmann 2002a, Hoffmann 2002b, Cinner et al. 2005a, Cinner et al. 2005b).

The lessons learned in these case studies provide for potential management options around Tutuila which has well established western institutions, an active research community and a very strong Polynesian cultural identity. In addition to NOAA CRED's research around American Samoa, NOAA's National Ocean Service runs the Fagatele Bay National Marine Sanctuary on Tutuila and the National Park Service runs preserves on multiple islands. Local authority falls to the American Samoa Department of Marine and Wildlife Resources, which is responsible for resource management on the islands and within territorial waters. There is a high degree of collaboration between local and regional entities as exemplified by American Samoa Coral Reef Initiative the collaborative efforts of its Coral Reef Advisory Group which was created by the Governor of American Samoa to provide him with advice on coral reef management and science (<http://doc.asg.as/CRAG/>). These national and regional authorities have created eight different MPA which are complemented by an additional 9 community based programs which are based around the traditional practice of the village having authority of its adjacent reef and other marine resources. The proliferation of these community MPA demonstrate the American Samoan cultural affinity for managing land and sea resources on the basis of well defined geographical units.

Management practices on this scale could be well monitored using the MTU approach, while research by McClannahan et al. (2006) indicates that community-based MPAs are more effective at reaching conservation goals than more centralized approaches. Thus, refined MTU analyses could be used to assess the effectiveness of MPA management practices around the island to guide further management decisions and expand upon previous research identifying best MPA practices. The use of local

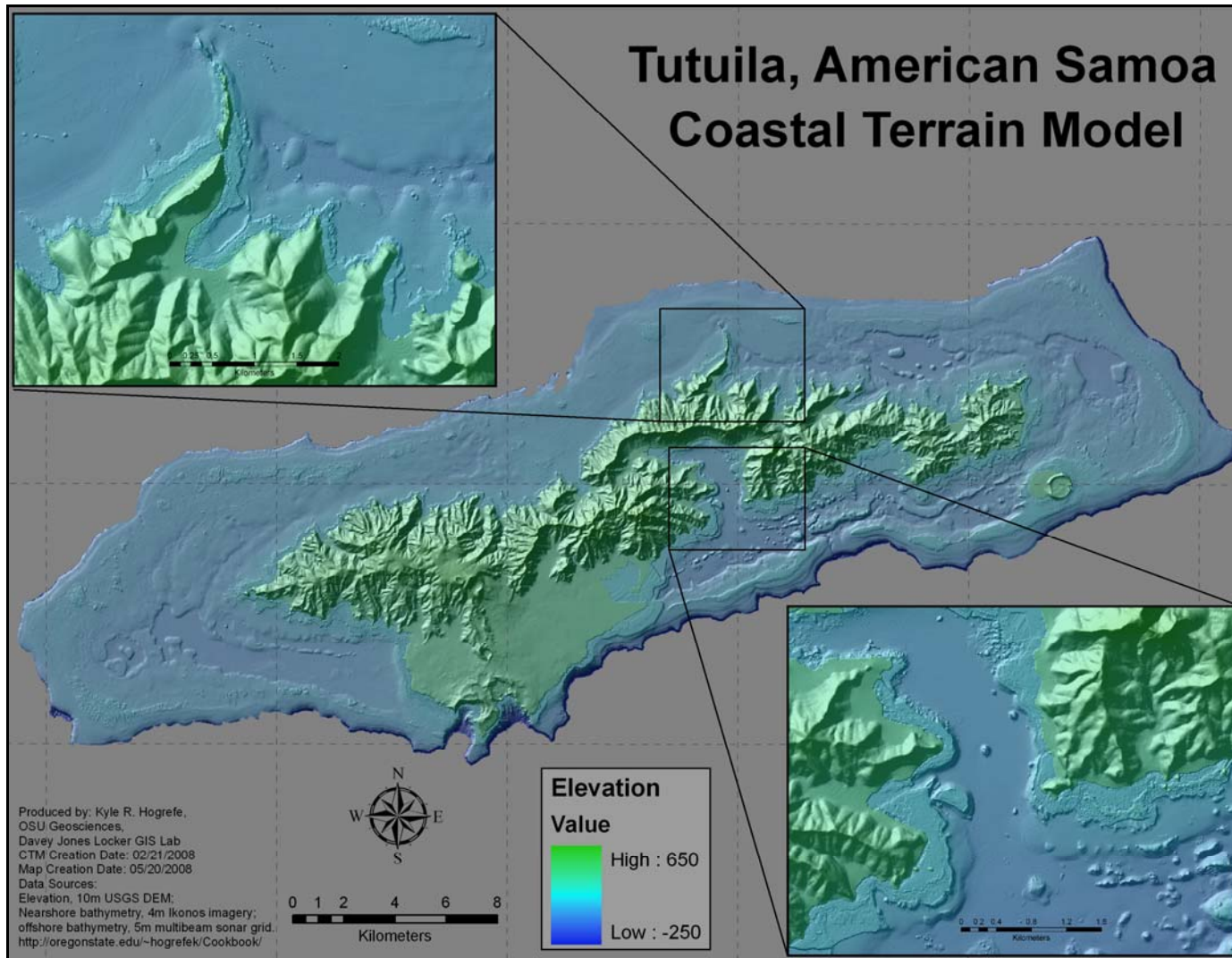
knowledge of the distribution and state of coral reef resources is important to accurate resource assessment and for creating the social capital needed for reliable compliance with MPA measures (Hoffmann 2002a, Hoffmann 2002b, Cinner et al. 2005a, Cinner et al. 2005b). Such knowledge can be effectively integrated into geographic information systems (GIS) to make this invaluable information available to resource managers (Aswani and Hamilton 2004). American Samoa is well situated to take advantage of such technology due to the existence of the American Samoa GIS Users Group which is a grassroots effort to bring together private and public entities to share GIS data resources (<http://doc.asg.as>).

The current combination of Western and Polynesian cultural institutions along with readily available scientific data in American Samoa presents an opportunity for the successful management of coral reef resources. The already substantive accomplishments of resource management efforts in the territory could be bolstered by using the Tutuila CTM and the MTU approach of terrain analysis to provide scientific guidance for measures to mitigate the impact of land use to the marine environment through freshwater runoff. The successes and failures indicated by such an assessment should be viewed in light of recent research that points to the inclusion of traditional management practices and knowledge in MPA measures as essential to achieving conservation goals. Such consideration will serve to protect the health of the coral reefs in American Samoa while respecting, protecting and utilizing the knowledge of the local cultural system that has fostered the reef for centuries.

## References

- Aswani, S. & R. J. Hamilton (2004) Integrating indigenous ecological knowledge and customary sea tenure with marine and social science for conservation of bumphead parrotfish (*Bolbometopon muricatum*) in the Roviana Lagoon, Solomon Islands. *Environmental Conservation*, 31, 69-83.
- Cinner, J. E., M. J. Marnane & T. R. McClanahan (2005a) Conservation and community benefits from traditional coral reef management at Ahus Island, Papua New Guinea. *Conservation Biology*, 19, 1714-1723.
- Cinner, J. E., M. J. Marnane, T. R. McClanahan, T. H. Clark & J. Ben (2005b) Trade, tenure, and tradition: Influence of sociocultural factors on resource use in Melanesia. *Conservation Biology*, 19, 1469-1477.
- Hoffmann, T. C. (2002a) Coral reef health and effects of socio-economic factors in Fiji and Cook Islands. *Marine Pollution Bulletin*, 44, 1281-1293.
- Hoffmann, T. C. (2002b) The reimplementation of the Ra'ui: Coral reef management in Rarotonga, Cook Islands. *Coastal Management*, 30, 401-418.
- McClanahan, T. R., M. J. Marnane, J. E. Cinner & W. E. Kiene (2006) A comparison of marine protected areas and alternative approaches to coral-reef management. *Current Biology*, 16, 1408-1413.
- Mumby, P. J., E. P. Green, A. J. Edwards & C. D. Clark (1999) The cost-effectiveness of remote sensing for tropical coastal resources assessment and management. *Journal of Environmental Management*, 55, 157-166.

## **Appendices**

**Appendix A: Tutuila, American Samoa Coastal Terrain Model.**

## Appendix B: Data processing “Cookbook” of instructions to deriving bathymetry from multispectral satellite imagery

### Digital Image Processing “Cookbook”:

#### A method to derive bathymetric data from high spatial resolution multi-spectral imagery

Produced by: Kyle R Hogrefe  
 Master’s Candidate - Oregon State University, Dept. of Geosciences  
 2/22/08

### Document Purpose

This document will provide a step by step outline, with comments concerning processing methods and accuracy issues, for a methodology to create raster grid of shallow-water (<20 meters of depth) bathymetric data from multi-spectral satellite imagery. It records image processing steps of the second run through an image specific methodology. The establishment of this methodology will be an iterative process so that processes can be improved. Some of the specifics of each processing step will vary depending on source data and file type, however, tools and considerations for each step will be described.

### Inputs

#### Tutuila/Rose

Multi-beam Sonar (collected by CRED/PIBHMC)

Collection date: February/March 2004, 2006  
Data Range: 0- 300 meters  
Instrument: 240 kHz RESON 8101-ER  
Resolution: 5x5 meter  
Processing: Noise editing and conversion to 5 meter grid.  
File Type: Arc ASCII (.asc)

#### Tutuila

IKONOS Satellite Image (purchased from GeoEye, Inc.)

Collection date/time: March 3, 2002/21:38 GMT  
Pertinent bands: Band 1 (blue): 445 – 516 nanometers  
 Band 2 (green): 506 – 595 nanometers  
 Band 3 (red): 632 – 698 nanometers  
 Band 4 (Near IR): 757 – 852 nanometers  
Resolution: 4x4 meter nominal  
Processing: Geometric correction (only)  
File Type: NITF (National Imagery Transfer Format)

USGS Digital Elevation Model

Rose

IKONOS Satellite Image (purchased from GeoEye, Inc.)

Collection date/time: March 3, 2002/21:38 GMT

Pertinent bands:

Band 1 (blue):	445 – 516 nanometers
Band 2 (green):	506 – 595 nanometers
Band 3 (red):	632 – 698 nanometers
Band 4 (Near IR):	757 – 852 nanometers

Resolution: 4x4 meter nominal

Processing: Geometric correction (only)

File Type: ERDAS Imagine (.img)

Complete sets of metadata are available.

**Software Used**

ArcGIS 9.2

ENVI 4.3

Microsoft Excel 2003

S-PLUS (statistical analysis software)

**Processing Method: Overview****1) Viewing of Images**

Software: ENVI, ArcGIS

**2) Data Conversion from DN (digital number) to Radiance**

Software: ENVI

**Atmospheric Correction (Comments)****3) Correct for Atmosphere and Water Surface Reflection (deglinting)**

Software: ENVI, Microsoft Excel

**4) Linearize spectral decay as a function of depth**

Software: ENVI

**5) Mask Values not Applicable to Depth Derivations**

Software: ENVI

**6) Georectify Images**

Software: ENVI, ArcGIS

**7) Extract Linearized Spectral Values and Depth Data**

Software: ArcGIS

## 8) Perform Multiple Linear Regression Analysis and Derive Bathymetry

Software: Microsoft Excel, S-PLUS, ENVI

## 9) Integrate Derived Bathymetry with Sonar Bathymetry

Software: ArcGIS

### Processing Method: Step Descriptions

#### 1) Viewing and Georectification of Images

Making sure that the IKONOS image and multibeam bathymetry grid are georectified is a very important preprocessing step because this analysis depends on gathering pixel information from the same position in each data source. Any number of issues can arise with image projections and the geometric corrections that the satellite imagery undergoes. Different georectification and file type issues were encountered through the first two iterations of this process, first using imagery of Rose Atoll and then the Island of Tutuila, are discussed.

The IKONOS images made available for bathymetric derivations around Tutuila were in the NITF format and the multibeam data were in ASCII format. The NITF files cannot be opened directly in ENVI without an additional (and costly) software extension and license; however, they can be opened in ArcGIS and converted for use in ENVI.

Additionally, for this iteration, I procured a free “plug in” called “ENVI Reader for ArcGIS” that enables the use of the “ENVI Standard” file type in ArcGIS. The plug in is available at <http://www.itvis.com/> and comes with installation and use instructions.

Opening the Bathymetry data in ArcMap (**Tutuila and Rose**):

- The multibeam bathymetry is in ESRI ASCII format and must be converted to a raster to be viewed in ArcMap. (In my case it was named *rose\_5m.asc*.)
  - Use *ArcToolbox > Conversion Tools > To Raster > ASCII to Raster* to create a raster grid of the bathymetry.
  - Use “Float” for output data type
  - Start naming and saving things intelligently – you’ll end up with lots of files.
- The spatial reference of both the raster bathymetry and the data view will be undefined at this point.
  - Use *ArcToolbox > Data Management Tools > Projections and Transformations > Define Projection* to define the projection as defined in the metadata. (D\_WGS\_1984)

- Choose the newly converted raster grid as the “Input Dataset”.
  - Use the browse button to define the “Coordinate System”
    - Click the “Select” button
    - Open the “Geographic Coordinate Systems” folder
    - Open the “World” folder
    - Choose “WGS 1984.prj”
    - Click “OK” (twice)
- Use *ArcToolbox > Data Management Tools > Projections and Transformations > Raster > Project Raster* to actually project the raster that was just defined.
- Choose the newly defined grid as the “Input raster”
  - Use “Output raster” to save the new raster in the proper place and name it wisely.
  - Use the browse button next to “Output coordinate system” to provide projection parameters.
    - Click the “Select” button
    - Open the “Projected Coordinate Systems” folder
    - Open the “UTM” folder
    - Open the “Wgs 1984” folder
    - Scroll over to “WGS 1984 UTM Zone 2S.prj”
    - Click “OK” (twice)

It is important to open this file and indicate its spatial reference first so that ArcGIS can match up IKONOS data (the spatial reference is different in this case) “on the fly”.

The bathymetry raster grid is now ready for use once IKONOS imagery has been prepped for processed radiance value extraction – read on!

### Viewing IKONOS imagery and preparing it for processing in ENVI (**Tutuila**)

The IKONOS imagery is in NITF format and must first be opened in ArcGIS and then converted to a TIFF file for use in ENVI. Note: Each band (blue, green, red and NIR) came as its own file and I needed two scenes for this project. Thus, four files for each scene must be opened and converted and then compiled in ENVI.

- To open the NITF files:
  - In ArcCatalog, with the “Preview” tab active:
    - Left click on the file and say yes to the “Calculate Pyramids?” inquiry.
    - Right click on the same file and choose “Calculate Statistics” from the options that pop up.
      - Accept the defaults

- Now the files can be previewed in ArcCatalog to choose the desired files to include in the ArcMap project.
  - Either drag and drop the files from ArcCatalog to ArcMap or use the “Add Data” button within ArcMap.
- The files will once again display as a black box – to view them...
  - Right click on the just added raster layer and select “Properties”
  - Click the “Symbology” tab
    - For a multi-band image, ensure “RGB composite” is highlighted
    - For a single band image, ensure “Stretched” is highlighted
  - In the “Stretch” frame
    - Click the “Type” drop down list and select “Standard Deviations”
    - Accept the default of 2 and click OK
- To convert the files for use in ENVI
  - In ArcMap, right click on the file in the table of contents.
    - Choose *Data > Export Data* from the pop up menu
    - From the “Format:” drop down list choose “TIFF”
    - Give the file a good name and storage location and click OK
    - The resultant TIFF files can be opened in ENVI with their spatial reference data intact.

Opening files in ENVI and multiple processing steps to prepare for bathymetric derivations

- To view the files in ENVI:
  - On the main ENVI toolbar, left click on *File > Open External File > Generic Formats > TIFF/GeoTIFF*
    - If the error message “This does not appear to be a valid .tif file” pops up, it means you’ve added the files to ArcMap or ArcCatalog and still have these programs running.
    - Close whichever ArcGIS projects are running and ENVI should open them just fine.
- To compile the files into a multiband image:
  - In ENVI, have the files you wish to compile active (in the “Available Bands List” window)
  - Left click on *File > Save File As > ENVI Standard*
    - In the “New File Builder” window:
      - Left click on the “Import File...” button
        - Choose the desired bands and click OK

- Left click on the “Reorder Files...” button, to make sure the bands are in the same order as in IKONOS data and move them if not.
  - B1 = blue, B2 = green, B3 = red, B4 =NIR
- Name the file, direct it to a good storage spot and click OK

### Viewing IKONOS imagery and preparing it for processing in ENVI (Rose)

To View the Data in ENVI:

- Start up ENVI 4.3 and “Open Image File” to open the IKONOS (rose\_corrected.img) file and use the “Available Bands List” to choose “RGB Color” and assign blue, green and red to bands 1, 2 and 3 respectively.
  - In my case this resulted in the image opening up as raster gobbledygook (technical term).
  - My trouble shooting resulted in noticing the fact the ENVI was defaulting to the NAD27, rather than the WGS84, datum for its UTM co-ordinate system.
    - I used the *Map > Convert Map Projection* from the main tool bar to change the datum to WGS84 (using nearest neighbor resampling) which caused the image to display properly.
    - However, my exploration of the image exposed the fact the positional accuracy of the image was off by about 100 meters as judged by the known feature positions.
      - Converting back to NAD27 did not solve the problem.

So, to summarize the problem, the cursor position was not matching to the known position of specific geographical features. There offset was a consistent direction and distance from control points. To me this meant the UTM values assigned to each pixel were offset in a specific distance and direction. My best understanding of the problem is that somewhere in the projection conversions threw the positions off some how, but I could not get the display to work by any other method. My decision was to spatially subset the data to the area of concern (immediately around the atoll) and to correct the offset of the image using the subset.

To Spatially Subset the Image:

- From the main toolbar, use *Basic Tools > Resize Data (Spatial/Spectral)*
  - In the “Resize Data Input” window
    - Select the right (reprojected) .img file
    - Click the “Spatial Subset” button
      - Click on the “Image” button
      - Use the cursor to drag the box around the area of interest
      - Click OK
    - Leave the “Spectral Subset” as default

- In the “Resize Data Parameters” window
  - Use the default resampling method of Nearest Neighbor.
  - Select a good storage spot for your processed IKONOS imagery and name the file.
  - Again, choose wisely, there will be lots of files

To rectify the Image:

In order to correct for the specific direction/distance offset, I decided to change the UTM coordinates of the of the origin or “Tie Point” pixel. This, in turn, shifts the coordinates of the rest of the pixels.

- Right click on the name of the file in the “Available Bands List” window and choose “Edit Header”
  - Click on the “Edit Attributes” button and choose “Map Info...”
  - In the “Map Coordinate of Tie Point” section of this window you can change the UTM position of the upper left corner or tie point of the image.
  - I adjusted the image as an iterative process where I changed the tie point position base on my estimate of offset in the image, checked the control point apparent location against the physical feature it should represent and then adjust the tie point location again to try and account for the remaining offset.
    - I achieved a precision of five decimal places, when viewing the position data in decimal degrees, after six or seven iterations.

## 2) Data Conversion from DN (digital number) to Radiance

Satellite imagery comes to the user with the strength of the at sensor radiance represented by a digital number (DN). To this point of the process, it has been OK to just use the data in DN values, but for the next step it is essential to convert to radiance. The “calibration coefficients” for this conversion are supplied by the parent company (GeoEye, Inc. for IKONOS) and are based on the date of the imagery and radiometric resolution of the image.

- The equation to convert DN to radiance is:  $\text{Radiance} = \text{DN}/\text{Cal Coeff}$
- The coefficients provided were: Blue = 728, Green = 727, Red = 949 and NIR = 843
- In the ENVI main toolbar, click *Basic Tools > Band Math*
- In the “Band Math” window, create the formulas to utilize the above formula and calibration coefficients. (ENVI help is quite good and very useful in figuring out band math.)
- My “Band Math” equations were thus:
  - $\text{float}(b1)/728$
  - $\text{float}(b2)/727$
  - $\text{float}(b3)/949$
  - $\text{float}(b4)/843$

- There will now be four “single band” images that will be compiled into a multiband image later, but, at this point, leave them as single band images for further processing.
- To facilitate upcoming steps, compile the individual band images in a multi-band image as described above ( under Viewing IKONOS imagery and preparing it for processing in ENVI (Tutuila)

**Note about atmospheric correction:**

Atmospheric correction is essential to deriving depth through the comparison of radiance values because atmospheric effects would mask the measure of variable spectral band attenuation through the water column upon which this measurement depends. Various methods exist for atmospheric correction. Absolute atmospheric correction methods rely on algorithms that use measures of environmental and instrument variables to correct and image. Other methods are more empirical, relying on proxy measures within the image used to adjust values for the effects of the atmosphere. One method (to be explored in the future) relies on creating a linear transform based on the brightest and darkest pixel value in each band. Another, called dark pixel subtraction, is effectively applied in images with areas of deep water. The method relies on the assumption that all radiation incident to the water’s surface is either absorbed or reflected. This darkest pixel in the image obviously contains minimal reflected light and the rest of the energy is absorbed so that any remaining radiance value in the pixel represents atmospheric effects. Subtracting the spectral value of each band in the pixel from its respective band across the image corrects for atmospheric effect.

The following process corrects for atmosphere (while also deglinting) in a manner analogous to dark pixel subtraction.

**3) Correct for Atmosphere and Water Surface Reflection (deglinting)**

Variable sun glint across images is a result of the ocean swell and chop causing widely variable incident angles for the reflection of the Sun’s radiation. Methods originated by Hochberg, et al. (2003) and refined by Hedley, et al. (2005) are effective in removing this glint and improving determinations made from the “de-glinted” imagery. The following steps outlined using ENVI functions are based on a four step process proposed in Hedley (2005).

Note: Eric Hochberg (in conversation) suggests that suitable atmospheric correction is accomplished by not subtracting the minimum NIR value in the application of the final equation in step 4. This makes steps 1 and the minimum NIR value from step 2 moot, but the spatial subset produced in step 2 is still applicable. The Rose product resulted from going through all steps (with step 1 accomplished by dark pixel subtraction). The deglinting/atmospheric correction for the Tutuila product commenced with the spatial subset from step 2, through step 3 and uses the adjusted formula in step 4 (below).

- 1) Radiometrically correct image using conventional method. (Hedley, 2005)
- 2) Select a sample area (or areas) of the image displaying a range of sun glint, but where the image would be expected to be more or less homogenous if the sun glint was not present (e.g. over deep water). Determine the minimum Near Infrared ( $\text{Min}_{\text{NIR}}$ ) value in this sample.
  - In ENVI, use the “ROI Tool” as described above to create and save a new ROI that covers a wide range of sunglint.
  - Also in the “ROI Tool”, click on the basic stats button and look at the information for Band 4 (which is the NIR).
    - Record the minimum NIR value.
    - You’ll be able to access this figure again later in processing.
- 3) For each band to have sun glint removed, perform a linear regression of NIR brightness (x-axis) against the band signal (y-axis) using the selected pixels. The slope of the regression line is the output of interest.
  - In ENVI use the “ROI Tool” option of “Subset data using ROI” and the just made ROI to create a new image that is only the glare pixel subset.
  - Display this new subset image
  - From the main tool bar click *File > Save File As > ASCII*
    - In the “New File Builder” window, click the “Import File” button and choose the glint subset file from the list.
    - Click the “Spectral Subset”
      - Choose the first band
      - Click OK
    - In the “Output to ASCII Parameters” window set the output style to XYZ Format.
      - Name the new 1 band file appropriately and store it in the right spot.
    - Repeat this process making a file for each of the first four bands (blue, green, red, NIR)
  - In Microsoft Excel:
    - Open each of the files just created using the formatting wizard
      - Each of the files will have an ID, a UTM position(s), and a DN value (we’ve yet to convert to radiance) for each pixel
      - Choose one of the files as your base and compile each of the columns of DN values into it
        - Label each column appropriately
        - Have the band 4 column be first in sequence (to facilitate using the chart wizard.)

- Use the Chart Wizard, create three different scatter plots with NIR DN values on the x axis and the DN values of each of the other bands on the y axis.
  - Add a trend line to each of the charts and display its linear equation (slope/intercept)
  - Record the slope of each bands trend line from these plots.
- 4) To deglint and atmospherically correct band  $i$  for all pixels in the image, subtract the product of  $b_i$  and the NIR brightness of the pixel from the pixel value in band  $i$  (following equation).
  - $R'_i = R_i - b_i (R_{NIR})$
  - In ENVI on the main tool bar, click *Basic Tools > Band Math*
  - In the “Band Math” window, create the formulas to utilize the above formula.
  - In the Tutuila work, ( $Min_{NIR}$  was not included) slopes for bands 1, 2 and 3 were 0.7884, 1.1551 and 0.8781 respectively so that my formulas were formatted as follows:
    - $float(b1) - 0.7884 * float(b4)$
    - $float(b2) - 1.1551 * float(b4)$
    - $float(b3) - 0.8781 * float(b4)$
  - In the final “Band Math” window select the files to be referenced by b1, b2, b3 and b4 as each formula is used to correct its respective band.

**4) Linearize spectral decay as a function of depth** (Base on Lyzenga, 1985 - with changes suggested by Eric Hochberg)

- Create a spatial subset of the atmospherically corrected and deglinted image from step 4.
  - This can be produced using the same ROI/spatial subset process as used in step 4-2, but must subset the most recent image.
- Determine the minimum spectral value for each band.
  - From the ENVI main toolbar, select *Basic Tools > Statistics > Compute Statistics*
  - Choose the just created spatial subset as the Input File, click OK
  - Record the minimum value for each band
    - For the Tutuila product my figures were
      - B1: 0.423909
      - B2: 0.261377
      - B3: 0.065501
- Subtract this average value and take the natural log of this figure for the entirety of each band.

- The formula:  $R_{\text{Linear}} = \text{Ln}(R_i - R_{\text{min}})$
- In ENVI on the main tool bar, click *Basic Tools > Band Math*
- In the “Band Math” window, create the formulas to utilize the above formula and figures.
- In the Tutuila work my formulas were formatted as follows:
  - $\text{alog}(\text{float}(b1) - 0.423909)$
  - $\text{alog}(\text{float}(b2) - 0.261377)$
  - $\text{alog}(\text{float}(b3) - 0.065501)$
- In the final “Band Math” window select the files to be referenced by b1, b2, b3 as each formula is used to linearize its respective band.

## 5) Mask values not applicable to Depth Derivations

### Mask NaN Values

The digital image processing methods conducted in steps 4 and 5 are applicable only to deriving depth (or substrate) data from aquatic environments and thus result in rather absurd figures for any land areas in the image. These figures interfere with further statistical calculations needed for processing and translation between ENVI and ArcGIS. To get rid of irrelevant data:

- Have your three single band files active in the “Available Bands List” window.
- On the ENVI main toolbar, click on *Basic Tools > Masking > Build Mask*
  - Choose the display that entails the band of interest
  - In the “Mask Definition” window, click the “Options” dropdown list and check “Selected Areas “off””
  - In the “Mask Definition” window, click the “Options” dropdown list and select “Mask NaN Values”
    - Highlight the file for which a mask is to be created and click OK.
    - Choose a good output file name and place
    - The mask file will be added to the “Available Bands List”
  - Masks for the other two bands can be created at this point without closing the “Mask Definition” window
- On the ENVI main toolbar, click on *Basic Tools > Masking > Apply Mask*
  - Choose the file to which a NaN mask is to be applied as the input file and click OK.
  - In the “Apply Mask Input File” window, click the “Select Mask Band” button
    - In the “Select Mask Input Band” window, choose the mask appropriate to the input file and click OK.
  - In the “Apply Mask Parameters” window, accept the mask value of 0, give the file a good name and location and click OK.

### Cloud/Land Masking

In the context of converting spectral data to bathymetric information, cloud masking serves the purpose of nullifying the value of pixels that contain clouds or cloud shadow since accurate depth cannot be derived from this spectral information. There are some methods to create masks by radiance values that may be unique to a feature. My testing of this approach revealed that there was too much spectral overlap between clouds and bright sand/coral rubble in shallow areas to employ such a method. I deemed the best approach would be to manually create a cloud/shadow mask by visual assessment of the image.

To create a mask and apply it to an image:

- In ENVI, open the desired file.
  - From the main tool bar, click on *Basic Tools > Region of Interest > ROI Tool*
  - With the “ROI Tool” open you can...
    - Use the mouse/cursor to draw shapes around each cloud and its shadow
      - Left click and hold it down to drag a line with the mouse
      - Left click and release to register points to be connected
      - Double right click to close and accept each shape.
    - Save ROI for later use as a mask
      - In the “ROI Tool” window click on *File > Save ROIs...*
      - Choose the right region (if more than one made)
      - Save it to a good place with a good name.
- From the image display tool bar, click on *Tools > Build Mask...*
  - In the “Mask Definition” window:
    - Click on *Options* and make sure that *Selected Areas “Off”* and *Selected Attributes (Logical OR)* have checkmarks.
    - Click on *Options > Import ROIs*
      - If your ROI is active, you can select it from the list. If it is not, you can navigate to the saved .roi file by clicking on the “Open ROI file...” button
      - Name and save the mask file in a good spot.
- From the main tool bar, click on *Basic Tools > Masking > Apply Mask*
  - Select the image to which the mask will be applied as the input file.
  - Click on the “Select Mask Band” button and choose the mask file that was just created in the last step.
    - Accept other defaults
    - Name it and put it away

## 6) Georectify Processed Imagery with Sonar Bathymetry

The IKONOS images are in a Geographic Lat/Long projection with the WGS84 datum while the multi-beam data is projected in UTM, zone 2S using the WGS84 datum.

I was not able to solve this problem using just ArcGIS tools, probably because ENVI files viewed in ArcGIS cannot be reprojected in ArcGIS. The solution was the use of both programs in re-projection.

- To re-project the ENVI files to correct the geographic offset:
  - On the ENVI main toolbar, click *Map > Convert Map Projection*
  - Select the file of concern and click OK
- In the “Convert Map Projection Parameters” window click on the “Change Proj...” button
  - Highlight “UTM”
  - Click the “Datum” button and select “WGS-84”
  - Use the toggle arrows to select zone 2 and be sure to indicate S (south)
  - Leave everything else as the defaults (especially the resampling at nearest neighbor so that pixel values are not changed).
  - Give the file a good name and storage place.

This file is now in the same projection and has the same spatial reference as the multibeam data. It is also the spatial reference of the Arcmap project (as long as the multibeam data was imported first. However, the actual offset will remain when the file is added to the project. ArcGIS needs to be “told” that this data is in the right projection and spatial reference.

- Import the ENVI file into ArcGIS as described above for the importation of the IKONOS NTF files.
- In ArcToolbox, select *Data Management Tools > Projections and Transformations > Raster > Project*
  - Choose the imported file that was just reprojected in ENVI
  - The input coordinate system will be referenced from the file
  - Indicate a good name and storage spot for the output file
  - 
  - To be absolutely sure that the output coordinate system will match that of the sonar bathy and the project ...
  - Click the button to the right of the input box for the “Output coordinate system”
  - Click the “Import...” button
  - Navigate to the projected bathymetry file, select it and click OK
  - Verify the displayed information and click OK
  - Accept the rest of the defaults and click OK

NOW the datasets are georectified, however in completing this process I discovered yet another issue. There appears to be a referencing problem when there is extensive use of both ENVI files and ArcGIS raster grids in the same ArcMap project even once the files are in the same geographic projection. This throws, again, throws off data referencing by point location. To circumvent this issue, I created an ArcMap project specifically for opening and viewing ENVI files and exported each file as an Arc raster grid for use in another project for working with the multi-beam bathymetry, processed spectral values and derived bathymetry.

- To export the ENVI file as an ESRI raster grid:
  - Right click on the file in the project's table of contents
    - Click *Data > Export Data*
    - In the "Export Raster Data" window
      - Use the dropdown arrow next to "Format:" to select GRID.
      - Give the file a name of less than 13 characters (Arc rule) and click OK.

Note: It is useful to start putting raster grids that have been prepared for data extraction (There should be a bathymetry grid and grids for IKONOS bands one and two that have been the applicable steps above.) into a geodatabase.

## 7) Extract Linearized Spectral Values and Depth Data

The nuts and bolts description of this step is to open the multibeam sonar and the corrected and linearized spectral data and extract data from each of the raster datasets at a consistent set of 150 - 200 points. To get started open the ArcMap project that was initiated back in step one. (or create another one and just re-import the data.)

- If need be, import the bathymetry raster grid and the ENVI files (as described in step 1).
- Double check the georectification of the data as previously described.
- Create a new **point** feature class and add it to the project.
  - In ArcToolbox use, *Data Management Tools > Feature Class > Create Feature Class*
  - Based on the overlay between the spectral and multibeam bathymetry grids, create on the order of 150 - 200 points by which to spectral and depth values.
    - Avoid placing points in areas that have been masked for clouds in the ratio data.
    - Avoid placing points in areas where depth exceeds 25 meters.
  - Add location data to each of the points made
    - In ArcToolbox, open *Data Management Tools > Features > Add XY Coordinates*
    - Input the point feature just created
    - Open the attribute table of the feature to verify addition of x, y locations

- Extract the data from both the multibeam sonar grid and the spectral data grids
  - In ArcToolbox, open *Spatial Analyst Tools > Extraction > Extract Values to Points*
    - Choose the point feature with x, y locations as the input point feature and one of the raster grids as the input raster.
    - Name and locate the output file properly
    - Add the feature to the project (should be automatic)
    - Repeat this with the other data sets
    - The .dbf file (of the several created) can be opened in Excel for the next step

### 8) Perform multiple linear regression analysis and use the resultant formula and coefficients to derive depth

- Create a new Excel worksheet and use the import wizard to open each .dbf file created by ArcGIS for each of the extracted point features.
  - While using the import wizard, begin with row 5 so that the header information is not included when opened in excel.
  - Use the extracted depth file as a base and copy/paste the linearized blue and green spectral values into two additional columns.
    - Label columns appropriately
    - Save the file

Note: There are a number of statistical analysis software programs available for the performance of a multiple linear regression analysis. S-PLUS what was available to me and the description of how I used it follows.

- Perform a multiple linear regression using S-PLUS.
  - On the main toolbar, click *File > Import Data > From File*
    - In the “Import from File” window, click the browse button and navigate to the Excel file that was just created
    - Leave the defaults and click OK
  - On the main toolbar, click *Statistics > Regression > Linear...*
    - In the “Linear Regression” window under the “Model” tab
      - Click the dropdown arrow next to “Dependant:” and choose the name of the column that contains the extracted depths.
      - Use the scroll bar next to “Independent:” and choose the names of the columns that contain the extracted linearized spectral data for the blue and then the green bands
      - Next to “Formula:” a formula that looks something like: **Depth~Band.1.2+Band.2.2** will appear

- All the defaults under all the other tabs should be fine, so click OK
- Lots of statistics will result; the figures important to this analysis are the coefficient values that appear as follows:
- Example Data:

	Value	Std. Error	t value	Pr(> t )
(Intercept)	6.0839	3.3739	1.8032	0.0731
Band.1.2	-2.6775	1.2128	-2.2077	0.0286
Band.2.2	11.6426	2.1936	5.3074	0.0000

- The applicable formula is not immediately apparent in the program, but it is of the form:  $D = a + (b_i)(x_i) + (b_j)(x_j)$ 
  - Where:
    - D = depth
    - a = intercept
    - b = slope
    - x = the linearized spectral value (radiance - radiance<sub>min</sub>) calculated in step 4.
- Use ENVI to derive depths.
  - Open the ENVI files that have been taken all processing steps previously performed in ENVI.
  - On the main tool bar, click *Basic Tools > Band Math*
  - In the “Band Math” window, create the formulas to utilize the above formula and figures.
  - Using the above information the ENVI band math formula would be of the form:  $6.0839 - 2.6775*\text{float}(b1) + 11.6426*\text{float}(b2)$

Note: At this juncture it’s important to point out that neither step 7 nor this entire process is as straight forward or “fool proof” as the instructions might imply. Regarding step 7, I went through several iterations before I had a product that I was satisfied with. I repeated it with extracted values correlated with depth of < 25 meters, < 20 meters and < 15 meters. The < 20 meter product was the most satisfactory, but I still came up with positive values in areas that I was sure (from on site experience and a good look at the original image) had shallow depth of water. My solution to this was to “bring in the tide” by adjusting the Y intercept value to produce deeper depths. This adjustment resulted not only in depths figures where values were positive, but also in a better match of deeper derived depths with the multi-beam bathymetry.

Regarding the whole process, I’ve only derived satisfactory shallow water bathymetry for one of the two images that I was working with for Tutuila. My successful product resulted from an image (central Tutuila) with close to flat calm conditions. The product for western Tutuila had much more severe glint conditions and my product had a depth range of only ~2 meters, between 10 and 12 meters. Communication with Eric Hochberg indicates that the glint in the image is extreme and that multiple negative values result from the lint correction due to likely whitecaps in the image. High quality original imagery is paramount.

## 9) Integrate Derived Bathymetry with Sonar Bathymetry

### Derived Bathymetry preparation and integration

- Import the ENVI derived bathymetry file (**step 6**) into the project containing the multi-beam bathymetry.
  - Verify georectification
- Edit the derived bathy grids so that only grid cells with a value between -20 and 0 contain data as follows:
- Reclassify the derived bathy grids into a new raster where each grid cell with a value between 0 and -20 is changed to 1 and values outside this range are changed to NoData.
  - Use (in ArcToolbox) *Spatial Analyst Tools > Reclass > Reclassify* to create a new raster grid
    - Click the “Classify” button
    - Use the dropdown list to change “Method” to Equal Interval
    - Change the number of “Classes” to 3
    - Change “Method” back to Manual
    - Set the displayed “break values” to:
      - -20
      - 0
      - The maximum positive default (**This should be the default**, however, I’ve had the program fail to recognize the highest positive value. I this occurs, simply set the positive value sufficiently high to include unrecognized values.)
        - Click “OK”
    - Assign all of the pixels that had a value between 0 and -20 a new value of 1.
    - Assign all of the pixels that had a value outside of this range a new value of “NoData”.
      - Click “OK”
  - Use Raster Calculator to multiply the values in this new grid by the values in the derived bathy grid.
    - Open “Raster Calculator” which is found in Spatial Analyst tools.
    - In the “Raster Calculator” expression builder window:
      - Double click on the derived bathymetry grid
      - Click once on the multiply button
      - Double click on the reclassified image that has only has values of “1” and “NoData”
        - Verify that the displayed formula is correct
        - Click “OK”





- To open the ArcGrid command line window:
  - Click the “Start” button in the lower left of your main Windows display and mouse through the dropdown lists to Programs > ArcGIS > ArcInfo Workstation > Grid
    - The command line window will have the command prompt of **Grid:** visible. This is the important window.
    - The other window is for displaying grids, I minimized and did not use it since I was working interactively with an open project.
  - To create a workspace (reference to where the desired files are stored) type:
    - **Grid:** arc CREATEWORKSPACE <path>
      - “arc” directs the program to interpret files in the workspace as arc files.
      - <path> should be where the grids to be worked with are stored.
        - Example:  
J:\hogrefek\TutCTM\_0108\Tut\_IKONOS\_GRD\_2
  - To direct ArcGrid to this workspace (so the program knows where to find files):
    - **Grid:** arc WORKSPACE <path>
  - Enter the expression that will begin filling gaps of “NoData” values in the bathymetry grid without changing original data values. Type:
    - **Grid:** New\_Grid =  
con(isnull(Old\_Grid),focalmean(Old\_Grid,rectangle,4,4),Old\_Grid)
      - “New\_Grid” should be replaced by the name for the new file with gap fills.
      - “Old\_Grid” should be replaced by the input file with gaps.
      - Type “help” at the **Grid:** prompt to access full descriptions of the commands involved in this expression.
    - Description of this function’s utility, as found at ESRI Support (<http://support.esri.com/>) follows:

I did find another solution in the ArcInfo mosaic help text:

"The MOSAIC function itself will not interpolate to fill missing data which may happen while putting a set of grids into one composite entity. The following GRID expression may help to solve the problem by interpolating values of the missing cells. It will fill gaps of up to three rows or columns of NODATA cells (the length of the gap is unrelated) with the mean cell value of the 4 x 4 square, leaving the valid existing data unchanged. If the gap is wider than 3 cells, the size of the focal window may be very conservatively increased.

Grid: final\_mosaic = con(isnull(gap\_mosaic), focalmean(gap\_mosaic, rectangle,4,4), gap\_mosaic) "

My gap was a max of 5 cells wide so I increased the focal window to a 6x6 square. You also have to change the "final\_mosaic" to a new grid name and the "gap\_mosaic" to your old grid name with the gaps in it. This worked great for me, filling the entire gap without changing values anywhere else. Fortunately my gaps were in areas of very little topographic change so a mean of the surrounding cells is okay, if you are interpolating over an area of high relief this command may not be appropriate.

- It may be necessary to run multiple iterations of the expression to entirely fill gaps, by replacing the input file with the most recent gap filled file and changing the output file name.
- Once the “NoData” gaps are filled to the analyst’s satisfaction, the grid is ready to mosaic with the derived bathymetry mosaic.
  - The edges of the raster that you gap filling will get new values too. This could effect the how well the derived and sonar bathy values match up along this edge (could be beneficial!).
  - More gap filling will occur to later grid mosaics, some remaining gaps are OK as long as now unwanted values are showing through “NoData” pixels.

### DEM preparation

The DEM was initially in the NAD1983 datum using the GRS80 ellipsoid with a resolution of 10 meters.

- When the DEM opened in ArcMap it had no geographic reference.
- In ArcToolbox use *Data Management Tools > Projections and Transformations > Define Projection* as described earlier in **Viewing and Georectification of Images**. Except ...
  - In “Geographic Coordinate Systems” choose “North America” and choose “North American Datum 1983.prj”
    - Click “OK”
  - Now the DEM can be reprojected
- In ArcToolbox use *Data Management Tools > Projections and Transformations > Raster > Project* as described earlier in **Viewing and Georectification of Images**. Except ...
  - Note that the “Input coordinate system” is NAD83 as you just defined it.
    - This is fine, for “Output coordinate system” use the “Import” button as described to assign WGS\_1984\_UTM\_Zone\_2S
    - Click “OK”

- In ArcToolbox use *Spatial Analyst Tools > Reclass > Reclassify* to change the grid cell size from 10 meter resolution to 5 meters as described previously in this section.

### Mosaic Derived Bathy, Sonar Bathy and DEM

At this point all raster grids should be in the same projection and have the same raster resolution and may have some preliminary “NoData” gap filling done. Time to Mosaic!

- Mosaic the sonar and derived bathy grids using *Data Management Tools > Raster > Mosaic* as recently described in this section.
  - The sonar bathy is most likely most correct, so assure that grid cells from the sonar bathy get priority in the mosaic.
- Fill “NoData” gaps that exist in the new mosaic using the ArcGrid command line window and the provided expression as described above.

Note: Small “Nodata” gaps left from bogus depth derivations in surf and shallow reef areas were filled with three or four iterations of running the expression. These values can be considered a good estimate of what the depth derivation process might have predicted.

Large “Nodata” gaps left from cloud masking were also filled using the gap fill expression. In the case of the largest gaps, it took 30 iterations to fill them. Of course, the further away from the edge of the original data, the more questionable the depths estimated by the expression. However, no handier or more accurate method exists within Arc (to my knowledge) to accomplish these fills without changing original data in the raster. Further, as the edge of estimated depths advances across gaps through multiple iterations, previously estimated values are not changed resulting in a progressive estimate across the gaps. Though I would not consider these estimated area specifically accurate representation of the terrain in the area, I would consider them reasonably accurate estimate of the terrain based of the best available data.

There are many questionable depth values that advance into the “NoData” hole that represents the island. These values will be superseded by DEM land values in the next mosaic step.

- Once satisfied with the combined sonar/derived bathy mosaic add the 5 m resolution DEM by once again using *Data Management Tools > Raster > Mosaic*.
  - The DEM is most likely most correct where the grids overlap, particularly if extensive gap filling has been conducted as noted just above. So, assure that grid cells from the DEM get priority in the mosaic.
  - Gap filling could be conducted once again if determined necessary.

## Appendix C: U.S. Census Bureau Data

**Table 1: Census Data MTU Assignments**

### Census Data MTU Assignments

MTU	FPL	Village	Census Unit Area (m <sup>2</sup> )	2000 Population	MTU Land Area (km <sup>2</sup> )	MTU Population Density (people/km <sup>2</sup> )
1	48920	Malaeloia Aitulagi	3622508.719	597		
1	49400	Malaeloia Ituau	270785.719	627		
1	24900	Fagalii	1652958.203	259		
1	13700	Asili	1368797.125	250		
1	8100	Amaluia	1802898.984	179		
1	68900	Seetaga	700564.453	270		
1	2500	Afao	1400112.875	188		
1	84100	Utumea West	670042.984	44		
1	76900	Taputimu	883542.266	640		
1	8900	Amanave	837947.078	287		
1	4500	Agugulu	401742.766	45		
1	56900	Nua	934654.109	207		
1	50500	Maloata	3006815.688	17		
1	64900	Poloa	855157.219	203		
1	29700	Failolo	619912.000	128		
1	44900	Leone	5812198.766	3568		
1*	25700	Fagamalo	1904429.96	20		
1*	87300	Vailoatai	412919.953	330		
1*	36100	Futiga	1041120.75	183		
<b>Totals</b>			<b>28199109.617</b>	<b>8042</b>	<b>/28.199109=</b>	<b>285.18</b>
2*	25700	Fagamalo	1904429.96	20		
2	100	Aasu	777784.188	364		
2	12800	Aoloau	5472841.469	778		
<b>Totals</b>			<b>15155055.62</b>	<b>1162</b>	<b>/15.155056=</b>	<b>76.67</b>
3	27300	Fagasa	4243933.313	900		
3*	62500	Pago Pago	3504030.56	278		
<b>Totals</b>			<b>7747963.873</b>	<b>1178</b>	<b>/7.747964 =</b>	<b>152.04</b>
4	66500	Sailele	1415742.500	100		
4	12100	Aoa	1728147.281	507		
4	4900	Alao	1490300.563	528		
4	81700	Tula	1357542.250	413		
4	61700	Onenoa	1026042.625	153		
4	53700	Masausi	838125.938	178		
4	54500	Masefau	4185745.281	435		
4	3300	Afono	3005366.281	530		
4	89700	Vatia	5694983.375	648		
4*	18500	Aunuu	763070.094	238		
<b>Totals</b>			<b>21505066.188</b>	<b>3730</b>	<b>/21.505066=</b>	<b>173.45</b>

5*	18500	Aunuu	763070.094	238		
5	56100	Mesepa	792848.219	481		
5	15300	Aua	2832894.344	2193		
5	9700	Amaua	871352.656	102		
5	16100	Auasi	660043.469	125		
5	83300	Utumea East	368534.813	64		
5	44100	Leloaloea	869554.594	534		
5	62230	Pagai	369226.313	122		
5	11300	Anua	311637.781	265		
5	20100	Auto	826699.250	258		
5	14500	Atuu	89399.719	413		
5	6500	Alega	796030.375	54		
5	28900	Fagatogo	1843725.656	2096		
5	82500	Utulei	865599.781	807		
5	48100	Malaeimi	3821770.125	1076		
5	26500	Faganeanea	1289407.969	183		
5	52900	Mapusagafou	2789210.813	1642		
5	57700	Nuuuli	7557305.250	5154		
5	22500	Fagaalu	1077917.850	1006		
5	55300	Matuu	1210916.737	385		
5	32900	Fatumafuti	102367.319	103		
5	40800	Laulii	1269996.031	937		
5	20900	Avaio	750233.500	57		
5	23300	Fagaitua	1398171.156	483		
5	7300	Alofau	1326786.094	495		
5	10500	Amouli	1635690.813	520		
5	17700	Aumi	2304784.188	249		
5*	32100	Falenui	336000.203	1028		
5*	75300	Tafuna	3472495.55	4205		
5*	62500	Pago Pago	5840050.94	4000		
		<b>Totals</b>	<b>48443721.6</b>	<b>29275</b>	<b>/48.443722=</b>	<b>604.31</b>
6*	32100	Falenui	336000.203	1028		
6*	75300	Tafuna	3472495.55	4205		
6	64100	Pavaiai	2410930.406	2200		
6	36900	Ilili	3347157.813	2513		
6*	88100	Vaitogi	1058721.38	449		
		<b>Totals</b>	<b>10625305.35</b>	<b>10395</b>	<b>/10.625305=</b>	<b>978.32</b>
7*	88100	Vaitogi	1058721.38	449		
7*	36100	Futiga	1388161	244		
		<b>Totals</b>	<b>2446882.38</b>	<b>693</b>	<b>/2.446882 =</b>	<b>283.217537</b>
8*	36100	Futiga	694080.5	0		
		<b>Totals</b>	<b>694080.5</b>	<b>0</b>	<b>/0.694081 =</b>	<b>0</b>

\* Indicates that census tract data has been divided between 2 or more MTUs.

**Table 2: Multiple MTU Census Tract Data Allocation**

Multiple MTU Census Tract Data  
Allocation

MTUs	FPL	Village	Census Unit Area (m <sup>2</sup> )	2000 Population	Allocation Comments
<b>1/2</b>	25700	Fagamalo	3808859.922	39	Allocation: half and half
<b>1/7/8/NA</b>	36100	Futiga	4164483	731	Allocation: 1/4 to 1, 1/3 to 7, Nothing to 8(Fagatele Bay).
<b>1/NA</b>	87300	Vailoatai	1238759.859	989	Allocation: Just 1/3 in 1, rest NA
<b>3/5</b>	62500	Pago Pago	9344081.5	4278	Issue: Census unit crosses over to N side of island - Most of pop HAS to be on Pago Pago side. Area = 5/8 to South (Pago) side and 3/8 to North side. Population in year 2000 = 4000 on Pago side and 278 on N side.
<b>4/5</b>	18500	Aunuu	1526140.188	476	half and half
<b>5/6</b>	32100	Faleniu	672000.406	2056	half and half
<b>5/6</b>	75300	Tafuna	6944991.094	8409	half and half
<b>6/7</b>	88100	Vaitogi	3176164.125	1347	Issue here: Census unit crosses over several NA catchments (no REA) with east and west ends of unit in MTUs 6 and 7. Central NA units probably effect both 6 and 7. Split 1/3 to 6, 1/3 to 7, 1/3 NA.

### Appendix D: REA Coral Reef Assessment Data MTU Summary

Site	Date	MTU	% Live CC	% Live CC MTU Avg.	Coral Colony Den.	Coral Colony Den. MTU Avg.	Gen. Rich.	Gen. Rich. MTU Avg.	Gen. Rich. MTU Total Count
TUT-06	2/25/2004	1	43		7.18		24		
TUT-07	2/25/2004	1	53		3.26		15		
TUT-23	2/24/2004	1	30		7.12		19		
		<b>1</b>		<b>42</b>		<b>5.9</b>		<b>19.3</b>	<b>29</b>
TUT-08	2/25/2004	2	15		3.06		14		
TUT-12	2/21/2004	2	10		2.30		12		
		<b>2</b>		<b>13</b>		<b>2.7</b>	<b>13</b>	<b>13</b>	<b>17</b>
TUT-13	2/21/2004	3	10		4.00		21		
TUT-18	2/20/2004	3	45		11.66		23		
TUT-19	2/21/2004	3	50		7.57		18		
		<b>3</b>		<b>35</b>		<b>7.7</b>		<b>20.7</b>	<b>30</b>
TUT-04	2/19/2004	4	35		7.96		22		
TUT-05	2/20/2004	4	43		7.84		18		
TUT-14	2/20/2004	4	40		7.08		22		
TUT-17	2/19/2004	4	28		11.74		24		
		<b>4</b>		<b>37</b>	<b>8.66</b>	<b>8.7</b>		<b>21.5</b>	<b>28</b>
TUT-01	2/22/2004	5	50		12.78		23		
TUT-02	2/22/2004	5	30		7.58		23		
TUT-10	2/23/2004	5	50		18.18		24		
TUT-15	2/18/2004	5	5		16.26		18		
TUT-16	2/19/2004	5	73		26.09		26		
TUT-20	2/22/2004	5	15		4.24		24		
		<b>5</b>		<b>37</b>		<b>14.2</b>		<b>23</b>	<b>37</b>
TUT-09	2/23/2004	6	70		31.20		21		
TUT-21	2/23/2004	6	40		30.40		27		
		<b>6</b>		<b>55</b>		<b>30.8</b>		<b>24</b>	<b>28</b>
TUT-11	2/24/2004	7	45		21.12		26		
		<b>7</b>		<b>45</b>		<b>21.1</b>		<b>26</b>	<b>26</b>
TUT-22	2/24/2004	8	50		16.48		24		
		<b>8</b>		<b>50</b>		<b>16.5</b>		<b>24</b>	<b>24</b>
TUT-06	2006	1	49		0.00		0		
TUT-07	2006	1	0		0.00		0		
TUT-23	2006	1	34		0.00		0		
		<b>1</b>		<b>28</b>		<b>N/A</b>		<b>N/A</b>	<b>N/A</b>
TUT-08	2006	2	18		0.00		0		
TUT-12	2006	2	15		0.00		0		
		<b>2</b>		<b>16</b>		<b>N/A</b>		<b>N/A</b>	<b>N/A</b>
TUT-13	2/19/2006	3	10		5.28		17		
TUT-18	2/19/2006	3	10		3.18		14		
TUT-19	2006	3	8		0.00		0		
		<b>3</b>		<b>9</b>		<b>4.23</b>		<b>15.5</b>	<b>17</b>

TUT-04	2/18/2006	4	16		3.84		20		
TUT-05	2/18/2006	4	30		5.32		14		
TUT-14	2/19/2006	4	15		4.20		15		
TUT-17	2/18/2006	4	16		5.22		18		
		<b>4</b>		<b>19</b>		<b>4.7</b>		<b>16.8</b>	<b>24</b>
TUT-01	2/22/2006	5	15		5.70		15		
TUT-02	2/22/2006	5	36		4.88		17		
TUT-10	2/24/2006	5	21		10.72		15		
TUT-15	2/22/2006	5	20		6.06		14		
TUT-16	2/23/2006	5	64		10.48		14		
TUT-20	2/23/2006	5	10		1.54		11		
		<b>5</b>		<b>28</b>		<b>6.6</b>		<b>14.3</b>	<b>27</b>
TUT-09	2/23/2006	6	60		11.28		16		
TUT-21	2/25/2006	6	20		8.98		22		
		<b>6</b>		<b>40</b>		<b>10.1</b>		<b>19</b>	<b>25</b>
TUT-11	2/25/2006	7	39		8.22		19		
		<b>7</b>		<b>39</b>		<b>8.2</b>		<b>19</b>	<b>19</b>
TUT-22	2/25/2006	8	27		7.00		19		
		<b>8</b>		<b>27</b>		<b>7</b>		<b>19</b>	<b>19</b>

## Appendix E: Correlation Co-efficient Calculations.

### Correlation Co-efficient Calculations

#### 2004 REA Data

MTU	2000 Population Density (People/km <sup>2</sup> )	Average % Coral Cover	X*Y	X <sup>2</sup>	Y <sup>2</sup>	N	Corr. Coeff.
8	0	50	0	0	2500	8	
2	77	13	996.76308	5878.9150	169		
3	152	35	5321.3980	23116.144	1225		
4	173	37	6417.5575	30084.035	1369		
7	283	45	12744.789	80212.173	2025		
1	285	42	11977.825	81331.231	1764		
5	604	37	22359.450	365189.94	1369		
6	978.3248251	55	53807.865	957119.46	3025		
<b>Sum =</b>	<b>2553.199677</b>	<b>314</b>	<b>113625.64</b>	<b>1542931.9</b>	<b>13446</b>		<b>0.469</b>

MTU	2000 Population Density (People/km <sup>2</sup> )	Average Coral Density	X*Y	X <sup>2</sup>	Y <sup>2</sup>	N	Corr. Coeff.
8	0	16.5	0	0	272.25	8	
2	76.67408351	2.7	207.02002	5878.9150	7.29		
3	152.0399449	7.7	1170.7075	23116.144	59.29		
4	173.4475015	8.7	1508.9932	30084.035	75.69		
7	283.2175366	21.1	5975.8900	80212.173	445.21		
1	285.1863094	5.9	1682.5992	81331.231	34.81		
5	604.3094757	14.2	8581.1945	365189.94	201.64		
6	978.3248251	30.8	30132.404	957119.46	948.64		
<b>Sum =</b>	<b>2553.199677</b>	<b>107.6</b>	<b>49258.809</b>	<b>1542931.9</b>	<b>2044.82</b>		<b>0.715</b>

MTU	2000 Population Density (People/km <sup>2</sup> )	Average Generic Richness	X*Y	X <sup>2</sup>	Y <sup>2</sup>	N	Corr. Coeff.
8	0	24	0	0	576	8	
2	76.67408351	13	996.76308	5878.9150	169		
3	152.0399449	20.7	3147.2268	23116.144	428.49		
4	173.4475015	21.5	3729.1212	30084.035	462.25		
7	283.2175366	26	7363.6559	80212.173	676		
1	285.1863094	19.3	5504.0957	81331.231	372.49		
5	604.3094757	23	13899.117	365189.94	529		
6	978.3248251	24	23479.795	957119.46	576		
<b>Sum =</b>	<b>2553.199677</b>	<b>171.5</b>	<b>58119.776</b>	<b>1542931.9</b>	<b>3789.23</b>		<b>0.373</b>

MTU	2000 Population Density (People/km <sup>2</sup> )	Total Generic Richness	X*Y	X2	Y2		N	Corr. Coeff.
8	0	24	0	0	576		8	
2	76.67408351	17	1303.4594	5878.9150	289			
3	152.0399449	30	4561.1983	23116.144	900			
4	173.4475015	28	4856.5300	30084.035	784			
7	283.2175366	26	7363.6559	80212.173	676			
1	285.1863094	29	8270.4029	81331.231	841			
5	604.3094757	37	22359.450	365189.94	1369			
6	978.3248251	28	27393.095	957119.46	784			
<b>Sum =</b>	<b>2553.199677</b>	<b>219</b>	<b>76107.792</b>	<b>1542931.9</b>	<b>6219</b>			<b>0.486</b>

## 2006 REA Data

MTU	2000 Population Density (People/km <sup>2</sup> )	Average % Coral Cover	X*Y	X2	Y2		N	Corr. Coeff.
8	0	27	0	0	729		6	
3	152.0399449	9	1368.3595	23116.144	81			
4	173.4475015	19	3295.5025	30084.035	361			
7	283.2175366	39	11045.483	80212.173	1521			
5	604.3094757	28	16920.665	365189.94	784			
6	978.3248251	40	39132.993	957119.46	1600			
<b>Sum =</b>	<b>2191.339284</b>	<b>162</b>	<b>71763.004</b>	<b>1455721.7</b>	<b>5076</b>			<b>0.587</b>

MTU	2000 Population Density (People/km <sup>2</sup> )	Average Coral Density	X*Y	X2	Y2		N	Corr. Coeff.
8	0	7	0	0	49		6	
3	152.0399449	4.2	638.56776	23116.144	17.64			
4	173.4475015	4.7	815.20325	30084.035	22.09			
7	283.2175366	8.2	2322.3838	80212.173	67.24			
5	604.3094757	6.6	3988.4425	365189.94	43.56			
6	978.3248251	10.1	9881.0807	957119.46	102.01			
<b>Sum =</b>	<b>2191.339284</b>	<b>40.8</b>	<b>17645.678</b>	<b>1455721.7</b>	<b>301.54</b>			<b>0.690</b>

MTU	2000 Population Density (People/km <sup>2</sup> )	Average Generic Richness	X*Y	X2	Y2		N	Corr. Coeff.
8	0	19	0	0	361		6	
3	152.0399449	15.5	2356.6191	23116.144	240.25			
4	173.4475015	16.8	2913.9180	30084.035	282.24			
7	283.2175366	19	5381.1332	80212.173	361			
5	604.3094757	14.3	8641.6255	365189.94	204.49			
6	978.3248251	19	18588.171	957119.46	361			
<b>Sum =</b>	<b>2191.339284</b>	<b>103.6</b>	<b>37881.467</b>	<b>1455721.7</b>	<b>1809.98</b>			<b>0.011</b>

MTU	2000 Population Density (People/km <sup>2</sup> )	Total Generic Richness	X*Y	X2	Y2		N	Corr. Coeff.
8	0	19	0	0	361		6	
3	152.0399449	17	2584.6790	23116.144	289			
4	173.4475015	24	4162.7400	30084.035	576			
7	283.2175366	19	5381.1332	80212.173	361			
5	604.3094757	27	16316.355	365189.94	729			
6	978.3248251	25	24458.120	957119.46	625			
<b>Sum =</b>	2191.339284	131	52903.028	1455721.7	2941			<b>0.695</b>

#### 2004-2006 REA Data % Change

MTU	2000 Population Density (People/km <sup>2</sup> )	Average % Coral Cover	X*Y	X2	Y2		N	Corr. Coeff.
8	0	-46	0	0	2116		6	
3	152.0399449	-74.2857	-11294.39	23116.144	5518.3673			
4	173.4475015	-48.6486	-8437.986	30084.035	2366.6910			
7	283.2175366	-13.3333	-3776.233	80212.173	177.77777			
5	604.3094757	-24.3243	-14699.42	365189.94	591.67275			
6	978.3248251	-27.2727	-26681.58	957119.46	743.80165			
<b>Sum =</b>	2191.339284	-233.8647	-64889.62	1455721.7	11514.310			<b>0.517</b>

MTU	2000 Population Density (People/km <sup>2</sup> )	Average Coral Density	X*Y	X2	Y2		N	Corr. Coeff.
8	0	-57.5757	0	0	3314.9678		6	
3	152.0399449	-45.4545	-6910.906	23116.144	2066.1157			
4	173.4475015	-45.9770	-7974.597	30084.035	2113.8855			
7	283.2175366	-61.1374	-17315.19	80212.173	3737.7866			
5	604.3094757	-53.5211	-32343.32	365189.94	2864.5110			
6	978.3248251	-67.2077	-65751.05	957119.46	4516.8873			
<b>Sum =</b>	2191.339284	-330.8736	-130295.0	1455721.7	18614.154			<b>-0.608</b>

MTU	2000 Population Density (People/km <sup>2</sup> )	Average Generic Richness	X*Y	X2	Y2		N	Corr. Coeff.
8	0	-20.8333	0	0	434.02777		6	
3	152.0399449	-25.1207	-3819.360	23116.144	631.05323			
4	173.4475015	-21.8604	-3791.643	30084.035	477.87993			
7	283.2175366	-26.9230	-7625.087	80212.173	724.85207			
5	604.3094757	-37.8260	-22858.66	365189.94	1430.8128			
6	978.3248251	-20.8333	-20381.76	957119.46	434.02777			
<b>Sum =</b>	2191.339284	-153.3970	-58476.52	1455721.7	4132.6536			<b>-0.208</b>

MTU	2000 Population Density (People/km <sup>2</sup> )	Total Generic Richness	X*Y	X2	Y2		N	Corr. Coeff.
8	0	-20.8333	0	0	434.02777		6	
3	152.0399449	-43.3333	-6588.397	23116.144	1877.7777			
4	173.4475015	-14.2857	-2477.821	30084.035	204.08163			
7	283.2175366	-26.9230	-7625.087	80212.173	724.85207			
5	604.3094757	-27.0270	-16332.68	365189.94	730.46019			
6	978.3248251	-10.7142	-10482.05	957119.46	114.79591			
<b>Sum =</b>	2191.339284	-143.1167	-43506.04	1455721.7	4085.9953			<b>0.417</b>

## **Appendix F: Data processing “Cookbook” of processing steps taken in Arc Hydro**

### **Terrain Analysis Processing “Cookbook”:**

**A summary of steps taken to conduct a terrain analysis of the Tutuila CTM using the Arc Hydro data model and processing tools.**

Produced by: Kyle R Hogrefe  
 Master’s Candidate - Oregon State University, Dept. of Geosciences  
 6/20/08

### **Introduction**

This document will provide a step by step summary , with comments concerning processing methods and accuracy issues, of the Arc Hydro processing steps used to conduct a terrain analysis of the coastal terrain model (CTM) created for the island of Tutuila, American Samoa (Hogrefe et al., submitted). It should be noted that, due to time constraints, the full functionality of Arc Hydro was not utilized in this analysis. However, the data management functionality and the fundamental processing steps that were used were well suited for the marine/terrestrial unit (MTU) analysis conducted in the second manuscript of this thesis (Hogrefe and Wright, unpublished).

### **Inputs**

The Tutuila, American Samoa CTM (Hogrefe et al., submitted)

#### CTM Information:

Produced by: Kyle R. Hogrefe, OSU Geosciences, Davey Jones Locker GIS  
 Lab

Creation Date: 02/21/2008

Data Sources: Elevation, 10m USGS DEM

Near shore bathymetry, derived 4m IKONOS imagery

Off shore bathymetry, 5m multibeam sonar grid.

Projection: WGS 1984, UTM zone 2S

Resolution: 5 x 5 m

### **Software Used**

ArcGIS 9.2 by Environmental Systems Research Institute, Inc., Redlands, CA (ESRI) with the Arc Hydro data model and data processing tools. Arc Hydro was developed by a consortium established by the Center for Research in Water Resources of the University of Texas at Austin and the Environmental Systems Research Institute

## **Processing Steps and Data Model Use**

The Arc Hydro processing tools used in MTU determination are all found in the “Terrain Preprocessing” tool set. This level of processing just begins to use the functionality of the Arc Hydro data model, but the ability to tag files as particular types as part of the “Data Management” function (described below) enables further processing steps. The data model automatically creates a personal geodatabase and a layers folder for file storage and management as processing is initiated. All default tags were accepted during processing.

### **Data Management** (Source: Arc Hydro Help)

Arc Hydro manages the input/output to the tools by using tags that are automatically assigned by the functions to the selected inputs and outputs. A tag may be used as input by one function and as output by another one. For example, the "Flow Direction Grid" tag is an output from Flow Direction, and an input to Flow Accumulation.

The Data Management function in the Terrain Preprocessing menu provides a global view of the tags assignments for that menu in the active Map/Data Frame. The function also allows assigning, reassigning or resetting the tags. A tag may be reset by selecting "Null" as the corresponding layer. When a reset tag is used as output, the function presents the user with the default layer name associated to the tag. This default name is defined in the XML file and may be modified (see XML Manager).

How the function works

- The pull down menu next to each tag offers for selection only those themes in the active data frame that match the required theme type (line, point, polygon, grid).
- A "Null" option is available in the list. Selecting "Null" remove the theme assigned to that role.
- A layer may be assigned several tags. When a layer is used with an additional tag, the user is warned that at least one other tag has already been assigned to this theme.
- A tag may be assigned to one and only one layer at any time.

The specific processing steps used for MTU determination are presented in Table 1.

**Table 1: Tags defined in Arc Hydro “Terrain Preprocessing” used for MTU analysis.**

Tag	Output from	Input to
Hydro DEM		Flow Direction Flow Direction with Sinks Sink Segmentation
Flow Direction Grid	Flow Direction Flow Direction with Sinks	Adjust Flow Direction in Lakes Flow Accumulation Stream Segmentation Catchment Grid Delineation Drainage Line Processing
Flow Accumulation Grid	Flow Accumulation	Stream Definition Drainage Point Processing
Stream Grid	Stream Definition	Stream Segmentation
Link Grid	Stream Segmentation	Catchment Grid Delineation Drainage Line Processing
Catchment Grid	Catchment Grid Delineation	Catchment Polygon Processing Drainage Point Processing
Catchment	Catchment Polygon Processing	Adjoint Catchment Processing Drainage Point Processing
Drainage Line	Drainage Line Processing	Adjoint Catchment Processing
Adjoint Catchment	Adjoint Catchment Processing	
Raw DEM		Slope Hydro DEM

**Step 1: DEM Reconditioning (AGREE)** (Source: Arc Hydro Help)

The DEM Reconditioning function (DEM Manipulation menu) modifies Digital Elevation Models (DEMs) by imposing linear features onto them (burning/fencing). This function is an implementation of the AGREE method developed by Ferdi Hellweger at the University of Texas at Austin in 1997. For a full reference to the procedure refer to the web link

<http://www.ce.utexas.edu/prof/maidment/GISHYDRO/ferdi/research/agree/agree.html>.

The function needs two inputs that both have to be present in the map document:

**Input**

"Raw DEM" Grid

**Output**

"Agree DEM" Grid

Input/Output Management

If there is a grid theme that has a tag "Raw DEM", it will be used as a default for the input grid. If not, the user needs to select an existing grid theme name that will be tagged with the "Raw DEM" tag at the end of the operation.

If there is a linear feature class that has a tag "Agree Stream", it will be used as a default for the input feature class. If not, the user needs to select an existing linear feature class that will be tagged with the "Agree Stream" tag at the end of the operation.

If there is a grid theme that has a tag "Agree DEM", it will be used as a default for the output grid. If not, the user needs to specify a grid name that will be tagged with the "Agree DEM" tag at the end of the operation. If the specified output grid already exists, the user is prompted whether to remove the existing dataset.

The user needs to enter three reconditioning parameters:

- Stream buffer (cells) – this is the number of cells around the linear feature class for which the smoothing will occur.
- Smooth drop/raise – this is the amount (in vertical units) that the river will be dropped (if the number is positive) or the fence extruded (if the number is negative). This value will be used to interpolate DEM into the buffered area (between the boundary of the buffer and the dropped/raised vector feature).
- Sharp drop/raise – this is the additional amount (in vertical units) that the river will be dropped (if the number is positive) or the fence extruded (if the number is negative). This has the effect of additional burning/fencing on top of the smooth buffer interpolation. It needs to be performed to ensure preserving the linear features used for burning/fencing.

The values used for the AGREE parameters depend on the nature of the DEM and the issues that are being resolved. In many cases, a trial and error approach is needed before satisfactory results are obtained. Refer to the original paper for some guidelines on the initial parameter selection.

The reconditioned AGREE DEM should be processed with the Fill Sinks function to ensure that the potential sinks generated in the streams are removed. The resulting filled DEM will be used to compute the flow direction/flow accumulation.

Tutuila CTM Application: The following Arc Hydro default settings were accepted: Stream buffer = 5, Smooth drop/raise = 10, Sharp drop/raise 1000.

## Step 2: Fill Sinks (Source: Arc Hydro Help)

The Fill Sinks function (DEM Manipulation menu) fills sinks in a grid. If a cell is surrounded by higher elevation cells, the water is trapped in that cell and cannot flow. The Fill Sinks function modifies the elevation value to eliminate these problems. A Deranged Polygon feature class may be specified to define areas that should not be filled. A threshold may also be specified – in that cases only sinks, whose depth is lower than the threshold will be filled.

Note that the function works on a selected set of Deranged Polygon features, or on all features if there is no selected set. The polygons to use may further restricted by using the IsSink field to define the sinks (Populated by function Sink Selection).

The function takes as input a DEM grid ("DEM" tag), which can be either an unprocessed DEM or a preprocessed DEM created with functions Build Walls and/or DEM Reconditioning ("AgreeDEM " tag). The function produces as output a grid ("Hydro DEM" tag) where no sinks exist.

A default threshold may be set in the XML with the parameter FillThreshold located under the node FrameworkConfig/HydroConfig/ProgParams/ApFunctions/ApFunction (FillSinks).

### **Input**

"DEM" Grid  
 "Deranged Polygon" Feature Class  
 (optional)  
 Fill Threshold (optional)

### **Output**

"Hydro DEM" Grid

### **Input/Output Management**

If there is a grid theme that has a tag "DEM", it will be used as a default for the input grid. If not, the user needs to specify an existing grid theme name that will be tagged with the "DEM" tag at the end of the operation.

If there is a polygon feature class that has a tag "Deranged Polygon", it will be used as a default for the input polygon feature class. If not, the user needs to specify a feature class name that will be tagged with the "Deranged Polygon" tag at the end of the operation.

If there is a grid theme that has a tag "Hydro DEM", it will be used as a default for the output grid. If not, the user needs to specify a grid name that will be tagged with the "Hydro DEM" tag at the end of the operation. If the specified output grid already exists, the user is prompted whether to remove the existing dataset.

Filling sinks is an iterative process that can be time-consuming. The status of the processing will be displayed in the ArcMap status bar.

Filling sinks is an operation that needs to be executed with care. The resulting DEM will have no inner depressions, that is, all the runoff from the DEM will reach its edges. In most cases, this is a correct assumption (when depressions are the artifacts of DEM generation), but in some cases that is not correct (e.g. inner lakes). In such cases, the hydrologically correct DEM needs to be developed in a different manner outside of Arc Hydro, and provided to Arc Hydro for processing. The Fill Sinks operation should not be performed, but rather the hydrologically correct DEM should be used in place of the "Hydro DEM".

Tutuila CTM Application: The input DEM was the "Agree DEM" of the Tutuila CTM output from step 1. The Arc Hydro default of 10 was used for the "Fill Threshold". The "Deranged Polygon" option was not used.

### **Step 3: Flow Direction** (Source: Arc Hydro Help)

The Flow Direction function (Terrain Preprocessing menu) takes a grid ("Hydro DEM" tag) as input, and computes the corresponding flow direction grid ("Flow Direction Grid" tag). The values in the cells of the flow direction grid indicate the direction of the steepest descent from that cell.

If an Outer Wall Polygon is specified, the resulting Flow Direction Grid will be masked to this feature class. This allows getting rid of the expanded extent created by the Build Walls Function.

#### **Input**

"Hydro DEM" Grid  
 "Outer Wall Polygon" Feature Class  
 (optional)

#### **Output**

"Flow Direction Grid"

#### **Input/Output Management**

If there is a grid theme that has a tag "Hydro DEM", it will be used as a default for the input grid. If not, the user needs to select an existing grid theme name that will be tagged with the "Hydro DEM" tag at the end of the operation.

If there is a polygon feature class that has a tag "Outer Wall Polygon", it will be used as a default for the input polygon feature class. If not, the user needs to select an existing polygon feature class that will be tagged with the "Outer Wall Polygon" tag at the end of the operation.

If there is a grid theme that has a tag "Flow Direction Grid", it will be used as a default for the output grid. If not, the user needs to specify a grid name that will be tagged with the "Flow Direction Grid" tag at the end of the operation. If the specified output grid already exists, the user is prompted whether to remove the existing dataset.

Tutuila CTM Application: The input DEM was the “Hydro DEM” output from step 2. The "Outer Wall Polygon" option was not used. There were no user defined parameters to be set.

#### **Step 4: Flow Accumulation** (Source: Arc Hydro Help)

The Flow Accumulation function (Terrain Preprocessing menu) takes as input a flow direction grid ("Flow Direction Grid" tag). It computes the associated flow accumulation grid ("Flow Accumulation Grid" tag) that contains the accumulated number of cells upstream of a cell, for each cell in the input grid.

##### **Input**

"Flow Direction Grid"

##### **Output**

"Flow Accumulation Grid"

##### **Input/Output Management**

If there is a grid theme that has a tag "Flow Direction Grid", it will be used as a default for the input grid. If not, the user needs to select an existing grid theme name that will be tagged with the "Flow Direction Grid" tag at the end of the operation.

If there is a grid theme that has a tag "Flow Accumulation Grid", it will be used as a default for the output grid. If not, the user needs to specify a grid name that will be tagged with the "Flow Accumulation Grid" tag at the end of the operation. If the specified output grid already exists, the user is prompted whether to remove the existing dataset.

Flow accumulation processing is the most time consuming task in the terrain preprocessing and can take a lot of time to complete. It requires significant computer memory (at least 64MB of RAM, preferably more) and a significant amount of hard disk space (about 5 times the size of the final flow accumulation GRID). If the function fails to operate properly, the most likely reason is the lack of hard disk space. The lack of memory can greatly increase the time required for processing.

Tutuila CTM Application: The input was the "Flow Direction Grid" output from step 3. There were no user defined parameters to be set.

#### **Step 5: Stream Definition** (Source: Arc Hydro Help)

The Stream Definition function (Terrain Preprocessing menu) takes a flow accumulation grid ("Flow Accumulation Grid" tag) as input and creates a Stream Grid ("Stream Grid" tag) for a user-defined threshold. This threshold is defined either as a number of cells (default 1%) or as a drainage area in square kilometers.

This initial stream definition (and related Catchments definition) has no meaning for later basin processing (except for performance during the extraction stage), since all parameters can be changed. In general, the recommended size for stream threshold definition (which in turn defines the sub basin delineation during preprocessing) is 1% of the overall area. For increased performance on large DEMs (over 20,000,000 cells), the size of the threshold may be increased to reduce the stream network and the number of catchment polygons.

The area may be entered only if the ground unit has been set in the spatial references (Refer to How to Define ground unit and z-unit for additional information). The resulting stream grid contains a value of "1" for all the cells in the input grid that have a value greater than the given threshold. All other cells in the Stream Grid contain no data.

**Input**  
"Flow Accumulation Grid"

**Output**  
"Stream Grid"

#### Input/Output Management

If there is a grid theme that has a tag "Flow Accumulation Grid", it will be used as a default for the input grid. If not, the user needs to select an existing grid theme name that will be tagged with the "Flow Accumulation Grid" tag at the end of the operation.

If there is a grid theme that has a tag "Stream Grid", it will be used as a default for the output grid. If not, the user needs to specify a grid name that will be tagged with the "Stream Grid" tag at the end of the operation. If the specified output grid already exists, the user is prompted whether to remove the existing dataset.

The user will then be prompted to enter a threshold to define the stream. This threshold is defined as a number of cells: the default is 1% of the maximum flow accumulation value.

Tutuila CTM Application: The input was the "Flow Accumulation Grid" output from step 4. The default stream definition parameter was set to an accumulation value of 45,431 based on the 1% Arc Hydro threshold. This setting resulted in a very sparse stream network. After testing several settings, a threshold accumulation value of 2500 was determined to provide a drainage network of suitable complexity to describe the terrain patterns.

#### **Step 6: Stream Segmentation** (Source: Arc Hydro Help)

The Stream Segmentation function (Terrain Preprocessing menu) creates a grid of stream segments that have a unique identification. Either a segment may be a head segment, or it may be defined as a segment between two segment junctions. All the cells in a particular segment have the same grid code that is specific to that segment.

**Input**

"Flow Direction Grid" Grid  
 "Stream Grid" Grid

**Output**

"Link Grid" Grid

**Input/Output Management**

If there is a grid theme that has a tag "Flow Direction Grid", it will be used as a default for the first input grid. If not, the user needs to select an existing grid theme (of flow direction type) that will be tagged with the "Flow Direction Grid" tag at the end of the operation.

If there is a grid theme that has a tag "Stream Grid", it will be used as a default for the second input grid. If not, the user needs to select an existing grid theme that will be tagged with the "Stream Grid" tag at the end of the operation.

If there is a grid theme that has a tag "Link Grid", it will be used as a default for the output grid. If not, the user needs to specify a grid name that will be tagged with the "Link Grid" tag at the end of the operation. If the output grid already exists, the user is prompted whether to remove the existing dataset.

Tutuila CTM Application: The inputs were the "Flow Direction Grid" from step 3 and the "Stream Grid" from step 5. There were no user defined parameters to be set.

**Step 7: Catchment Grid Delineation** (Source: Arc Hydro Help)

The Catchment Grid Delineation function (Terrain Preprocessing menu) creates a grid in which each cell carries a value (grid code) indicating to which catchment the cell belongs. The value corresponds to the value carried by the stream segment that drains that area, defined in the input Link grid.

**Input**

"Flow Direction Grid"  
 "Link Grid"

**Output**

"Catchment Grid"

**Input/Output Management**

If there is a grid theme that has a tag "Flow Direction Grid", it will be used as a default for the first input grid. If not, the user needs to select an existing grid theme (of flow direction type) that will be tagged with the "Flow Direction Grid" tag at the end of the operation.

If there is a grid theme that has a tag "Link Grid", it will be used as a default for the second input grid. If not, the user needs to specify a grid name that will be tagged with the "Link Grid" tag at the end of the operation.

If there is a grid theme that has a tag "Catchment Grid", it will be used as a default for the output grid. If not, the user needs to specify a grid name that will be tagged with the "Catchment Grid" tag at the end of the operation. If the output grid already exists, the user is prompted whether to remove the existing dataset.

Tutuila CTM Application: The inputs were the "Flow Direction Grid" from step 3 and the "Link Grid" from step 6. There were no user defined parameters to be set.

### **Step 8: Catchment Polygon Processing** (Source: Arc Hydro Help)

The Catchment Polygon Processing function (Terrain Preprocessing menu) takes as input a catchment grid ("Catchment Grid" tag) and converts it into a catchment polygon feature class ("Catchment" tag). The adjacent cells in the grid that have the same grid code are combined into a single area, whose boundary is vectorized. The single cell polygons and the "orphan" polygons generated as the artifacts of the vectorization process are dissolved automatically, so that at the end of the process there is just one polygon per catchment.

#### **Input**

"Catchment Grid"

#### **Output**

"Catchment" Polygon Feature Class

#### **Input/Output Management**

If there is a grid theme that has a tag "Catchment Grid", it will be used as a default for the input grid. If not, the user needs to select an existing grid theme name that will be tagged with the "Catchment Grid" tag at the end of the operation.

If there is a polygon feature class that has a tag "Catchment", it will be used as a default for the output feature class. If not, the user needs to specify a feature class name that will be tagged with the "Catchment" tag at the end of the operation. If the output feature class already exists, the user is prompted whether to remove the existing dataset.

Fields created:

- HydroID: Unique identifier in the Hydro database. System generated.
- GridID: GridCode of the corresponding Catchment grid.

If the target database is an ArcSDE database, all the fields defined in the XML for the layer Catchment will also be created by the function. The following additional fields will be created when using the default XML:

- NextDownID
- JunctionID

Tutuila CTM Application: The input was the "Catchment Grid" from step 7. There were no user defined parameters to be set.

### **Step 9: Drainage Line Processing** (Source: Arc Hydro Help)

The Drainage Line Processing function (Terrain Preprocessing menu) converts the input Stream Link grid into a Drainage Line feature class. Each line in the feature class carries the identifier of the catchment in which it resides.

#### **Input**

"Link Grid"  
"Flow Direction Grid"

#### **Output**

"Drainage Line" Feature Class

#### **Input/Output Management**

If there is a grid theme that has a tag "Link Grid", it will be used as a default for the first input grid. If not, the user needs to select a grid name that will be tagged with the "Link Grid" tag at the end of the operation.

If there is a grid theme that has a tag "Flow Direction Grid", it will be used as a default for the second input grid. If not, the user needs to select an existing grid theme (of flow direction type) that will be tagged with the "Flow Direction Grid" tag at the end of the operation.

If there is a theme that has a tag "Drainage Line", it will be used as a default for the output line feature class. If not, the user needs to specify a feature class name that will be tagged with the "Drainage Line" tag at the end of the operation. If the output feature class already exists, the user is prompted whether to remove the existing dataset.

Fields created:

- GridID – Grid code of the catchment the drainage line segment belongs to.
- FROM\_NODE – From Node number of the drainage line segment.
- TO\_NODE – To Node number of the drainage line segment.
- HydroID – Unique identifier of the drainage line in the Hydro database.
- NextDownID – HydroID of the next downstream drainage line. Populated with "-1" if there is no next downstream line.

If the target database is an ArcSDE database, all the fields defined in the XML for the layer DrainageLine will also be created by the function. The following additional field will be created empty when using the default XML:

- DrainID

### Note

One of the tasks performed by this function is the identification of upstream-downstream relationship. In rare cases, this relationship cannot be determined automatically based on connectivity and DEM, and the user will be asked to identify whether a segment is an outlet or not. This situation usually occurs when a drainage line segment is very short and the elevation at its beginning and end is the same, thus preventing the application from identifying the correct directionality.

In such cases, the questionable segment will be highlighted, the application will zoom on it, and an input box will be brought up. The input box enables the user to zoom in or out of the segment and specify whether the segment is an outlet (most of the times) or not. This process is repeated for every such segment until the directionality is fully established.

The function may also create the two following empty fields in the feature class tagged as "Catchment":

- NextDownID – HydroID of the next downstream catchment.
- JunctionID – HydroID of the junction that serves as the outlet for the catchment.

Tutuila CTM Application: The inputs were the "Link Grid" from step 6 and the "Flow Direction Grid" from step 3. There were no user defined parameters to be set.

### Step 10: Adjoint Catchment Processing (Source: Arc Hydro Help)

The Adjoint Catchment Processing function (Terrain Preprocessing menu) generates the aggregated upstream catchments from the "Catchment" feature class. For each catchment that is not a head catchment, a polygon representing the whole upstream area draining to its inlet point is constructed and stored in a feature class that has an "Adjoint Catchment" tag. This feature class is used to speed up the point delineation process.

#### Input

"Drainage Line" Feature Class  
"Catchment" Feature Class

#### Output

"Adjoint Catchment" Feature Class

#### Input/Output Management

If there is a linear feature class that has a tag "Drainage Line", it will be used as a default for the first input theme. If not, the user needs to select an existing linear feature class that will be tagged with the "Drainage Line" tag at the end of the operation.

Required fields: HydroID, GridID, From\_Node, To\_Node, NextDownID

Field created: DrainID – HydroID of the Catchment in which the drainage line is located.

If there is a polygon feature class that has a tag "Catchment", it will be used as a default for the second input theme. If not, the user needs to select an existing polygon feature class that will be tagged with the "Catchment" tag at the end of the operation.

Required fields: HydroID, GridID

Fields created:

- NextDownID – HydroID of the next down catchment. Populated with "-1" if there is no downstream catchment.
- With SDE:
- DrainID – created empty (if not previously existing)
- JunctionID – created empty (if not previously existing)

If there is a polygon feature class that has a tag "Adjoint Catchment", it will be used as a default for the output feature class. If not, the user needs to specify a feature class name that will be tagged with the "AdjointCatchment" tag at the end of the operation. If the output feature class already exists, the user is prompted whether to remove the existing dataset.

Fields created:

- HydroID – Unique identifier of the Adjoint Catchment in the hydro database.
- GridID – GridID of the catchment located downstream from the Adjoint Catchment.

Tutuila CTM Application: The inputs were the "Drainage Line" Line Feature Class from step 9 and the "Catchment" Polygon Feature Class from step 8. There were no user defined parameters to be set.

### **Final Note:**

The "Adjoint Catchment" feature class is the final output for the series of Arc Hydro processing steps conducted to determine MTU in the second manuscript of this thesis. As described in Hogrefe and Wright (unpublished), five of these catchment polygons were used as MTU with no further analysis. Three more MTU were identified by combining multiple catchments by visual analysis.